molecules

Review

Ruthenium(II) Polypyridyl Complexes and Their Use as Probes and Photoreactive Agents for G-quadruplexes Labelling

Julie Jiang [1], Titouan Teunens [1,2], Jérôme Tisaun [1], Laura Denuit [1] and Cécile Moucheron [1,*]

1. Laboratoire de Chimie Organique et Photochimie, Service de Chimie et PhysicoChimie Organiques, Université Libre de Bruxelles, Avenue F. D. Roosevelt 50-CP 160/08, 1050 Brussels, Belgium; julie.jiang@ulb.be (J.J.); titouan.teunens@ulb.be (T.T.); jerome.tisaun@ulb.be (J.T.); laura.denuit@ulb.be (L.D.)
2. Laboratoire de Chimie des Matériaux Nouveaux, Université de Mons, Place du Parc 20, 7000 Mons, Belgium
* Correspondence: cecile.moucheron@ulb.be

Abstract: Due to their optical and electrochemical properties, ruthenium(II) polypyridyl complexes have been used in a wide array of applications. Since the discovery of the light-switch ON effect of $[Ru(bpy)_2dppz]^{2+}$ when interacting with DNA, the design of new Ru(II) complexes as light-up probes for specific regions of DNA has been intensively explored. Amongst them, G-quadruplexes (G4s) are of particular interest. These structures formed by guanine-rich parts of DNA and RNA may be associated with a wide range of biological events. However, locating them and understanding their implications in biological pathways has proven challenging. Elegant approaches to tackle this challenge relies on the use of photoprobes capable of marking, reversibly or irreversibly, these G4s. Indeed, Ru(II) complexes containing ancillary π-deficient TAP ligands can create a covalently linked adduct with G4s after a photoinduced electron transfer from a guanine residue to the excited complex. Through careful design of the ligands, high selectivity of interaction with G4 structures can be achieved. This allows the creation of specific Ru(II) light-up probes and photoreactive agents for G4 labelling, which is at the core of this review composed of an introduction dedicated to a brief description of G-quadruplex structures and two main sections. The first one will provide a general picture of ligands and metal complexes interacting with G4s. The second one will focus on an exhaustive and comprehensive overview of the interactions and (photo)reactions of Ru(II) complexes with G4s.

Keywords: ruthenium(II) complexes; G-quadruplexes; photoprobes; photoreactive agents; labelling

1. Introduction

When one thinks of DNA, one often thinks of the classical double-helix structure, B-DNA, that was discovered from X-ray data by Watson and Crick in 1953 [1]. In this form, two complementary and antiparallel strands are held together by hydrogen bonding between adenines and thymines or guanines and cytosines. Nevertheless, a wide variety of other structures exist such as the more commonly known A-DNA and Z-DNA or the less common ones such as i-motif [2,3] and four-way junctions [4,5] for example. Among them, G-quadruplexes (G4) are formed from guanine-rich sequences of DNA or RNA. In G-quadruplex structures, four guanines are associated by Hoogsten hydrogen bonds in a plane, which form a so-called G-quartet or tetrad, and a minimum of two tetrads stacked on top of each other is needed to form a G-quadruplex (Figure 1). These G4 structures can be stabilized by monovalent cations such as K^+ or Na^+ which can coordinate the oxygen of the carbonyl groups of guanines, as demonstrated in the 1960s by X-ray diffraction [6–8] and spectroscopic studies [9]. G-quadruplexes play an important role in gene expression [10,11] and their presence in the cell environment has been demonstrated at several sites and intensively studied at the telomeric ends of eukaryotic chromosomes [12,13]. At these telomeric ends, DNA is organized as a guanine-rich single strand rather than a double helix,

which allows a favored quadruplex conformation and a privileged interaction with small molecules [14–16]. Bioinformatics studies have predicted the occurrence of quadruplex structures at many locations in the genome, particularly in promoter regions, or in genes involved in cell replication [17]. Computational studies have indicated that quadruplex structures may number as many as 700,000 [17–19].
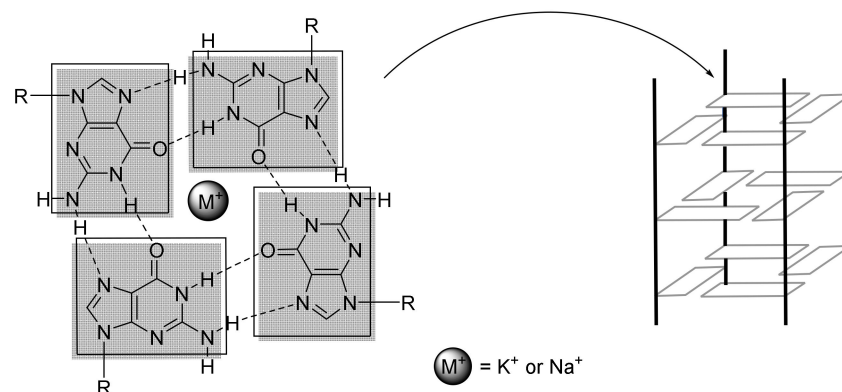
Figure 1. Structure of a G-tetrad and simplified schematic representation of a G-quadruplex.

Intensive research has been carried out over the past few decades to study G-quadruplexes as they have high potential to be used notably as therapeutic targets for cancer treatments thanks to their presence at the end of chromosomes [20]. They are crucial in cells as they play the role, among others, of cellular clock by shortening with each cell division, which finally brings cells to a state of senescence.

The stabilization of such G4 structures by small molecules or metal complexes is of key importance as this can inhibit the telomerase activity (activated in approximately 85–90% of cancer tumors), and thus, kill the cell through the induction of apoptosis. However, studying G-quadruplexes is not an easy task because they can adopt many different structures depending on the number and orientation of the strands that form the quadruplex, the stabilizing ions, or the sequence of nucleotides involved. Therefore, those structures will be briefly discussed in the next section. Afterwards a brief summary of the existing organic and metal complexes-based G-quadruplex ligands will showcase the great diversity of molecules able to interact with such G4. Lastly, an exhaustive presentation of ruthenium(II) polypyridyl complexes studied in presence of G-quadruplex structures will present their ability to interact and act as selective probes or potential anti-cancer agent which is the main focus of this review.

1.1. G-quadruplex Structures

G-quadruplexes are nucleic acid sequences containing a repeat of guanines which form quartets, linked together to the rest of the sequence forming loops [21–23]. The sequence allowing such a conformation can be summarized as follows:

$$G_{3-5}X_{B1}G_{3-5}X_{B2}G_{3-5}X_{B3}G_{3-5} \tag{1}$$

where the length and the composition of the sequence (X) that form the loops (B) vary from one structure to the other. A theoretical prediction model has been developed based on various G-quadruplex stability measurements. This model states that a structure can adopt a G4 conformation if it has a repeating unit comprising at least three consecutive guanines followed by at least one other base (usually several) [18,19].

$$G_{\geq 3}X_{1-7}G_{\geq 3}X_{1-7}G_{\geq 3}X_{1-7}G_{\geq 3}X_{1-7} \tag{2}$$

G-quadruplexes can be formed from one to four different nucleic acid strands. They are generally defined by a stack of at least two guanine tetrads.

The guanine quartets form the centre of the quadruplex by means of Hoogsteen hydrogen bonds [22], while the loops are located on the outside of the structure. The grooves formed by this structure are stabilized by phosphodiester bonds. In the case of a single-stranded structure, the sequence can be folded back on itself in different ways. The loops can be diagonal, lateral, or inverted, which leads to different G4 conformations.

The conformation adopted by a G4 structure will determine the direction of the strand base sequence. If a direction is arbitrarily defined, from top to bottom for example, it is possible to construct G4 structures in different ways (Figure 2). If all the guanine quartets participate in the top to bottom construction, a parallel structure will be spoken about (Figure 2A). If, on the other hand, half of the guanine quartets participate in the bottom-up construction, and the other half in the top-down construction, we speak of an antiparallel structure (Figure 2B–E). For single- or two-stranded G-quadruplexes, it is possible to observe a parallel conformation, implying that the top of the structure must be connected by a loop to the bottom of the structure for the adjacent strand. This is known as a propeller loop (Figure 2A) [24,25]. Another possibility is the antiparallel conformation, in which at least one of the strands is oriented in the opposite direction to the others. Although the loop can also exist in this type of structure, this implies the existence of another type of loop, connecting the upper (or lower) ends of the structures. Such a connecting loop between two adjacent vertices of posts is called a lateral loop (Figure 2B–D) [26–28]. When, on the other hand, the loop connects opposite posts, it will be called a diagonal loop (Figure 2C,E). Note that in this case, the direction of adjacent strands will alternate between parallel and antiparallel for steric reasons [29–33]. Furthermore, NMR studies have shown that guanines that do not constitute the quartet but are present in close proximity, for example in a loop, can participate in the stabilization of the overall structure [34].
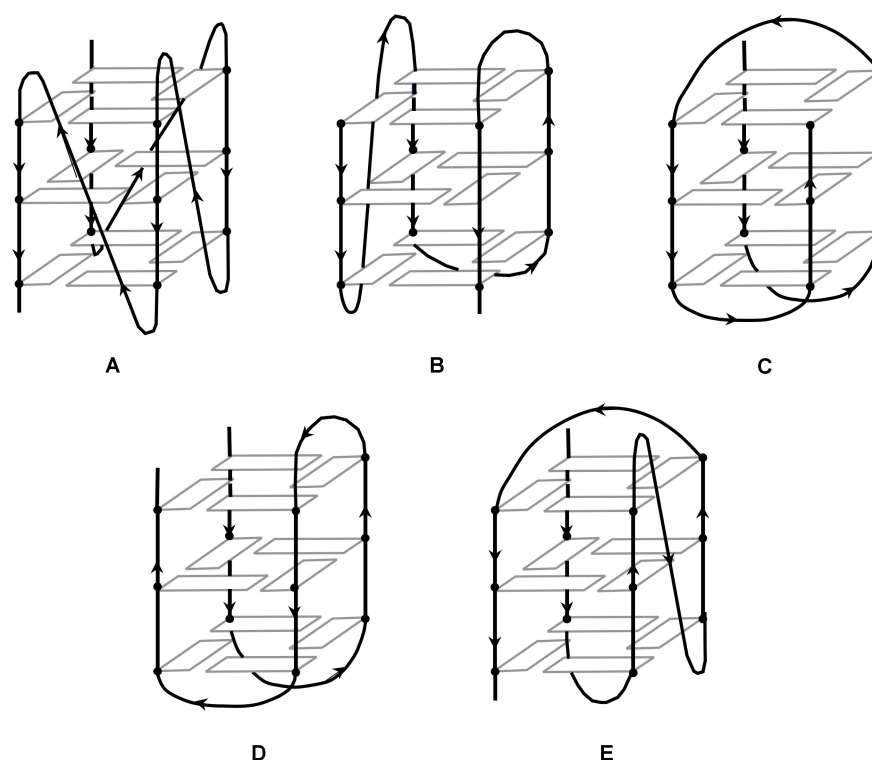
Figure 2. Schematic representation of various topologies adopted by simple unimolecular G-quadruplexes. (**A**)—Parallel conformation with three double chain reversal loops. (**B**)—Antiparallel conformation with one double chain reversal loop and two side loops. (**C**)—Antiparallel conformation with two side loops and a diagonal loop. (**D**)—Antiparallel conformation with three side loops. (**E**)—Antiparallel conformation with two diagonal loops and a double chain reversal loop [16,22].

The environment where the DNA strands are evolving has a major influence on the adopted conformation. The physiological environment controls the thermodynamic stability of the G-quadruplex due to the π-stacking existing by the induced conformation. The presence of positively charged ions that compensate for the overall negative charge of the DNA strand also plays a key role in the adopted structure. In particular, the presence of alkali ions such as Na^+ or K^+ will alter the parallel or antiparallel conformation of the quadruplex [35–41]. An NMR study published in 1993 showed that under sodium (Na^+) conditions, the quadruplex adopts an antiparallel conformation with one diagonal and two lateral loops (Figure 2C) [42]. However, in potassium (K^+) conditions, the sequence adopts a parallel conformation, with helical loops (propeller) (Figure 2A) [24,25]. The fact that the telomeric sequence can adopt a parallel conformation in potassium conditions was a surprise and led to numerous studies of quadruplexes in solution [35–40,43–45]. Because of the sensitivity of such systems to the environment, the conformations adopted by G-quadruplexes often coexist and easily switch from one to the other, suggesting that the two conformations are equi-energetic [35,39,46].

1.2. G-quadruplexes in Human Genome

1.2.1. Telomeres and Their Functions

Telomeres are found at the ends of chromosomes and consist mainly of a single strand of DNA. Their presence protects the rest of the chromosome and allows the conservation of the genetic code. With each cell division, this single strand is shortened until it reaches a critical length that triggers the cell death mechanism. This regulation based on the progressive shortening of the telomere prevents older cells from accumulating too many mutations that could alter gene expression [47]. Telomerase is expressed or over-expressed in 80–85% of cancer cells and is not expressed in healthy somatic cells [48]. This enzyme acts as a regulator of telomere length, preventing them from shortening.

1.2.2. Cellular Replication

The repeated sequence in human telomeres is a set of six bases: TTAGGG [49]. This sequence is accompanied by various proteins which have a necessary role for the protection of the telomere from the environment or in cell replication [50–52]. The function of the telomere is to protect the genetic information contained in the entire chromosome. Indeed, between 150 and 250 nucleotides are present at the 3′ end of the telomere sequence as a single strand and protect the rest of the chromosome from degradation or unwanted recombination [12]. Chromosomes are also protected by the presence and action of various proteins, among them hPOT1, a protein that interacts with TPP1, and whose role is to regulate the action of telomerase [53–55]. The absence of such proteins initiates the cell death response. The formation of more complex conformations such as G-quadruplexes competes with the action of these proteins, and stabilization of G4 structures by small molecules may also interfere with their action [56–61]. Studies have eventually determined that G-quadruplexes could present an anti-proliferative effect [62].

In a non-tumoral cell with a 24 h replication cycle, without an imported stabilizing molecule, a telomere of 5000 bases in length losing 100 bases per cycle would allow the cell to live between 40 and 50 days. In contrast, the use of molecules stabilizing G-quadruplex conformations shortens the lifetime of the cell drastically: only 7 to 10 days of life expectancy [63,64].

While the existence of G-quadruplex structures is no longer in question, their role in genetic processes is not well understood yet. Indeed, their presence in many gene promoter regions suggested that they might be of key importance in cell development, replication, and gene expression. In 2002, a study demonstrated that the transcription of *c-myc* (an oncogene) was adversely affected by the G4 conformation of the NHE III1 sequence upstream of the promoter sequence. In fact, if the sequence can retain its G-quadruplex conformation (by adding a stabilizer such as TMPyP4), *c-myc* is less expressed,

whereas if the G4 conformation is dropped (by mutation for example), *c-myc* expression is favoured [65]. This first example was followed by many others [66,67].

2. Classification and Characteristics of G4 Ligands

G-quadruplexes are dynamic structures in constant movement. In spite of this fact, there are lots of compounds capable of interacting with those ever-changing structures, and some of them can stabilize one or another conformation, leading to potential biological consequences.

Stabilization of G-quadruplex structures by small molecules was first demonstrated using an anthraquinone derivative **1** (Figure 3, diamidoanth) [68] and other studies have followed [20], mainly reporting the use of planar aromatic compounds, one end of which being positively charged [14,15,68]. Several studies have shown that the planar part of the molecule comes to rest on the external quartet, while intercalation between two guanine quartets has not been less observed so far [69–74]. Beyond the planar and positively charged ligands, telomestatin **2** (Figure 3) was of great interest to scientific research [75] and was the source of many more easily synthesized derivatives [76–79]. It has been shown that the size of the loops is important for molecular recognition [73].

diamidoanth

1

Telomestatin

2
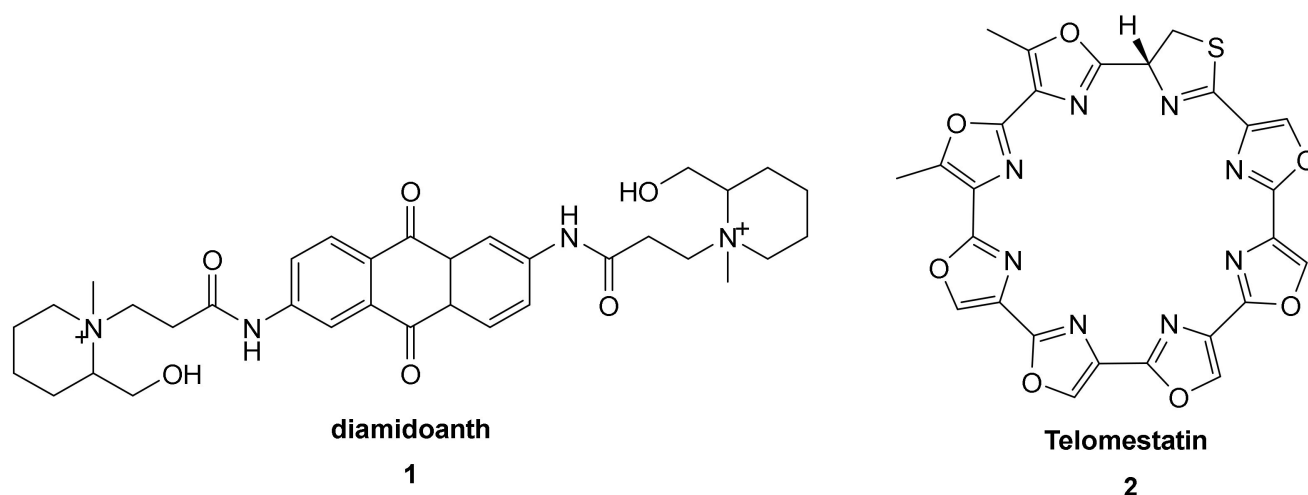
Figure 3. Structure of 2,6-bis[3-(4-methylpiperazino)proprionamido]-anthracene-9,10-dione **1** and telomestatin **2**.

Ligands displaying aromatic rings mainly interact with the G-quadruplex by π-stacking on the terminal quartets. In comparison, ligands displaying some lateral chains preferably interact with the grooves and loops. The presence of a protonated amino group will help the ligand to interact with the negatively charged phosphate groups. Ligands displaying a long charged lateral chain will be able to interact through the central channel. All the ligands display at least one of those properties (abilities), but some ligands can interact with G4-structures by more than one geometry.

G-quadruplexes present different interaction sites, among whom terminal quartets, internal quartets, grooves, loops, and the central channel (Figure 4) [16].
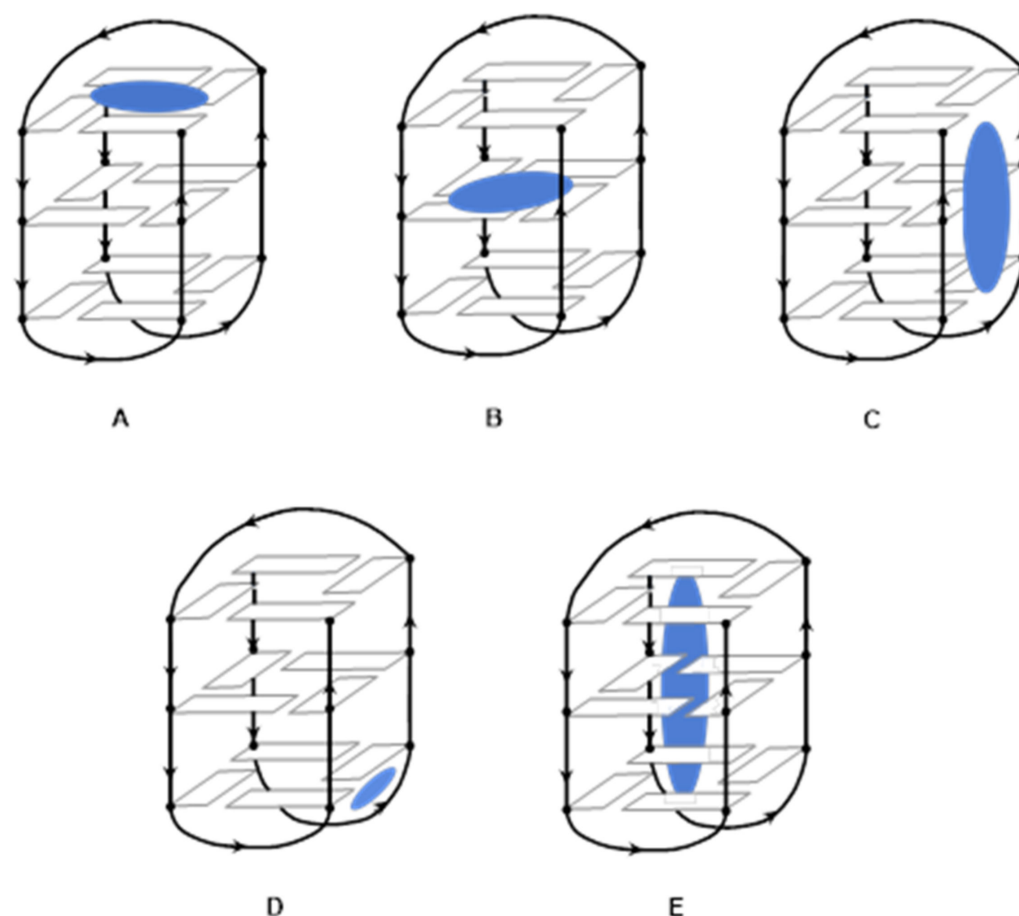
Figure 4. Interaction geometries between a G4-ligand and a G-quadruplex structure. (**A**)—(π-stacking) on an external quartet. (**B**)—intercalation between tetrads. (**C**)—interaction within a groove. (**D**)—interaction within a loop. (**E**)—interaction within the central channel.

2.1. Organic G4 Ligands

2.1.1. Stacking on the Terminal Tetrads

This interaction geometry is achieved by electrostatic, hydrophobic, and van der Waals interactions. The large aromatic surface resulting from the combination of four guanines allows better interaction with ligands displaying a large aromatic surface, making them more selective towards G4 structures than double-stranded DNA.
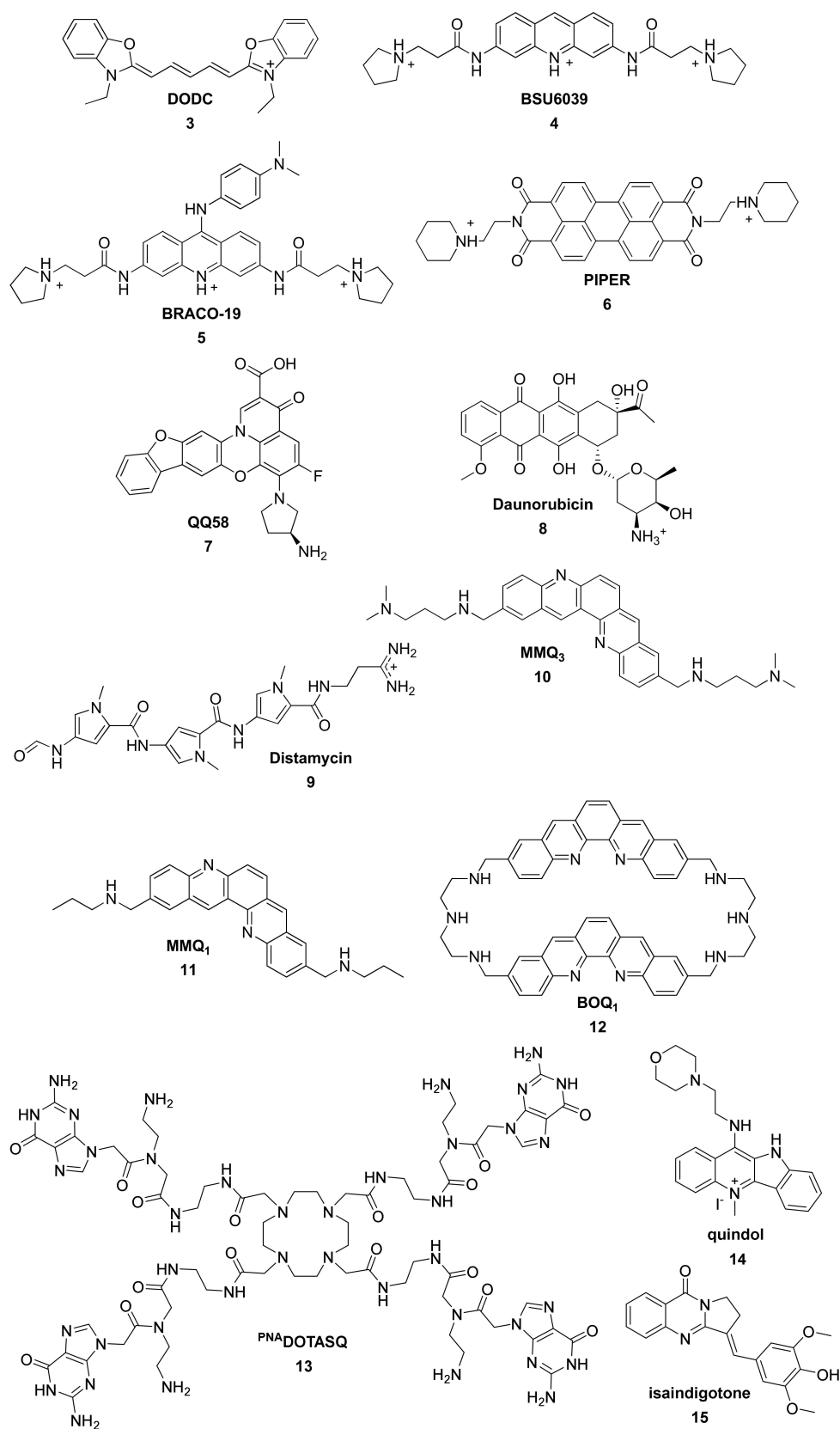
In Situ Protonated Ligands

While hydrophobicity must be sufficient to develop π-stacking with the external quartet, hydrophilia must also be present to allow the ligand to dissolve in water. This explains why several ligands have been designed to be protonated in experimental conditions.

In 1996, Shafer showed that the relatively simple and small DODC (DODC = 3,3′-diethyloxadicarbocyanine) (Figure 5, compound **3**) interacts with G4 structures [80].

In 1997, Hurley developed a derivative of 2,6-diamidoanthraquinone (Figure 3, compound **1**) which exhibits an inhibitive behavior to telomerase [68].

However, it turned out that those compounds were not selective enough to G-quadruplexes, and focus moved to acridine derivatives [81,82]. BSU6039 (Figure 5, compound **4**) was proved to interact by π-stacking [70,83] and based on these results, BRACO-19 (Figure 5, **5**) was synthetized. This ligand is able to interact with three different grooves of G-quadruplexes [73,84–87] and showed encouraging results on the non-proliferation of cancerous cells [58,84,88–90].

Figure 5. Structure of the in situ protonated ligands. **3**—DODC. **4**—BSU6039. **5**—BRACO-19. **6**—PIPER. **7**—QQ58. **8**—Daunorubicin. **9**—Distamycin. **10**—MMQ$_3$. **11**—MMQ$_1$. **12**—BOQ$_1$. **13**—^{PNA}DOTASQ in an open conformation. **14**—5-methyl-11-(2-morpholinoethylamino)-10H-indolo[3,2-b]quinolin-5-ium iodide (quindol). **15**—isaindigotone.

Then, Hurley developed in 1998 a series of ligands with an even more extended planar aromatic moiety. In this context, perylene diimide (PIPER) (Figure 5, compound **6**) displays a more hydrophobic core but seems less aggressive to telomerase activity [69]. Later, some Iron(II) complexes bearing this PIPER ligand were also studied [91].

In the early 2000s, the family of quinobenzoxazines was studied. QQ58 (Figure 5, compound **7**) [92,93], a fluoroquinophenoxazine (FQP), showed an interesting cellular activity, namely the inhibition of polymerase stop assay, driven by the effective binding to G-quadruplexes via stacking on the external tetrads. Furthermore, this fluoroquinophenoxazine showed potent inhibition of telomerase activity with an IC_{50} value of 28 μM [92].

In the meantime, research also targeted compounds known for their affinity to duplex DNA. In this context, Daunorubicin [94,95] (Figure 5, compound **8**) was shown to strongly interact with G-quadruplexes. Three ligands can interact with only one G4 [96]. In comparison, two molecules of distamycin [97] (Figure 5, compound **9**) interact top to tail inside a groove or on the surface of the external tetrads [98–102]. This time the small aromatic surface is compensated by the presence of two ligands side by side.

Covering a large surface of the tetrad seems to be the top of the parameter list to ensure better interaction with the G-quadruplexes. Therefore, elbow-shaped pentacyclic quinacridine ligands were designed to cover more efficiently the guanines of the external quartet. Studies on MMQ_3 (Figure 5, compound **10**) and MMQ_1 (Figure 5, compound **11**) showed strong inhibition of telomerase activity [103] due to the interaction geometry with G4s involving the covering of three guanines. It also demonstrated the importance of the lateral chains interacting with the grooves [104]. Platinum(II) complexes bearing similar ligands were designed later [105].

A dimer of quinacridine (BOQ_1) (Figure 5, compound **12**) was developed. The extended aromatic moieties allow it to interact more selectively with G-quadruplexes than with double-stranded DNA [106,107]. Another study showed that this compound could interact with the loops by adopting a half-closed conformation [108].

The dynamic change of conformation allows ^{PNA}DOTASQ (Figure 5, compound **13**) to rearrange itself when in interaction with the G4 structure, on the surface of the external quartet [109].

Lots of alkaloids were studied as potential G4-ligands. For example, two molecules of quindoline (Figure 5, quindol **14**) stack on the external tetrads of telomeric G-quadruplexes, resulting in a high affinity for the G4 [110]. Finally, besides the characteristic end-stacking binding mode, isaindigotone (Figure 5, compound **15**) interacts preferably with the grooves than the loops. Four molecules of this ligand were proved to interact simultaneously with antiparallel G4 structures [111].

N-methylated Ligands

Those ligands consist of a central aromatic unit with four nitrogen atoms. The nitrogen atoms located on the lateral aromatic rings are methylated, allowing easier solvation in water. Moreover, the weaker electronic density decreases the repulsion and allows better packing. TMPyP4 (Figure 6, compound **16**) [65,112–120] shows an inhibitive activity of telomerase ($IC_{50} = 8$ μM) [114] and also plays a role in the gene expression such as *c-myc*. The interaction occurs when a porphyrin unit stacks on the external quartet of the parallel G-quadruplex [121]. However, this ligand does not exhibit a much better affinity for G4 over double-stranded DNA [122–125]. Other binding geometries exist between this ligand and the G4 structures. Aside from π-stacking with the external quartet, it also can intercalate between two tetrads [121,126,127] and interact with the loops [72]. Some derivatives were studied as well. For example, 3,4-TMPyPz (Figure 6, compound **17**) exhibits a better selectivity for G4 structures, and a much higher affinity [128].
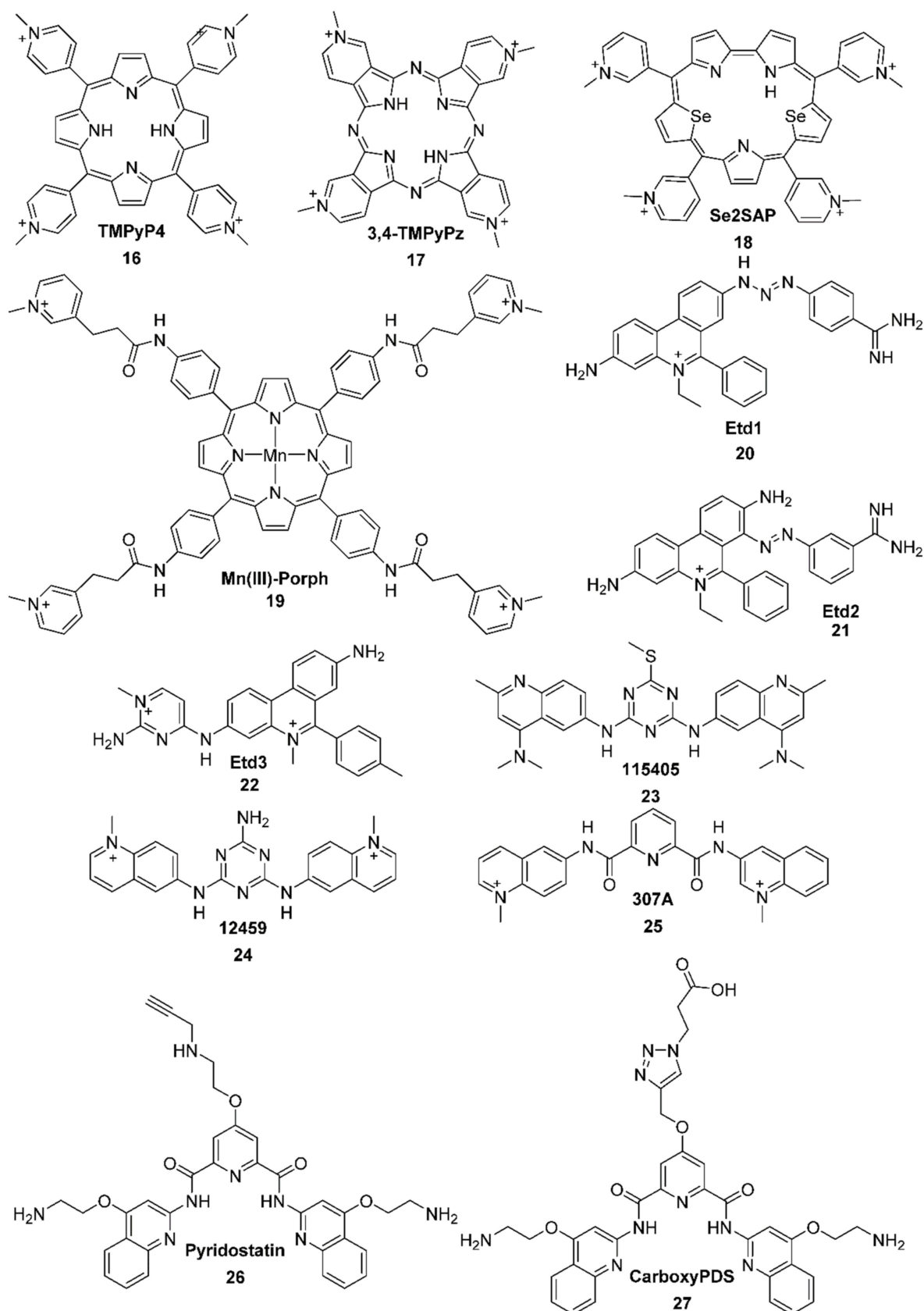
Figure 6. Structure of the N-methylated ligands. **16**—TMPyP4. **17**—3,4-TMPyPz. **18**—Se2SAP. **19**—Example of a Mn(III) complex bearing a porphyrin unit. **20–22**—Ethidium derivatives (Etd1, Etd2, Edt3). **23 + 24**—Triazine derivatives (115405, 12459). **25**—307A. **26**—Pyridostatin. **27**—CarboxyPDS.

To increase the selectivity for G4 structures over double-stranded DNA, a manganese(III) center was used in the core of the ligand, composed of a porphyrin unit connecting four lateral chains bearing methylated nitrogen atoms (Figure 6, Mn(III)-Porph **19**) [129]. It was shown that the porphyrin unit lies on the top of an external tetrad while the lateral flexible cationic arms interact with the grooves [129].

The aromatic unit of porphyrins was extended with the same goal in mind. In this context, Se2SAP (Figure 6, compound **18**) shows a better selectivity for G-quadruplexes over duplexes. The studies showed that its presence induces a change of conformation from parallel or antiparallel to a hybrid one [130,131].

Most of the ligands presented so far were quite large, but some smaller ligands were also used. For example, Mergny developed some derivatives of ethidium (Figure 6, Etd1 **20**, Etd2 **21**, Etd3 **22**) [132]. However, despite a good stabilization of G-quadruplexes and the inhibition of telomerase, they were quickly replaced by derivatives of triazine (Figure 6, 115405 **23**, 12459 **24**) [133–136] because of the carcinogen risks linked to ethidium bromide. In parallel, pyridocarboxamide derivatives were also studied [137,138]. Among these compounds, one of the most promising ones in terms of G-quadruplex vs duplex selectivity and telomerase inhibition activity (IC_{50} = 0.3 μM), 307A (Figure 6, compound **25**), proves to be an efficient stabilizer of *c-myc* G-quadruplex. Furthermore, this 2,6-pyridine-dicarboxamide derivate interferes with telomere maintenance and multiple steps of the cell division cycle, namely the S-phase.

Among the other ligands that were studied, pyridostatin (PDS) (Figure 6, compound **26**) shows an effect on the growth of cancerous cells by inducing replication as well as transcription-dependent DNA damage. After 48 h of incubation at a concentration of 10 μM, pyridostatin proves to be an efficient growth inhibitor of some human cancer cell lines [139]. Another one, carboxyPDS (Figure 6, compound **27**) shows a preference for RNA quadruplexes over DNA quadruplexes [140].

2.1.2. Intercalation between Guanine Tetrads

This interaction geometry is much less common. TMPyP4 intercalates between the quartet in absence of potassium cation. In the presence of the cation, the ligands preferably bind to the grooves or stack on the external quartet [121,141,142]. The experimental results are consistent with an intercalation between the tetrads [126,143]. The visible and circular dichroism (CD) spectra display the characteristic hypochromic redshift of the Soret band (420 nm) and a negative-induced CD band in the Soret region upon binding to the G-quadruplexes through intercalation. Furthermore, molecular modelling studies predicted this intercalative binding mode rather than π-stacking to either end of the tetrad.

2.1.3. Interaction with Grooves and Loops

The non-planar structure of peimine et peiminine (Figure 7, **28** and **29**, respectively) confers to those ligands a higher affinity due to a better fitting into the lateral grooves of parallel G-quadruplexes by electrostatic interactions. Indeed, as the antiparallel G4 conformation, which is more prevalent in Na^+ medium, has loops close to the grooves, these non-planar compounds display preferential binding to mixed-hybrid G-quadruplexes in K^+ medium due to steric hindrance of the antiparallel G4 conformation adopted in Na^+ medium. Temperature-dependent circular dichroism experiment results are in agreement with this observation and revealed selectivity over duplex DNA [144].
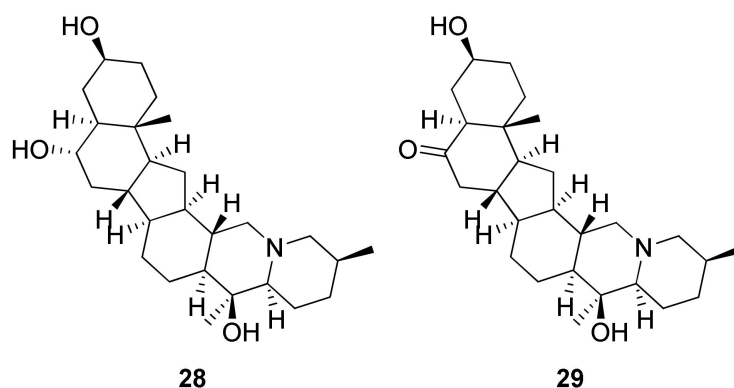
Figure 7. Structures of peimine **28** and peiminine **29**.

2.1.4. Central Insertion

Since the guanines' carbonyl groups face each other at the center of the quartet, the high electronic density attracts small cations such as K$^+$ and Na$^+$, which place themselves in the central channel. In this context, some ligands were designed with an aromatic part that interacts with the external quartet while a polyamine chain penetrates inside the central channel (Figure 8, **30**) [145].
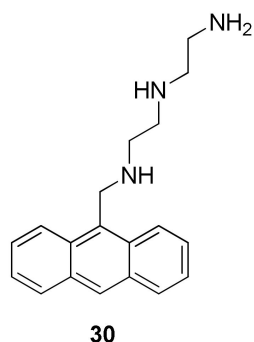
Figure 8. Structure of an anthracene with a polyamine chain.

2.2. Metal Complexes-Based G4 Ligands

Metal complexes display interesting photophysical properties that can be exploited to target G-quadruplexes. For instance, such complexes can emit light specifically when bound to G4 structures [146] or stabilize a telomeric G4 conformation [147].

Moreover, the presence of a metallic ion near the central channel can optimize the alignment of the aromatic moieties of the ligands and the guanines, resulting in a stronger interaction force [148].

2.2.1. Porphyrines

As explained before, TMPyP4 has been widely studied and metal complexes have been designed as well, leading to the synthesis of complexes with various metal cations: Cu(II) [149,150], Ni(II), Co(III), Au(III), and Mn(III) (Figure 9, **31–35**) [151].

Other Mn(III)-porphyrin complexes (Figure 9, **36** and **37**) were imagined to specifically target G-quadruplexes. For this purpose, the porphyrin unit stacks on the external tetrads while lateral arms interact with the grooves [129,152–154]. The resulting Mn(III)-porphyrin complexes display a lower inhibitory activity of telomerase than TMPyP4, but remain efficient G-quadruplex stabilizers. Other porphyrin complexes built around Zn(II) [128,155] have been studied such as the 3,4-TMPyPz zinc(II) porphyrazine [128]. By adding a metal center, the binding affinity towards G-quadruplexes was weakened compared to the 3,4-TMPyPz parent ligand, despite the four molecules of 3,4-TMyPyPz zinc(II) that can bind to telomeric G-quadruplex. Among other porphyrin, a protoporphyrin IX complex

incorporating a Fe(III) cation, also known as haemin, has been widely discussed and displays a strong binding affinity of 4.2×10^7 M^{-1} [156,157].
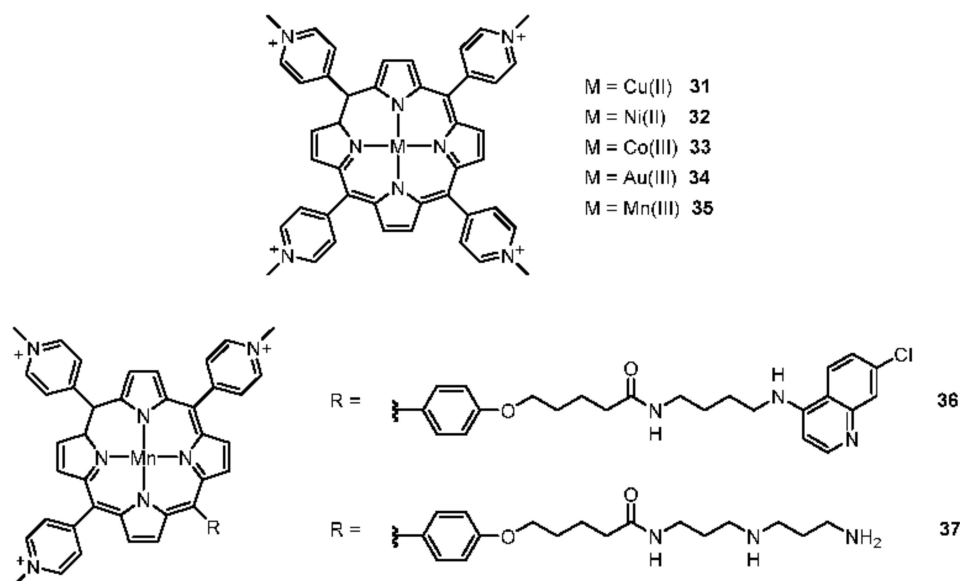
Figure 9. Structure of porphyrin ligands used with various metal ions for G-quadruplexes recognition.

2.2.2. Salphens

Another category of metal complexes is based on a salphen unit. Cu(II) and Ni(II)-salphen complexes (Figure 10, **38**, **39**) have been synthetized in this framework [148,158] and are good stabilizers of G4-structures in consequence of the stacking of the salphen rings on the external tetrads and the interactions of the lateral charged substituents with the grooves. The metal center is located above the central channel [159]. While complexes adopting a square planar geometry develop a good affinity for G4 quadruplexes, as expected, it was demonstrated that complexes with a square-based pyramidal geometry also develop a good affinity for G-quadruplex in addition to a good selectivity for those structures compared to duplex DNA. The vanadyl complex presented in Figure 10, **40** is a representative example of this family of salphen square-based pyramidal compounds [158].
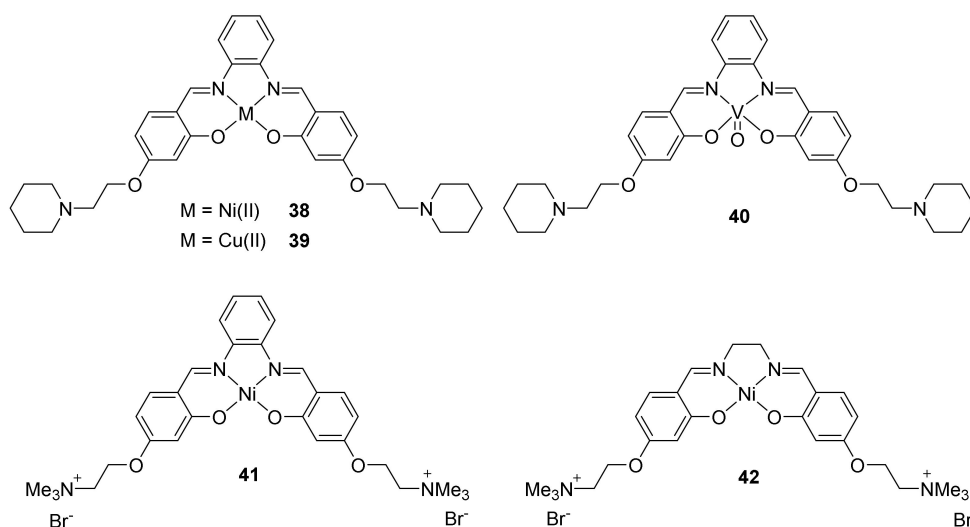
Figure 10. Structure of metalled salphen and salen complexes used for G-quadruplexes recognition.

Based on this concept, other metals were used and various complexes were developed: Ni(II), Pd(II), Cu(II), Co(III), Pt(II), or Zn(II) [160–169]. Most of these salphen or salen

complexes display a square planar geometry except the square-based pyramidal salphen complexes based on Co(III) [168].

A study compared two Ni(II) complexes bearing a salphen (**41**) or a salen (**42**) ligand (Figure 10) [170]. The presence of that supplementary aromatic ring increases the interaction by π-stacking. The presence of cationic groups on the lateral chains increases the affinity [170], whereas anionic groups decrease it [171].

2.2.3. Terpyridines and Other Square Planar Complexes

Square planar geometry adopted by Pt(II) and Pd(II) complexes wearing terpyridine ligands has been proved to be necessary for a good affinity when compared with Cu(II) and Zn(II) analogue complexes which are not planar [172]. The interaction geometry remains based on stacking on top of the external tetrads, but some studies demonstrated that interactions within the loops were also possible [173–175]. The terpyridine geometry was also modified to increase the affinity towards G-quadruplexes structures. Pt-bzimpy [176] (Figure 11, **43–45**) is a series of compounds synthesized for this purpose.
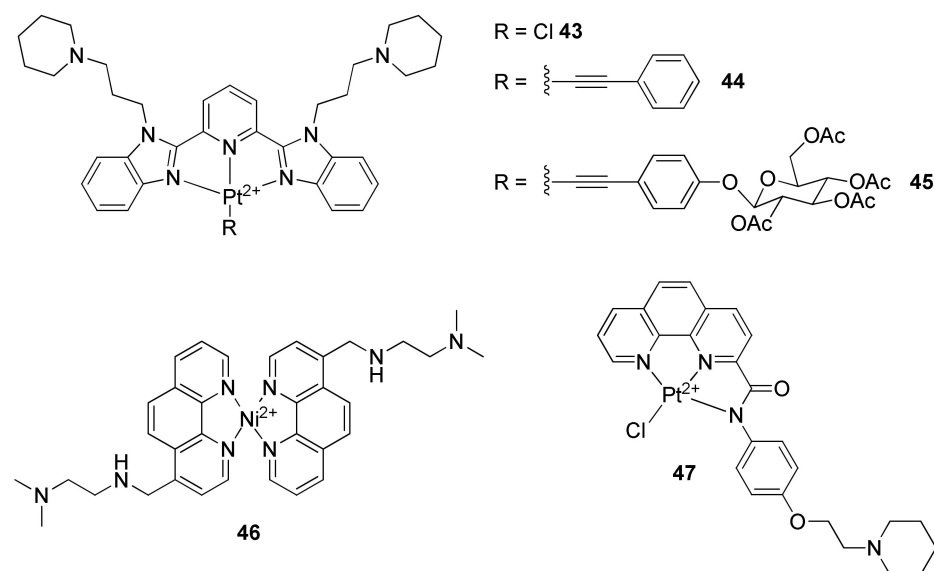
Figure 11. Structure of some terpyridines and other square planar complexes used for G-quadruplex recognition.

Another example is (K34)$_2$Ni(II) (Figure 11, **46**) which has a high affinity to the external tetrads thanks to its square planar geometry [177]. Another square planar Pt(II) complex based on a mono-substituted phenanthroline ligand (Figure 11, **47**) shows a good stabilization of G-quadruplexes by stacking on top of G-tetrads [178]. Molecular calculations also predicted the fitting of the piperidine sidearm into the pocket created by a TTA loop. Furthermore, this compound presents a 40-fold selectivity for G-quadruplexes over duplex DNA and is, therefore, more selective than BRACO-19. However, its telomerase inhibitory activity is less effective than BRACO-19 or TMPyP4, with an IC$_{50}$ value of 49.5 μM (compared to 2.5 μM [84] and 8 μM [114], respectively).

Besides those metal complexes adopting mainly a square planar geometry, complexes adopting an octahedral geometry have also been studied with G-quadruplexes as for example complexes based on Fe(III) [179] or Ir(III) [180–183]. Among those complexes, the ruthenium(II) complexes occupy a central place and will be at the core of the following sections.

3. Interactions of Ruthenium(II) Complexes with G-quadruplexes

Ruthenium(II) polypyridyl complexes are composed of one central ruthenium(II) cation and three chelating diimines. The first example of the luminescence of such complexes dates from the report of the luminescence of [Ru(bpy)$_3$]$^{2+}$ (bpy = 2,2′-bipyridine)

by Paris and Brandt [184], who paved the way for an impressive field of research. This luminescence arises from a metal-to-ligand charge transfer triplet excited state (^{3}MLCT) whose energy largely depends on the solvent used. The photophysical and electrochemical properties of Ru(II) polypyridyl complexes can be finely tuned by the structure of the chelating diimines which allowed their use in a plethora of applications involving light-induced processes [185,186]. A lot of these complexes are composed of one ligand of interest and two other "spectator" ancillary ligands which play an important structural role but do not control the photophysical or electrochemical properties of the complex. The best examples of ancillary ligands are the bpy and phen (1,10-phenanthroline) molecules and derivatives thereof such as the dmp (2,9-dimethyl-1,10-phenanthroline) or TAP (1,4,5,8-tetraazaphenanthrene) molecules (Figure 12) [187].
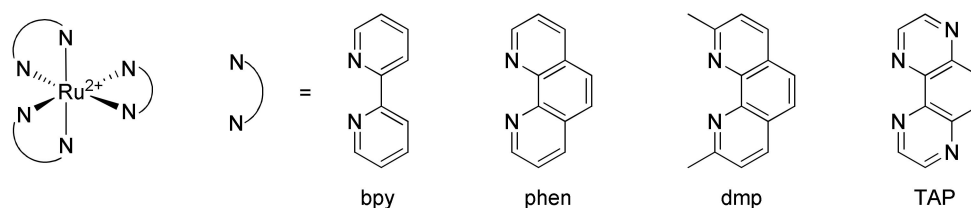

Figure 12. Schematic structure of ruthenium(II) polypyridyl complexes and of typical ancillary ligands.

The most famous compounds triggering the interest of ruthenium(II) polypyridyl complexes as powerful tools to study DNA are the [Ru(bpy)$_2$(**dppz**)]$^{2+}$ and [Ru(phen)$_2$(**dppz**)]$^{2+}$ (dppz = dipyrido[3,2-*a*:2′,3′-*c*]phenazine) complexes [188]. These complexes are called light-up probes as they are not luminescent in water but do emit brightly in DNA containing aqueous solutions. This light-switch ON effect can be explained by the presence of two different MLCT excited states whose relative energy position is very sensitive to the environment: one bright emissive state and one dark non-emissive state [189,190]. In water, the formation of hydrogen bonds with the nitrogen atoms of the pyrazinic cycle greatly stabilizes the dark state, which leads to a very strong luminescence quenching as no luminescence can be observed anymore. However, in apolar solvents or in presence of DNA, no hydrogen bonds are formed and the lowest excited state is the bright state, thus restoring the luminescence of the complex (Figure 13).
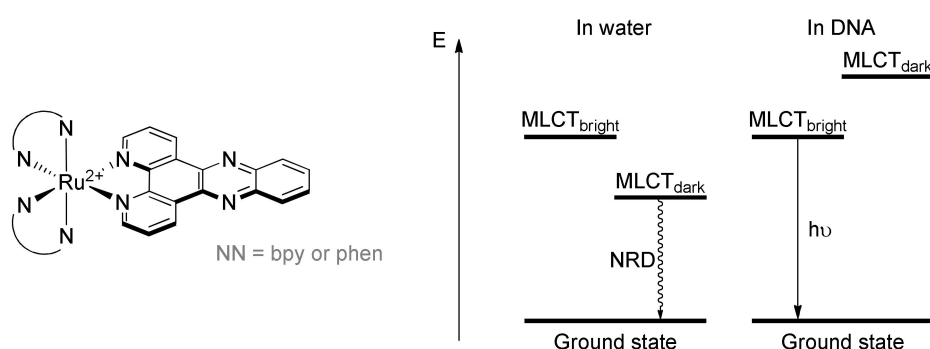

Figure 13. Structure of [Ru(L)$_2$(**dppz**)]$^{2+}$ (L = bpy or phen) and energy diagram of the excited states involved in the light-switch effect in function of the environment around the complex. NRD = non-radiative decay.

The first studies involving ruthenium(II) complexes and G-quadruplexes started with [Ru(bpy)$_3$]$^{2+}$ as Szalai and Thorp compared its cyclic voltammogram in the presence of G4s relative to the results obtained with duplex DNA (B-DNA) [191]. Their work revealed that guanines of G-quartets are more accessible to the complex than guanines of duplexes. However, the three-dimensional structure of G4s does not allow for sufficiently compact stacking to constitute an increase in the reactivity observed for sequences with successive guanines in duplex DNA.

On top of that, other very well-known homoleptic ruthenium(II) complexes, namely [Ru(phen)$_3$]$^{2+}$ and [Ru(TAP)$_3$]$^{2+}$ (TAP = 1,4,5,8-tetraazaphenanthrene), were studied in the presence of G4 structures as well [192]. These complexes only interact weakly with G-quadruplexes. However, it appears that [Ru(phen)$_3$]$^{2+}$ interacts through different binding modes, namely by end-stacking and intercalation into the minor groove, which can induce slight deformation in the G-quadruplex structures.

The following section will focus on the interaction of ruthenium(II) polypyridyl complexes with G-quadruplexes starting with mononuclear and then polynuclear complexes. The main focuses of this section are first dppz containing complexes as their interaction with G4s are the most understood due to the advanced techniques used for their study. Afterwards, ruthenium(II) complexes containing a π-extended ligand will be thoroughly explored as large aromatic surfaces have been demonstrated to promote G-quadruplexes selectivity through improved interaction of the complexes with these structures.

The last section of this review will be discussing the photoreactivity of certain types of ruthenium(II) polypyridyl complexes with G-quadruplexes for their irreversible labelling.

3.1. Monometallic Ruthenium(II) Complexes

3.1.1. Ruthenium(II) dppz and dppz Derivative Complexes

The first examples of the use of [Ru(L)$_2$(**dppz**)]$^{2+}$ (L = bpy or phen) as sensor for G-quadruplexes dates from 2010 with two studies carried out by Shi et al. [193,194]. Both complexes show an increase in luminescence when interacting with either G-quadruplexes or i-motif DNA. However, the increase is more intense with G-quadruplexes indicating a better protection of the complex from this type of structure and thus better interaction. Furthermore, the increase in luminescence is more important with mixed-hybrid G-quadruplexes which are more prevalent in K$^+$ medium, whereas the luminescence increase is lower with antiparallel G-quadruplexes which are more present in Na$^+$ medium. This indicates a further potential selectivity of such complexes towards specific structures of G-quadruplexes. These first studies showed promising results and paved the way for further understanding of the interaction of these complexes with G-quadruplexes and the consequent impact on the photophysical behavior of dppz containing Ru(II) complexes.

As both DNA and the studied complexes are chiral, the following studies explored the possible differences of the interaction of Δ and Λ enantiomers of [Ru(L)$_2$(**dppz**)]$^+$ with G-quadruplexes [195,196]. Interestingly, the Λ enantiomer of both complexes show a slightly stronger binding than the Δ enantiomer, which is contrary to the observations reported when such complexes interact with double-stranded DNA instead of G-quadruplexes. On the other hand, the chirality of the complexes does not have an impact on the affinity of the complex towards different structures of G-quadruplexes (hybrid or antiparallel) indicating the absence of appreciable stereoselective G-quadruplex binding.

Using ultrafast time-resolved infrared spectroscopy allowed a recent investigation on the binding site of [Ru(phen)$_2$(**dppz**)]$^{2+}$ with various G-quadruplex structures in solution [197]. This technique allows one to get information on both the excited state of the complex (bright or dark state) and on the influence of the dipole of the excited complex on the interacting DNA bases. As expected, different structures of G-quadruplexes induce a different geometry of interaction with the striking highlighting of the thymine base interactions in the binding of the complex with the Na$^+$-stabilized antiparallel human telomer quadruplex (Figure 14B). This indicates that instead of stacking on to the terminal guanine quartets, [Ru(phen)$_2$(**dppz**)]$^{2+}$ seems to bind in the loop region of the antiparallel G-quadruplex structure. However, for the other structures studied, signals attributed to the interaction of the complex with guanines indicates that the complex is stacked on the terminal guanine quartets with varying degrees of interaction with other DNA bases depending on the size and flexibility of the loops (Figure 14A,C,D).
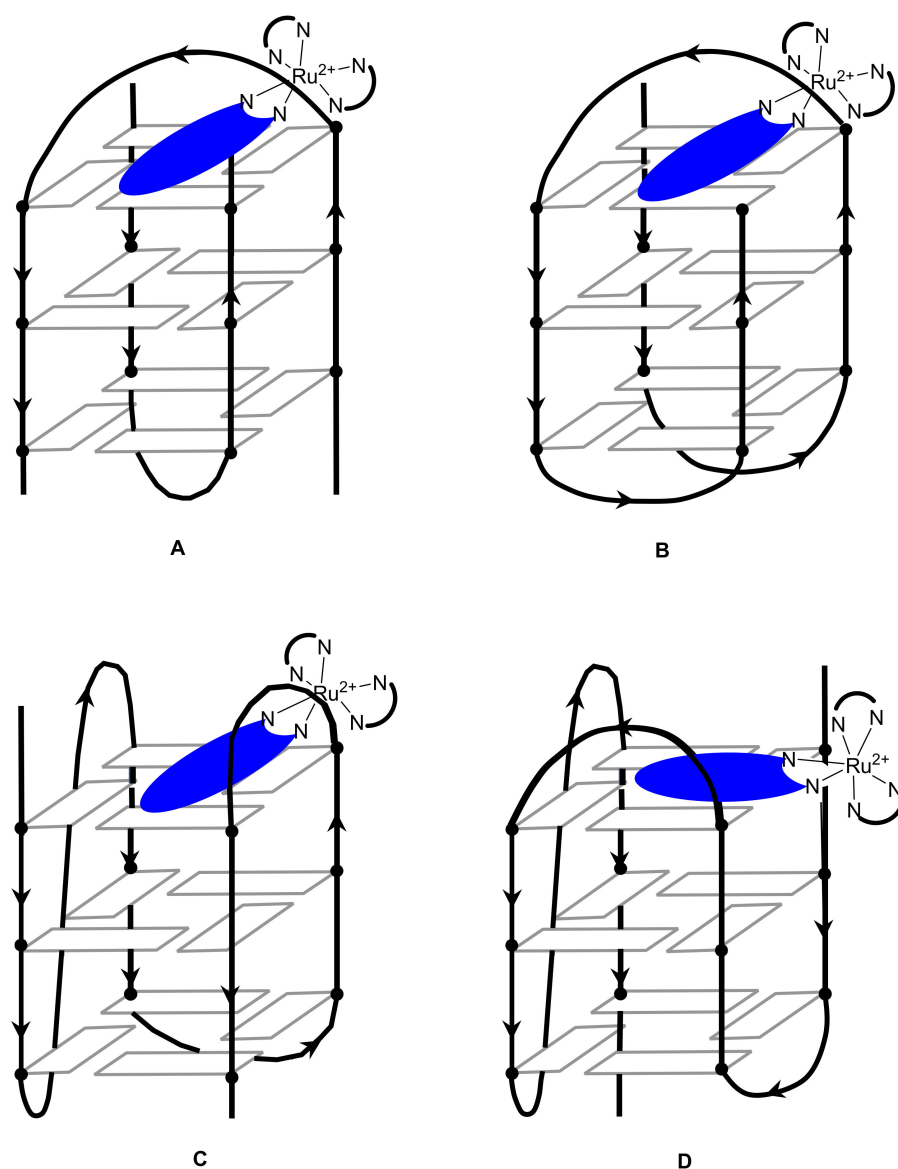
Figure 14. Binding interactions of [Ru(phen)$_2$dppz]$^{2+}$ with (**A**)—G4T4G4 (K$^+$), (**B**)—G-HT (Na$^+$), (**C**)—G-HT (K$^+$) Hybrid 1, (**D**)—G-HT (K$^+$) Hybrid 2; using time-resolved infrared spectroscopy as proposed by Devereux et al. [197] (G4T4G4 = *Oxytricho nova* telomere sequence [d(G$_4$T$_4$G$_4$)]$_2$, G-HT = human telomere sequence d[AG$_3$(T$_2$AG$_3$)$_3$]).

Even more recently, the ultrafast excited state dynamics of [Ru(phen)$_2$(**dppz**)]$^{2+}$ was studied in order to investigate the influence of the microenvironment around the complex on the population of both the bright and dark states [198]. The ultrafast dark state formation and decay rates are the most sensitive to the amount of water near the complex. The faster formation of the dark state (10.5 ps) for [Ru(phen)$_2$(**dppz**)]$^{2+}$ interacting with the antiparallel Na$^+$-stabilized human telomeric sequence when compared to the 15.6 ps obtained in presence of *Oxyticha nova* G-quadruplex sequence indicates that the microenvironment of the complex is more hydrophilic for the former interaction site. This finding agrees with the previously discussed study which pointed out that the complex interacts with the loops of this antiparallel Na$^+$-stabilized structure of G-quadruplex. Such loops allow a faster water exchange since they offer a more flexible environment for the complex.

These recent studies underscore the ability to potentially discriminate different secondary structures of DNA with such complexes and thus emphasize the need to understand their behavior in a precise way. Furthermore, the ability to greatly modify the structure of

the dppz-type ligands (Figure 15) opens the way to further development in the quest for even more selective probes which are discussed here below.
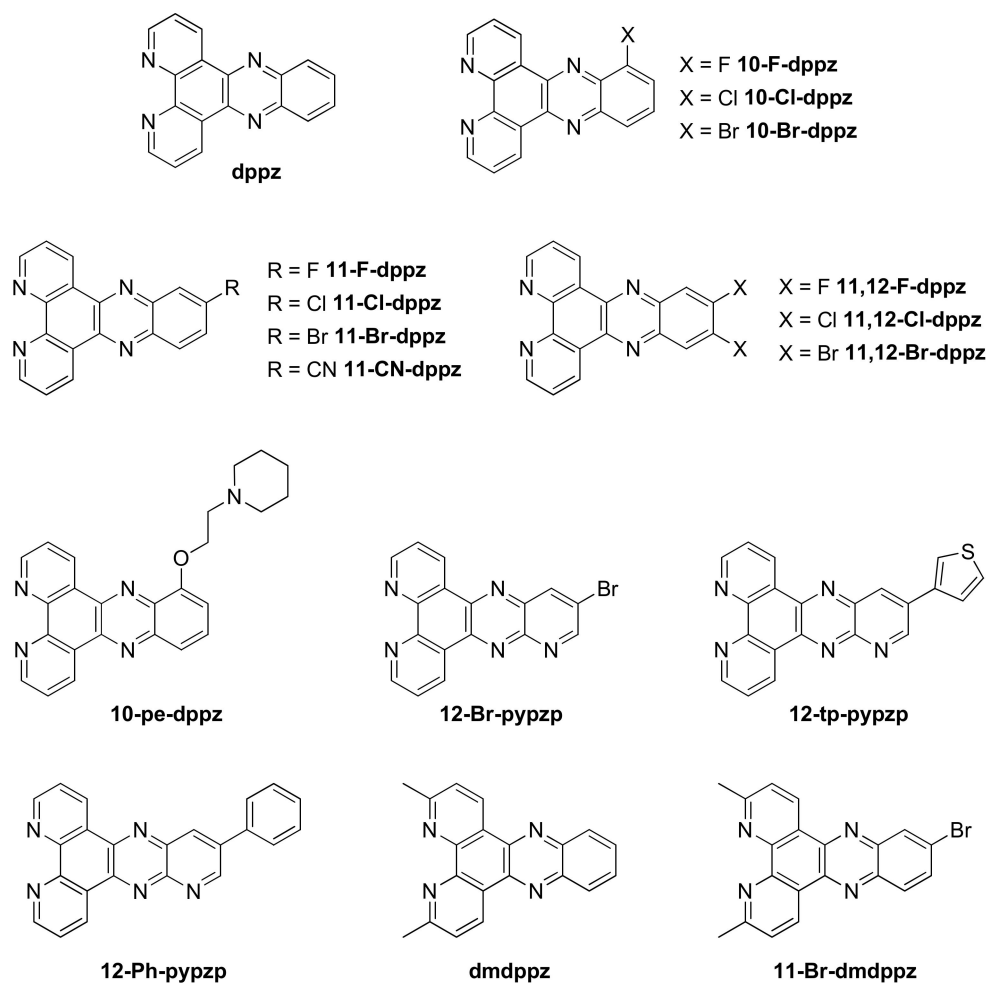
Figure 15. Structure of dppz and closely related ligands used to form ruthenium(II) complexes studied in presence of G-quadruplexes.

Obtaining a crystal structure of a complex interacting with a G-quadruplex is rather challenging due to the various structures they can adopt. However, in 2019 two reports were published on the crystal structure of Λ-[Ru(TAP)$_2$(**dppz**)]$^{2+}$ [199] and the closely related Λ-[Ru(TAP)$_2$(**11-CN-dppz**)]$^{2+}$ as well as Δ-[Ru(phen)$_2$(**11-CN-dppz**)]$^{2+}$ (Figure 15) [200] bound with the G-quadruplex forming heptamer d(TAGGGTT). Out of the four binding modes found for Λ-[Ru(TAP)$_2$(**dppz**)]$^{2+}$, none of them show the complex stacking on one of the ends of the G-quadruplex. Indeed, the four structures obtained show that the complex is rather interacting with the thymine–adenine loop regions, which agrees with the recent spectroscopic findings in solution. The different binding sites observed might also explain the various degrees of protection from water of the complex and thus the various lifetimes measured in solution. Adding a simple cyano group on the dppz ligand to form [Ru(TAP)$_2$(**11-CN-dppz**)]$^{2+}$ drastically changes the obtained crystal structure. Indeed, the Λ enantiomer is shown to interact directly with the G-tetrad plane (Figure 16A), which is not the case for [Ru(TAP)$_2$(**dppz**)]$^{2+}$. On the contrary, Δ-[Ru(phen)$_2$(**11-CN-dppz**)]$^{2+}$ does not interact directly with the G-quartet but rather with the terminal T-T pairs (Figure 16B). These findings further illustrate the need to use advanced techniques to better understand the implications of small structural changes of the complexes on their ability to interact with G-quadruplexes.
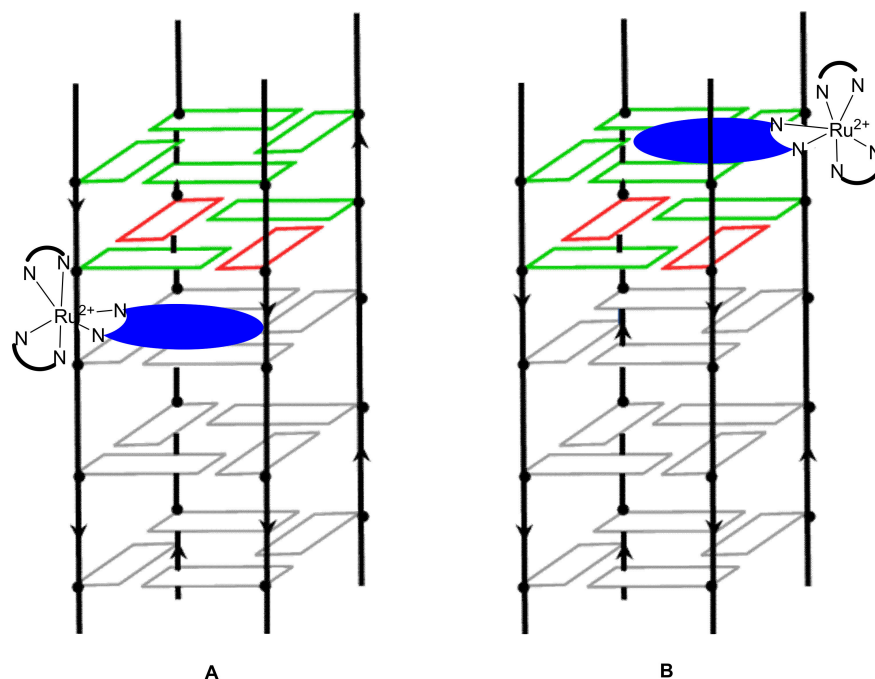
Figure 16. Binding interactions of (**A**)—Λ-[Ru(TAP)$_2$(11-CN-dppz]$^{2+}$ and (**B**)—Λ-[Ru(phen)$_2$(11-CN-dppz]$^{2+}$ with parallel tetramolecular G-quadruplex d(TAGGGTTA) using X-ray crystallography as proposed by McQuaid et al. [200] where adenine, guanine and thymine are colored in red, grey, and green, respectively and the 11-CN-dppz ligand is colored in blue.

A few articles illustrate the impact of small structural changes on the binding affinity and sensing ability of various complexes in presence of various structures of G-quadruplexes [201–205]. However, despite showing drastic differences in the emission profile of the complexes in function of their structure and the type of G-quadruplexes they bind to, the lack of systematic study with thorough structural investigation does not allow the establishment of a systematic structure–activity relationship.

Some complexes containing two dppz ligands have also been investigated ([Ru(**NMe-bpy**)(**dppz**)$_2$]$^{4+}$, [Ru(**NEt-bpy**)(**dppz**)$_2$]$^{4+}$, [Ru(**βAla-bpy-CONH$_2$**)(**dppz**)$_2$]$^{2+}$ and [Ru(**Arg-bpy**)(**dppz**)$_2$]$^{2+}$) (Figure 17) [206,207] but no drastic differences other than a slightly higher affinity to the G-quadruplexes can be noticed from the complexes containing only a single dppz ligand. However, the introduction of a peptide sequence (L-octaarginine) on the complex changes its selectivity between different G-quadruplex structures.
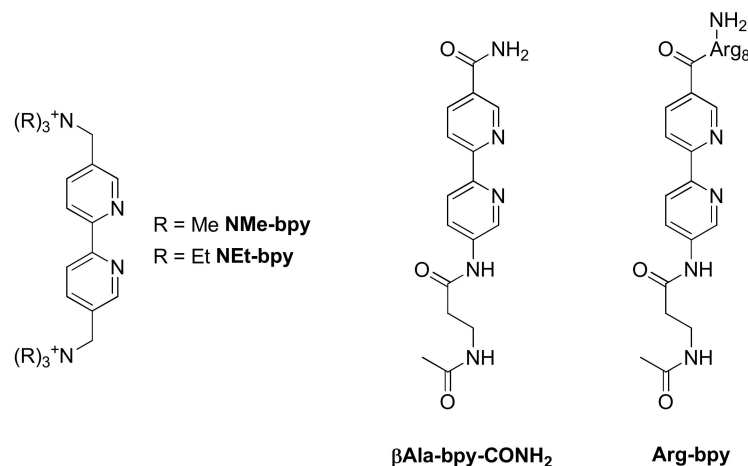
Figure 17. Structure of ancillary ligands used with dppz-containing ruthenium(II) complexes.

Incorporating methyl groups at positions 3 and 6 of the dppz ligand alters the well-studied [Ru(bpy)$_2$(**dppz**)]$^{2+}$ into a dual photochemical "light-switch" and DNA damaging agent [208]. The new complex, [Ru(bpy)$_2$(**dmdppz**)]$^{2+}$ (dmdppz = 3,6-dimethyl-dipyridophenazine) (Figure 15), undergoes photo-induced ligand ejection in organic solvents and upon interaction with duplex and G-quadruplex DNA, consequently generating a ligand-deficient and reactive metal center which then leads to covalent metalation of DNA. The photo-ejection is confirmed by a redshift in the absorption spectra and decreased extinction coefficient, with a selective ligand ejection since only the dmdppz ligand is ejected.

A small structural change by adding a bromine atom at position 11 (**11-Br-dmdppz**) (Figure 15) enhances the G-quadruplex selectivity while maintaining the ligand ejection phenomenon [205]. However, these strained complexes, [Ru(bpy)$_2$(**dmdppz**)]$^{2+}$ and [Ru(bpy)$_2$ (**11-Br-dmdppz**)]$^{2+}$, are more likely to interact with one side of hybrid G-quadruplex structures by binding through an end-capping mode on the lateral loop end due to the distorted planar dppz ligand.

Another structural change on the dppz ligand by incorporating a flexible chain generates a new complex [Ru(bpy)$_2$(**10-pe-dppz**)]$^{2+}$ (10-pe-dppz = 10-(2-(piperidin-1-yl)ethoxy) dipyrido[3,2-*a*:2′,3′-*c*]phenazine) (Figure 15), displaying a great ability to stabilize the G-quadruplex conformation in the K$^+$ medium by interacting through the stacking mode on the G-tetrads [209]. Further studies, through polymerase chain reaction (PCR) stop and telomerase repeat amplification protocol (TRAP) assays, show the potential use of this ruthenium(II) complex as a telomerase inhibitor with no acute cytotoxicity at the same time with an IC$_{50}$ value of 38.8 μM.

3.1.2. Ruthenium(II) Complexes Bearing a π-Extended Ligand

In view of designing new ruthenium(II) complexes as probes for G-quadruplexes, researchers started extending the conjugated system of the aforementioned dppz ligand. A series of complexes containing the **dppzi** (= dipyrido[3,2-*a*:2′,3′-*c*]phenazine-10,11-imidazole) (Figure 18) ligand were therefore reported by Shi et al. [210,211]. Similar to [Ru(phen)$_2$(**dppz**)]$^{2+}$, [Ru(bpy)$_2$(**dppzi**)]$^{2+}$ shows a preferred interaction with G-quadruplexes relative to i-motif. Additionally, this complex binds preferentially to the mixed-hybrid G-quadruplex rather than the antiparallel basket-type conformation, which is consistent with the higher stabilizing effect observed in the K$^+$ buffer [210]. The greater binding affinity towards the mixed-hybrid G-quadruplex over that towards antiparallel G-quadruplex seems to follow the same trend as what was observed with the other studied [Ru(L)$_2$(**dppzi**)]$^{2+}$ complexes (L stands either for phen or dmp = 2,9-dimethyl-1,10-phenanthroline) [196]. Further studies revealed the effect of the ancillary ligands on the spectral properties of the complex upon interaction with G-quadruplexes. [Ru(phen)$_2$(**dppzi**)]$^{2+}$ is emissive in the absence and presence of G-quadruplexes, whereas adding the -CH$_3$ substituent on the ancillary phen ligands results in no luminescence at all for [Ru(dmp)$_2$(**dppzi**)]$^{2+}$, regardless of the considered experimental conditions [196]. Surprisingly, however, [Ru(bpy)$_2$(**dppzi**)]$^{2+}$ displays a so-called reversible "light-switch" behavior that can be regulated by the competition of [Fe(CN)$_6$]$^{4-}$ ions and G-quadruplex DNA. In fact, upon the addition of G-quadruplexes, the emission intensity of [Ru(bpy)$_2$(**dppzi**)]$^{2+}$ is enhanced by about 2.5 while the luminescence is completely quenched upon the addition of [Fe(CN)$_6$]$^{4-}$ ions in the absence of G-quadruplex DNA. The luminescence can be restored by adding an excess of G-quadruplexes to the system containing both the G4-bound complex and [Fe(CN)$_6$]$^{4-}$ ions [210].
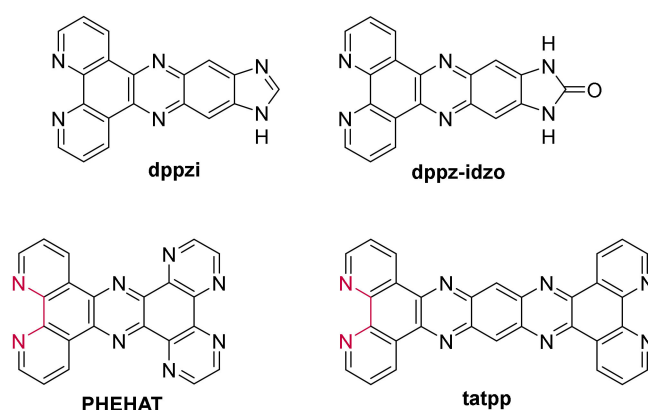
Figure 18. Structure of the π-extended symmetrical ligands form ruthenium(II) complexes studied in presence of G-quadruplexes.

On the contrary, the ancillary ligands do not have any effect regarding the binding modes of each complex with G4-quadruplexes, namely stacking on the center between the parallel loop and the terminal G-quartet in Na^+ buffer and π-stacking on the terminal G-quartets in K^+ buffer. By adding the -CH_3 substituents, the resulting complex presents more steric hindrance preventing [Ru(dmp)$_2$(**dppzi**)]$^{2+}$ from interacting less efficient with G-quadruplex DNA than the bpy- and phen-analogue complexes [210,211].

As these complexes do not display high emission enhancement upon binding to G-quadruplex DNA, further small structural changes were made by introducing an imidazolone group to the dppz ligand. A noteworthy emission intensity enhancement was observed upon the addition of G-quadruplexes to the [Ru(L)$_2$(**dppz-idzo**)]$^{2+}$ complexes (L = bpy or phen; **dppz-idzo** = dppz-imidazolone (Figure 18)) in K^+ medium [212,213]. Interestingly though, [Ru(phen)$_2$(**dppz-idzo**)]$^{2+}$ displays a pH-controlled light-switch effect while being in the presence of G-quadruplexes. In the acidic pH region below 1.4, the complex shows no luminescence, whereas the addition of OH^- ions and adjusting the pH to 4.5 restores the emission [212]. This reversible light-switch effect can be explained by the dissociation of the G-quadruplex to random-coil single-stranded DNA (ssDNA) at pH 1.4, the complex being not bound anymore to this random-coil structure and thus not protected from a water environment.

Further studies explored the binding behaviors of the Δ and Λ enantiomers of [Ru(bpy)$_2$ (**dppz-idzo**)]$^{2+}$ with G-quadruplexes [195]. Reminiscent of the parent Λ-[Ru(bpy)$_2$(**dppz**)]$^{2+}$ enantiomer, Λ-[Ru(bpy)$_2$(**dppz-idzo**)]$^{2+}$ shows a stronger binding affinity with antiparallel G-quadruplex than the Δ enantiomer, which marks a great difference compared to double-stranded DNA binding. However, no chiral selectivity towards hybrid or antiparallel G-quadruplex structures was observed for the Δ and Λ isomers. Both isomers bind to G-quadruplexes by π-π stacking interactions, with a supplementary binding mode through groove binding for the Λ isomer.

More recently, Shi et al. investigated the influence of multiple factors, such as tail and loop length, linkers, and ionic concentration, on the enantioselectivity of these isomers towards the G-quadruplex structures [214]. As expected, cation concentration (K^+ or Na^+) influences the enantioselectivity, which is the most notable at a low concentration. Nonetheless, no remarkable chiral selectivity was observed otherwise except that the initial enantioselectivity disappears or weakens with the increasing length of TTA loops.

Simultaneously, complexes bearing an even more extended conjugated system were investigated [192]. Moucheron et al. focused their interest on a Ru(II) compound containing the planar DNA intercalating **PHEHAT** (=1,10-phenanthrolino[5,6-*b*]1,4,5,8,9,12-hexaatriphenylene) ligand (Figure 18). In the presence of G-quadruplexes, this complex also displays "light-switch ON" properties and concomitantly induces a high stabilization of G4s, with a preference towards the hybrid conformation. Furthermore, under these conditions, [Ru(phen)$_2$(**PHEHAT**)]$^{2+}$ shows a large selectivity towards G4 structures over duplex structures, as confirmed by competitive

experiments. Molecular modelling of the binding of [Ru(phen)$_2$(**PHEHAT**)]$^{2+}$ to hybrid G4s gave further insight into the G4 vs duplex selectivity, showing that the G4 selectivity is due to the interaction with loops as well as the π-interaction between the adenine bases and the PHEHAT ligand [192].

Besides a high affinity of 10^6 M^{-1}, no further systematic study was conducted for [Ru(phen)$_2$(**tatpp**)]$^{2+}$ (tatpp = tetraazapyridopentacene) (Figure 18) bearing an even larger intercalative ligand than PHEHAT to provide fundamental insights into the interaction of the ruthenium(II) complex with the G4 scaffold [215].

While the foregoing ruthenium(II) polypyridyl complexes carried symmetrical planar extended ligands, the following paragraphs will be discussing the interaction of ruthenium compounds based on an elbow-shaped or non-symmetrical planar ligand with G-quadruplexes. These compounds were designed to improve the G4 vs duplex selectivity since most of the reported G-quadruplex ligands bind by π-stacking on the external G-quartets, whereas only a few can interact with grooves/loops and G-quartets simultaneously.

Further structural changes were consequently made on the [Ru(L)$_2$(**dppz**)]$^{2+}$ compounds by incorporating an indoloquinoline moiety [147,216], part of the alkaloid group, already discussed and reported as efficient G-quadruplex ligands. The resulting complexes efficiently stabilize the G-quadruplex structures and show moderate (~10^5 M^{-1}) [147] to high (~10^7 M^{-1}) [216] binding constants through binding by the characteristic π-π stacking interaction. Interestingly, [Ru(phen)$_2$(**mitatp**)]$^{2+}$ (**mitatp** = 5-methoxy-isatino[1,2-*b*]-1,4,8,9-tetraazaphenylene) (Figure 19) can induce the formation of a parallel G-quadruplex structure [147], hitherto rarely reported, as most ruthenium(II) polypyridyl complexes convert the human telomeric sequence into an antiparallel or hybrid conformation. On another note, the absence of a methoxy group generates a complex with a higher binding constant and provides the ability to discriminate between different G-quadruplex structures [216].

Liao et al. eventually incorporated a flexible chain on the mitatp ligand to design a new complex, namely [Ru(bpy)$_2$(**pemitatp**)]$^{2+}$ (**pemitatp** = 5-methoxy-1-(2-(piperidin-1-yl)ethyl)-isatino[1,2-*b*]-1,4,8,9-tetraazatriphenylene) (Figure 19), capable of effectively affecting the activity of the telomerase and stabilizing G-quadruplexes [209]. Similar to the structurally similar complex [Ru(bpy)$_2$(**10-pe-dppz**)]$^{2+}$, this compound shows no acute cytotoxicity at concentrations up to 3 μM, with an IC$_{50}$ of 39.7 μM.

To improve the G4 binding ability and selectivity to a greater extent, the Moucheron and Demeunynck groups designed a new series of complexes with a π-extended acridine-derived ligand (Figure 19) [217,218]. The G4 interaction of those elbow-shaped ruthenium(II) complexes was assessed by fluorescence resonance energy transfer (FRET)-melting assays against an array of quadruplex-forming DNA and RNA sequences and a duplex DNA sequence. These studies revealed that the complexes stabilize both DNA and RNA G-quadruplexes. Furthermore, they can discriminate between quadruplex and duplex sequences as demonstrated by competitive experiments. Their selectivity towards G-quadruplexes over duplexes is partly attributed to the acridine moiety of the π-extended ligands [218], thus allowing more favorable π-stacking interactions between the ligand and the G-quadruplexes, already reported by Neidle [219,220]. Further FRET-melting experiments showed that beyond the interaction with the external quartets, these complexes also interact with the loops [218].
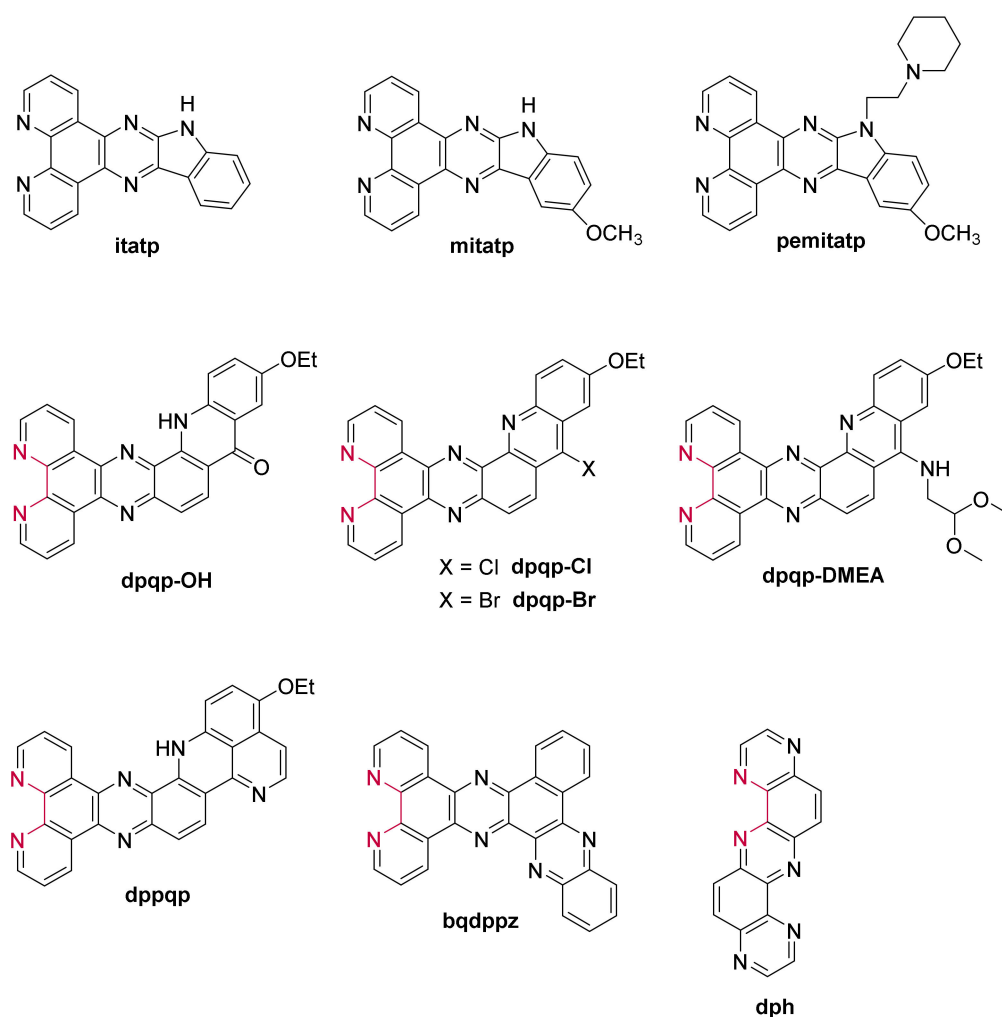
Figure 19. Structure of the π-extended non-symmetrical ligands to form ruthenium(II) complexes studied in presence of G-quadruplexes.

Additionally, the complexes bearing a halide substituent on the acridine moiety, [Ru(phen)$_2$(**dpqp-Cl**)]$^{2+}$ and [Ru(bpy)$_2$(**dpqp-Br**)]$^{2+}$ (dpqp = dipyrido[3,2-*a*:2′,3′-*c*]quinolino[3,2-*h*]phenazine), display remarkable spectroscopic properties upon interaction with nucleic acids, which make them very interesting light-up probes. They show little to no luminescence at all in aqueous solution and moderate luminescence with duplexes, while there's a remarkable luminescence enhancement (up to 330) in the presence of G-quadruplexes. The combined studies also showed that they are efficient at labelling G-quadruplex structures even against an excess of duplex DNA in two orders of magnitude higher concentrations. Following the particular light-up properties of the acridine derived ruthenium(II) complexes, the most promising complex, [Ru(bpy)$_2$(**dpqp-Br**)]$^{2+}$ was further assessed through preliminary cellular luminescent labelling studies by incubation of melanoma B16F10 cells [218]. Confocal images of the cancer cells gave insights into the main labelling sites, the nucleoli, and diffuse perinuclear cytoplasmic foci. These results are evocative of previously reported quadruplex-selective smart probes [221,222], suggesting that the complex primarily labels RNA G-quadruplexes, rooted in the nucleolus and cytoplasmic assemblies of ribonucleoprotein particles [218].

Another ruthenium complex based on the non-symmetrical ligand **bqdppz** (= benzo[*j*]quinoxalino[2,3-*h*]dipyrido[3,2-*a*:2′,3′-*c*]phenazine) (Figure 19) [223,224] was investigated and revealed a remarkable luminescent enhancement towards hybrid G-quadruplex as opposed to the antiparallel structure. Due to the steric hindrance gener-

ated by the loops, end-stacking on hybrid G-quadruplexes is more favorable, which allows a preferential stabilization of this hybrid structure.

Recently, Elias et al. designed a ruthenium(II) complex incorporating a new planar-extended ligand, based on a pyrazino core, the **dph** (= dipyrazino[2,3-*a*:2′,3′-*h*]phenazine) (Figure 19) [225]. A combined analysis of the spectroscopic properties, computational data, and Surface Plasmon Resonance (SPR) experiments showed that this complex exhibits a higher affinity and specificity towards G-quadruplexes than double-stranded DNA (4.8×10^4 M^{-1} vs 1.3×10^3 M^{-1}). Despite displaying two binding modes, mainly the π-stacking interaction between the dph ligand and guanines from the G-quartet with minor contribution by insertion into the groove, the binding affinity for G-quadruplexes remains lower than the previously reported ruthenium(II) complexes.
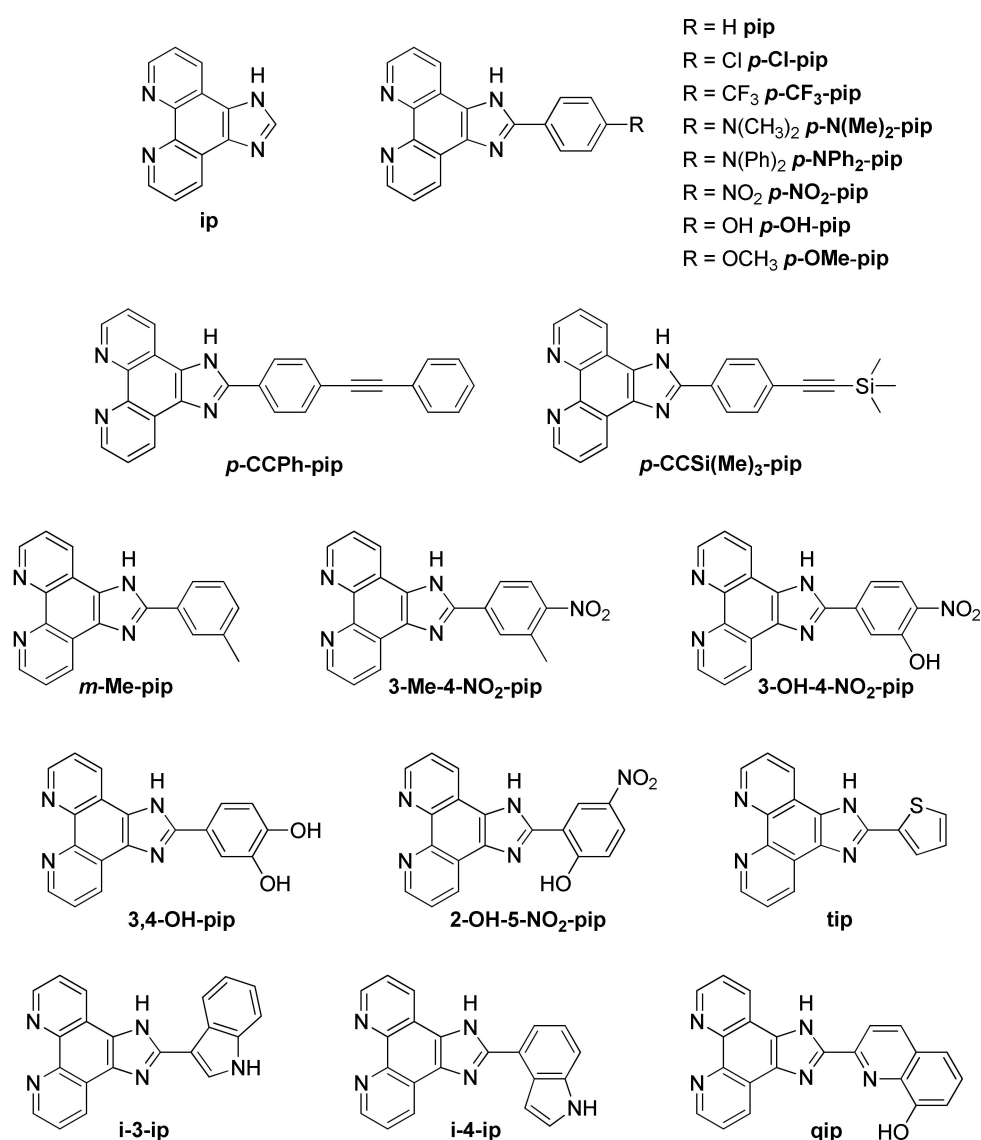
3.1.3. Ruthenium(II) Complexes Bearing Imidazo-Phenanthroline Ligands

Besides the studies involving ruthenium(II) complexes based on an extended planar ligand, other researches focused on complexes bearing a smaller moiety, the imidazo-phenanthroline. The structure of all the imidazo-phenanthroline derivatives used as ligand to form ruthenium(II) complexes studied in the presence of G-quadruplexes are presented in Figure 20.

Contrary to complexes containing a dppz-based ligand, complexes bearing an imidazo-phenanthroline ligand are luminescent in water. They consequently do not show a light-switch ON effect in the presence of DNA. Nevertheless, their luminescence still increases to various extents in presence of different DNA structures, which allows one to assess their interaction with G-quadruplexes. These complexes do show a stronger affinity towards G-quadruplexes over double-stranded DNA [226–236]. The small variations on the structure of the ligands does influence the binding constant of the complex with G-quadruplexes which goes from 10^4 M^{-1} for less efficient binders ([Ru(bpy)$_2$(**i-3-ip**)]$^{2+}$) [235] to almost 10^7 M^{-1} for complexes with high affinity ([Ru(phen)$_2$(***p*-OMe-pip**)]$^{2+}$, [Ru(phen)$_2$(***p*-OH-pip**)]$^{2+}$ or [Ru(phen)$_2$(***p*-NPh$_2$-pip**)]$^{2+}$) [227,228,233]. It was shown that imidazo-phen-based complexes bearing phen ancillary ligands have a stronger affinity for G-quadruplexes than complexes with bpy ligands [226,229,230,234,237,238]. This is due to the higher hydrophobicity of phen ligands which enhances the interaction of the corresponding complexes in the grooves and loops of G-quadruplexes. The Λ-enantiomer does also show a higher binding affinity due to a more favorable interaction geometry with G-quadruplexes [227,228,231,235]. Two studies led by Liu et al. also show that having more than one imidazo-phen-based ligand does not lead to higher affinities of the complex with the G-quadruplexes as seen for [Ru(**ip**)$_3$]$^{2+}$, [Ru(**ip**)$_2$(**pip**)]$^{2+}$, [Ru(**ip**)(**pip**)$_2$]$^{2+}$ and [Ru(**pip**)$_3$]$^{2+}$ whose binding constant are 1.05×10^6 M^{-1}, 1.03×10^6 M^{-1}, 2.5×10^5 M^{-1} and 4.7×10^5 M^{-1}, respectively [239,240].

Since these complexes do not show the light-switch ON effect desired for the design of molecular probes, they have not been studied for this kind of application. Instead, the main interest of imidazo-phen-containing complexes is their use as potential drugs for the inhibition of telomerase activity and potential agents for cancer treatment which is discussed below.

Recently, a few complexes containing a nitro group have been studied ([Ru(L)$_2$(**3-OH-4-NO$_2$-pip**)]$^{2+}$, [Ru(L)$_2$(**2-OH-5NO$_2$-pip**)]$^{2+}$, [Ru(bpy)$_2$(***p*-NO$_2$-pip**)]$^{2+}$ and [Ru(bpy)$_2$(**3-Me-4-NO$_2$-pip**)]$^{2+}$ with L = bpy or phen) [237,238,241]. These complexes show the same light-switch ON property as dppz-containing complexes and are selective towards G-quadruplex structures over double- or single-stranded DNA. This light-switch ON effect can be attributed to the highly stabilizing hydrogen bonding between water and the nitro group which is prevented when the complex interacts with G-quadruplexes.

Figure 20. Structure of the imidazo-phenanthroline (ip) ligands and other closely related complexes used to form ruthenium(II) complexes studied in presence of G-quadruplexes.

The ability of these complexes to inhibit the action of the telomerase enzyme is mainly monitored through PCR-stop (Polymerase Chain Reaction) and TRAP (Telomerase Repeated Amplification Protocol) assays. As all the ruthenium(II) complexes containing an imidazo-phenanthroline derivative as ligand do show some binding affinity towards G-quadruplexes, they all tend to inhibit the replication of this DNA strand to some extent. However, their efficiency as potential anti-cancer drug is directly linked to their affinity for G-quadruplexes. In vitro studies to assess the cytotoxicity of these complexes for different types of cancerous cells show that depending on the type of cancerous cells, the IC_{50} value of these ruthenium(II) complexes goes from around 10 µM to a few hundred µM [226,229,232,234,235,237,239], with some complexes showing an IC_{50} comparable to that of Cisplatin as, for example, $[Ru(\textbf{ip})_2(\textbf{pip})]^{2+}$ which displays an IC_{50} of 14.4 µM against lung carcinoma epithelial cells (A549), whereas Cisplatin has an IC_{50} of 13.6 µM [237]. The complex $[Ru(phen)_2(\textbf{\textit{p}-CF_3-pip})]^{2+}$ even has an IC_{50} of 16.3 µM against breast cancer cells (MDA-MB-231) which is twice as low as Cisplatin under the same conditions (IC_{50} = 36.1 µM) [229].

Recently, Elias et al. reported a series of complexes based on the *p*-**Cl-pip** (2-(4-chlorophenyl)-1*H*-imidazo[4,5-*f*][1,10]phenanthroline) ligand (Figure 20) [242], aiming

initially at designing new photo-oxidizing complexes by introducing TAP moieties either as ancillary ligands, by modifying the phenanthroline imidazole ligand with TAP leading to the *p*-**Cl-piTAP** (2-(4-chlorophenyl)-1*H*-imidazo[4,5-*f*]pyrazino[2,3-*h*]quinoxaline) ligand (Figure 21) or by combining both methods. The studied complexes show high affinities for G-quadruplexes, namely displaying similar affinities as that reported for BRACO-19 and are selective towards G-quadruplexes. Theoretical calculations predicted two binding modes: π-stacking over external G-tetrads and insertion of the complex into the TTA loop [242]. The high affinity towards G-quadruplexes motivated those authors to evaluate the cell penetration ability of these complexes into U2OS osteosarcoma cells. However, the luminescence in the cells was too weak to be detected by confocal microscopy except in the case of [Ru(phen)$_2$(*p*-**Cl-pip**)]$^{2+}$, which revealed efficient at penetrating the cells, even inside the nucleus, after 24 h of incubation. Additionally, preliminary photo-cytotoxicity experiments were conducted on U2OS osteosarcoma cells. As expected, the [Ru(TAP)$_2$(*p*-**Cl-pip**)]$^{2+}$ complex was revealed to be photo-cytotoxic by inducing 100% cell mortality under irradiation. However, [Ru(phen)$_2$(*p*-**Cl-pip**)]$^{2+}$ exhibited remarkable photo-cytotoxicity as well. Therefore, it seems more likely that this effect might be due to singlet oxygen photosensitization in contrast to the typical type I photoreaction (i.e., photoinduced electron transfer (PET)) expected for TAP complexes. Additionally, this might be the first example of photo-cytotoxic ruthenium(II) complexes that does not involve the inhibition of telomerase activity, as these cancer cells do not express the telomerase enzyme. Nonetheless, further studies are necessary to give deeper insight into their photo-cytotoxicity.
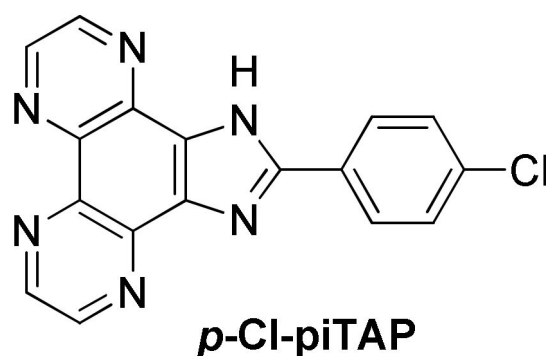
Figure 21. Structure of the imidazo-TAP ligand studied by Elias et al. [242].

A few examples of ruthenium(II) complexes used for their interaction with G-quadruplexes do not fall in the previously discussed categories. The ligands composing these complexes are represented in Figure 22. The complexes containing the **dpq-df** (dipyrido(3,2-*a*:2′,3′-*c*)quinoxaline-difuran) or **bmbbipy** (*N*,*N*′-bis(4-methyl-benzothiazol-2-yl)-2,2′-bypiridine-4,4′-dicarboxyamide) ligands do show a significant light-up effect when put in presence of G-quadruplex DNA [146,243]. The complexes based on the **ptpn** (3-(1,10-phenanthroline-2-yl)-*as*-triazino[5,6-*f*]1,10phenanthroline), **phen-Se** (1,10-phenathrolineselenazole), and **biim** (2,2′-bisimidazole) ligands do not show any significant light-up properties and have thus been studied as potential anti-cancer drugs [244–246]. They show similar binding affinity and cytotoxicity as the previously discussed mononuclear complexes.

Two biologically active molecules (**ASC** (Ascididemin) and **Emodin**) have also been used to form the [Ru(L)$_2$(**ASC**)]$^{2+}$ (L = bpy, phen or dpq) and [Ru(bpy)$_2$(**emodin**)]$^{2+}$ (Figure 23) complexes in order to combine the cytotoxic activity of the free ligands with the high binding affinity of ruthenium(II) complexes towards G-quadruplexes [247,248].
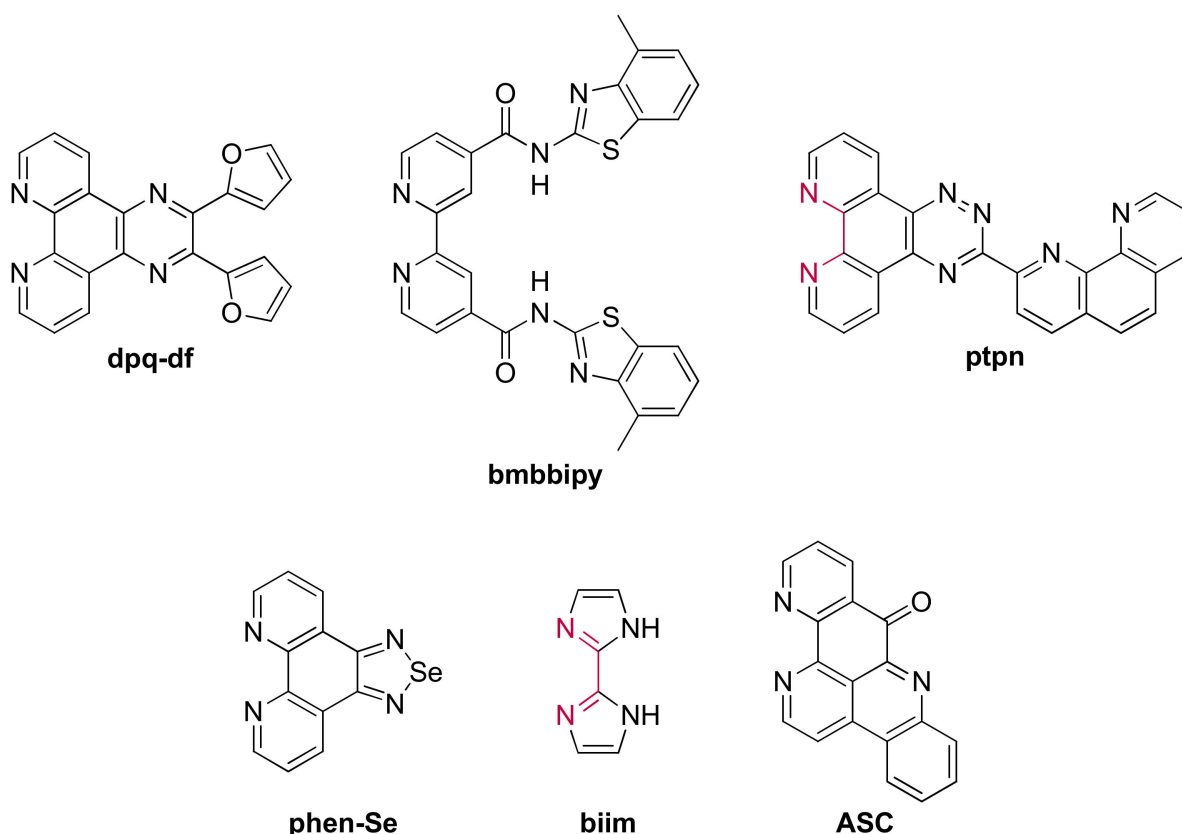
Figure 22. Structure of other types of ligands used to form ruthenium(II) complexes studied in presence of G-quadruplexes.
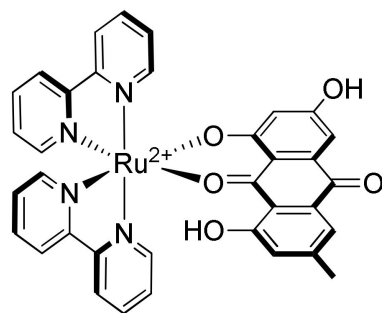
Figure 23. Structure of the [Ru(bpy)$_2$(**emodin**)]$^{2+}$ complex studied by Mei et al. [248].

Three complexes bearing a planar tetradentate ligand composed of two phenanthroline moieties linked by an amine (Figure 24) have been synthesized by Shao et al. [249]. The new geometry obtained with these complexes allowed to obtain a higher selectivity of interaction for G-quadruplexes over double-stranded DNA, with [Ru(NH$_3$)$_2$(**bpa**)]$^{2+}$ (bpa = *N*,*N'*-bis-(1,10-phenanthrolin-2-yl)-amine) showing a binding constant of around 4.5×10^5 M^{-1} towards various G-quadruplexes whereas no binding constant could be determined due to the lack of affinity for double-stranded DNA.

R$_1$ = NH$_3$, R$_2$ = NH$_3$
R$_1$ = NH$_3$, R$_2$ = DMSO
R$_1$ = NH$_2$CH$_3$, R$_2$ = NH$_2$CH$_3$
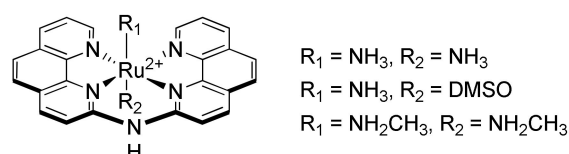
Figure 24. Structure of the complexes using the constrained bpa ligand studied by Shao et al. [249].

The complexes discussed in this section show that the diversity of ligands used to form ruthenium(II) complexes studied for their interaction with G-quadruplexes should not be limited to dppz derivatives.

3.1.4. Ruthenium(II) Complexes Bearing Schiff Base-Type Ligands

Recent advances have revealed the importance of designing more flexible ligands to identify G4 scaffolds over duplex DNA due to favored groove interactions [250,251]. Research in designing new ruthenium(II) complexes carrying a more flexible ligand arose naturally, with the recent example of complexes carrying a Schiff base-type ligand. This type of ligand (Figure 25) was selected because it presents multiple single bonds allowing free rotational movements [252]. Additionally, the salphen moiety found in the **salicyl(pip)-** and **coumarin**-based complexes allows the possible chelation of a second metal center, which will be discussed later in this review.
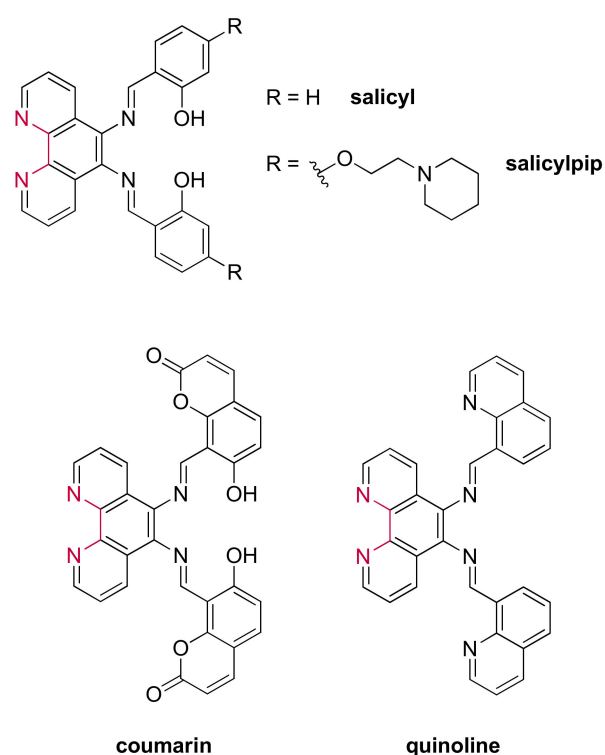

Figure 25. Structure of the Schiff base ligands used to form the ruthenium(II) complexes studied in the presence of G-quadruplexes.

These studies showed that the luminescence of the complexes significantly increases in the presence of genetic material. However, only $[Ru(phen)_2(\textbf{salicyl})]^{2+}$ and $[Ru(phen)_2(\textbf{coumarin})]^{2+}$ revealed to be promising at differentiating between the different DNA structures. Complementary studies by circular dichroism confirmed these results by displaying a more important stabilization effect on G4s relative to duplex DNA; therefore, displaying the selectivity of these complexes towards G-quadruplexes. It appears that the addition of positively charged piperidine chains on the salphen moiety increases the affinity towards G-quadruplexes, allowing a more favorable interaction with the grooves, already reported for the previously mentioned metal salphen complexes. An enhancement of the affinity was also observed with $[Ru(phen)_2(\textbf{coumarin})]^{2+}$ and $[Ru(phen)_2(\textbf{quinoline})]^{2+}$ for which the salicyl moiety has been replaced by a coumarin or quinoline moiety, respectively. This enhancement was attributed to higher π-stacking interactions through the coumarin or quinoline moiety compared to the salicyl part. Nevertheless, the affinity towards G-quadruplexes of these new Schiff base complexes is of

the same order of magnitude when compared to other ruthenium(II) complexes already reported in the literature.

These compounds were evaluated in their ability to penetrate U2OS osteosarcoma cells due to their promising luminescence properties. The studied complexes penetrate the cells but with different intracellular localization (outside and inside the nucleus). Incorporating piperidine fragments leads to an increased ability of the complexes to target the genetic material, which follows the trend of the high affinity of those compounds towards G-quadruplexes. These Schiff base ruthenium(II) compounds were found to be capable of labelling the nucleoli, very dense in nucleic acids. Consequently, the cytotoxicity of these Schiff base compounds was investigated, both in the dark (IC_{50} = 47 to >100 μM) and under irradiation (IC_{50} = 0.33 to 2.1 μM). Under the experimental conditions, the complexes only exhibited very low toxicity in the dark, whereas cell viability was remarkably affected under irradiation. Surprisingly, the presence of the piperidine arms increased the photo-cytotoxicity but also induced slightly higher toxicity in the dark [252].

3.2. Bimetallic and Trimetallic Ruthenium(II) Complexes

The First G-quadruplex "Light-Switch" Ruthenium(II) Complexes

Pioneering work carried out by the Barton group that identified the "light-switch" effect of [Ru(bpy)₂(**dppz**)]²⁺ and [Ru(phen)₂(**dppz**)]²⁺ upon interaction with duplex DNA [253,254], has marked a milestone in the application of ruthenium(II) complexes as probes for genetic material. Following this discovery, Thomas et al. investigated the use of dinuclear Ru(II) complexes as potential G-quadruplex probes in 2006 [255]. These [{Ru(bpy)₂}₂(**tpphz**)]⁴⁺ and [{Ru(phen)₂}₂(**tpphz**)]⁴⁺ complexes incorporate the **tpphz** bridging ligand (Figure 26), with a more extended aromatic ring system than dppz, and therefore structurally reminiscent of some of the aforementioned G4-binding ligands.
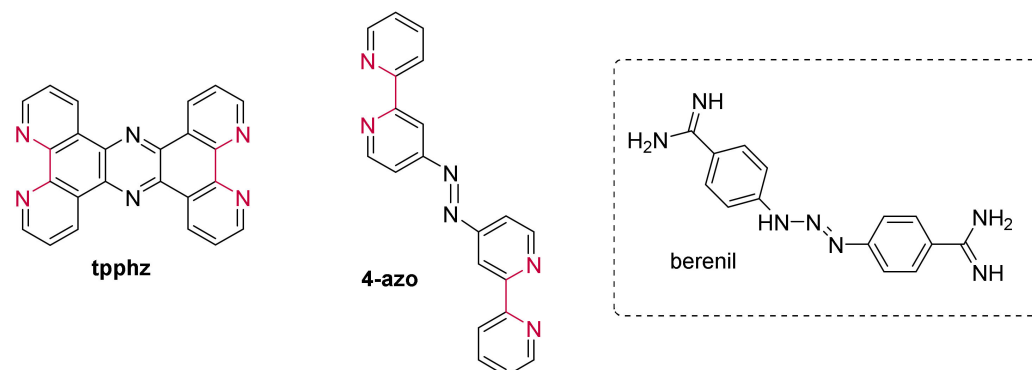
Figure 26. Structure of the tpphz and 4-azo ligands to form the dinuclear ruthenium(II) complexes studied by Thomas et al. in the presence of G-quadruplexes [255–259].

These dinuclear complexes bind to G4 structures with a preference for the antiparallel human telomere sequence over duplex structures. Furthermore, an emission enhancement by ~2.5 times with a more pronounced hypsochromic shift in the presence of G-quadruplexes than observed for duplex DNA was detected [255]. This finding made these complexes the first G-quadruplex "light-switches" at that time, able to differentiate between the interaction with different DNA structures [255,256].

Further studies revealed that chirality also is a relevant factor in the interaction of the investigated complexes with the G-quadruplex structure. A combined analysis of NMR and molecular dynamics simulations demonstrated that the binding affinity of the ΛΛ-[{Ru(phen)₂}₂(**tpphz**)]⁴⁺ is 40 times higher than the ΔΔ isomer (2.95×10^7 M⁻¹ vs 1.16×10^5 M⁻¹). Only the ΛΛ isomer can interact through threading in the diagonal loop while the ΔΔ isomer binds mainly at the lateral loop [257].

Following their light-switch properties, the cytotoxicity of these complexes towards commonly studied cell cultures, such as the MCF-7 human breast cancer cells, were in-

vestigated. Neither of these dinuclear compounds display any cytotoxicity after 24 h of incubation and show an IC_{50} value of 138 μM [258]. However, [{Ru(bpy)$_2$}$_2$(**tpphz**)]$^{4+}$ is only taken up by fixed cells and therefore can act as an indicator of cell mortality. On the other side, the dinuclear [{Ru(phen)$_2$}$_2$(**tpphz**)]$^{4+}$ complex demonstrated a successful penetration into live cells and is located throughout the cell cytosol but found in higher concentrations within the nucleus as well as within heterochromatin. Interestingly, this compound presents two different non-colocalized emission peaks and proves to be an excellent DNA structural probe, functioning to mark duplex and G-quadruplex structures [258].

Shortly afterwards, Thomas et al. investigated the effect of an azo-based tethered ligand on the interaction of ruthenium(II) complexes with G-quadruplexes [259]. The reported compound [{Ru(bpy)$_2$}$_2$(**4-azo**)]$^{4+}$ (**4-azo** = 4,4''-azobis(2,2'-bipyridine) carries a structurally similar ligand to the minor groove binder berenil and displays a colorimetric response of the buffer solution in the presence of G-quadruplexes. Further investigations are still needed to obtain a better comprehension of this phenomenon.

More recently, another dinuclear complex [{Ru(phen)$_2$}$_2$(**PHEHAT**)]$^{4+}$ (Figure 27), based on the π-extended **PHEHAT** bridging ligand, also revealed a "light-switch" behavior in the presence of G-quadruplexes [192]. However, in contrast to its mononuclear analogue mentioned earlier, this complex stabilizes more strongly the antiparallel conformation than the hybrid form of the human telomere sequence. Unfortunately, further studies indicated that this dinuclear complex shows no preference for neither G4 DNA nor duplex DNA despite being considered a good G4 ligand [192].
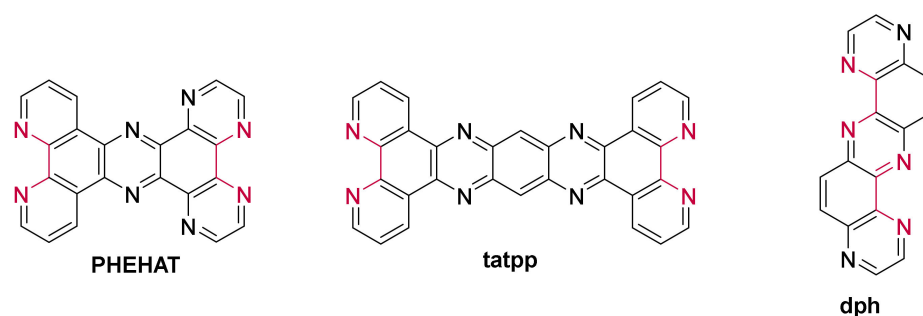

Figure 27. Structure of the π-extended ligands bridging ligands to form dinuclear ruthenium(II) complexes studied in the presence of G-quadruplexes.

A recent publication reported a dinuclear ruthenium complex based on the **tatpp** ligand (Figure 27) [215], which displays the highest affinity (K = 4.2 × 10^7 M^{-1}) for G-quadruplexes reported up to this point for a dinuclear ruthenium compound. Similar to [{Ru(phen)$_2$}$_2$(**tpphz**)]$^{4+}$ [255–257], [{Ru(phen)$_2$}$_2$(**tatpp**)]$^{4+}$ interacts with the G4 scaffold through two binding modes, mainly by end-stacking on the G-tetrads and interaction through the grooves [215]. Through thermodynamic studies, Lewis et al. attributed these two binding modes to the preferential binding of the Λ,Λ-enantiomer over that of the other two isomers.

Due to the two equivalent chelating sites of the previously mentioned **dph** ligand, the dinuclear ruthenium(II) complex (Figure 27) was synthesized and studied in the presence of G-quadruplex structures [225]. Similar to the mononuclear analogue, the dinuclear compound displays a modest binding affinity and selectivity towards G-quadruplexes.

A few dinuclear complexes based on the imidazo-phenanthroline ligand have also been investigated. The structure of the bridging ligands can be found in Figure 28. When compared to the mononuclear ruthenium(II) complexes containing one imidazo-phenanthroline ligand, these dinuclear complexes tend to have a higher binding constant. For example, [{Ru(bpy)$_2$}$_2$(**btip**)]$^{4+}$ and [{Ru(bpy)$_2$}$_2$(**bpip-OH**)]$^{4+}$ have a binding constant of 1.16 × 10^7 M^{-1} and 9.07 × 10^6 M^{-1} towards G-quadruplexes [260,261], whereas their mononuclear counter-parts [Ru(bpy)$_2$(**tip**)]$^{2+}$ and [Ru(phen)$_2$(*p*-**OH-pip**)]$^{2+}$ (Figure 20) have a binding constant of 6.33 × 10^5 M^{-1} and of around 8.5 × 10^6 M^{-1}, respectively [226,228]. While for the phenol containing imidazo-phen,

the increase in the binding constant is not dramatic, for the thiophene-containing complexes the binding constant of the dinuclear complex is twice as high as for the mononuclear complex.
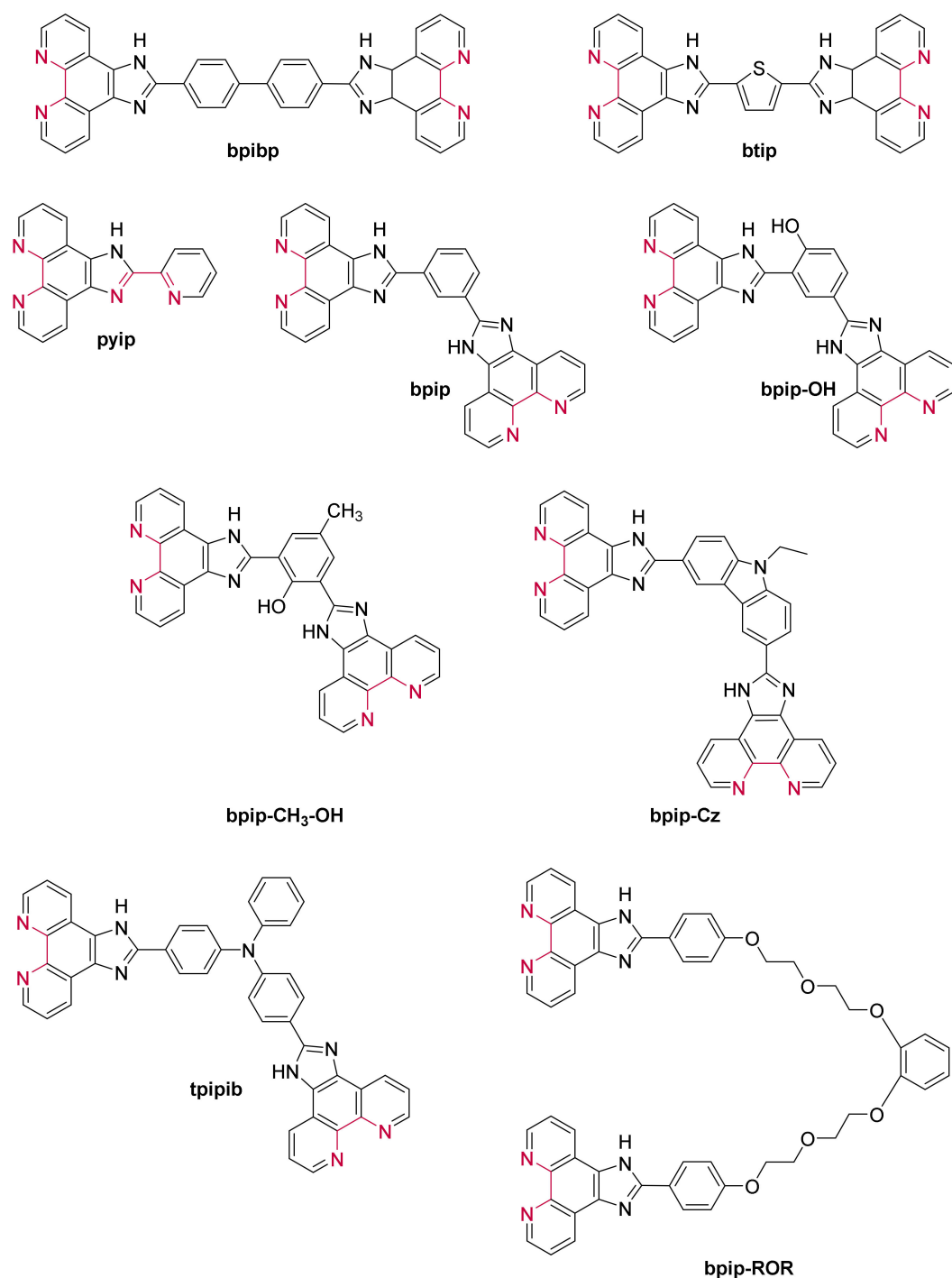
Figure 28. Structure of imidazo-phenanthroline ligands used to form dinuclear ruthenium(II) complexes studied in presence of G-quadruplexes.

The only complex showing significant light-up properties is [{Ru(bpy)$_2$}$_2$(**bpip-ROR**)]$^{4+}$ [262]. This light-up effect is explained by the ability of the noncyclic crown ether linking the two ruthenium(II) chromophores to interact with the K$^+$ cations present in the aqueous buffered solution used, leading to a luminescence quenching. However, when the complex is in presence of G-quadruplexes, its luminescence is restored due to their interaction with the G4 structure, preventing the quenching by the K$^+$ cations. No in-depth study has been carried out on the

interaction of other dinuclear ruthenium(II) complexes bearing a bridging imidazo-phen ligand (**bpibp**, **pyip**, **bpip**, **bpip-CH₃-OH**, **bpip-Cz,** and **tpipib**) with G-quadruplexes, but they have been investigated as potential anti-cancer drugs due to their ability to stabilize G-quadruplex structures [263–265]. Two examples of trinuclear ruthenium(II) complexes ([{Ru(bpy)₂}₃(**tpbip**)]6⁺ and [{Ru(bpy)₂}₃(**tptaip**)]6⁺) (Figure 29) have also been studied for the same purpose [266].

tpbip   tptaip
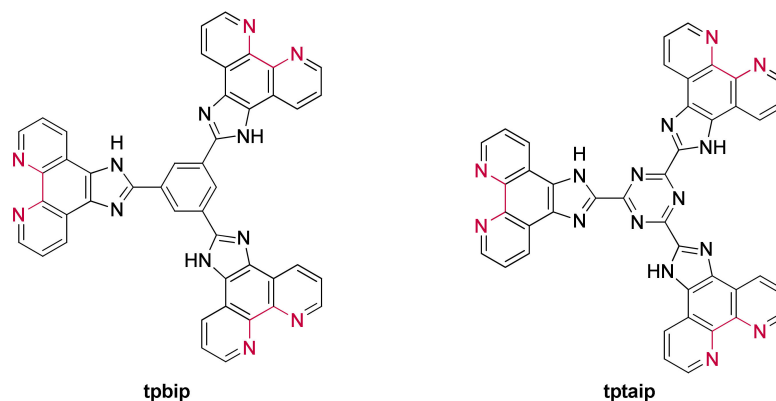
Figure 29. Structure of two bridging imidazo-phenanthroline ligands used to form trinuclear ruthenium(II) complexes studied for their interaction with G-quadruplexes.

In addition to dinuclear ruthenium(II) complexes, some bimetallic compounds were also studied in the presence of G-quadruplexes, such as those carrying a Schiff base-type ligand, previously mentioned (Figure 30) [252]. A second metal center was chelated to the salphen moiety to prevent any free rotation; therefore, leading to the stiffening of the ligand. However, the bimetallic Ru(II)-Ni(II) and Ru(II)-Pd(II) compounds are barely luminescent under the experimental conditions, making them less apt to be exploited in biological assays. Surprisingly, the Ru(II)-Pt(II) complexes exhibit much stronger luminescence alone in the solution. Furthermore, their emission is enhanced and accompanied by a hypsochromic shift once they interacted with the G4 scaffold.

R = H, M = Ni(II) **salicyl-Ni**
R = H, M = Pd(II) **salicyl-Pd**
R = H, M = Pt(II) **salicyl-Pt**
R = (piperidine chain) M = Ni(II) **slaicylpip-Ni**
R = (piperidine chain) M = Pd(II) **slaicylpip-Pd**

coumarin-Ni
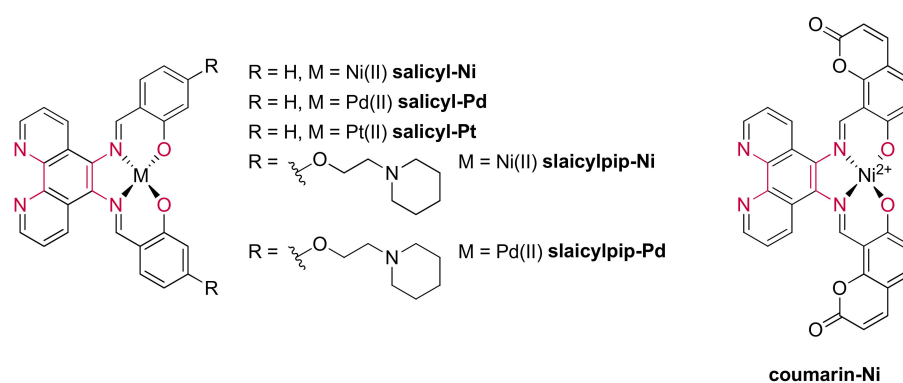
Figure 30. Structure of the Schiff base bridging ligands used to form the bimetallic compounds studied in the presence of G-quadruplexes.

Globally, the stabilization of G-quadruplexes by the bimetallic compounds appeared to be less effective when compared to their monometallic analogues. However, a small increase in stabilization can be observed when piperidine chains are added to the salphen moiety. Adding these piperidine-derived compounds also seems to follow the trend of increasing the affinity of the bimetallic complexes towards G-quadruplexes, similar to their monometallic parent compounds. Additionally, the stiffening of the Schiff base subunit by the addition of the second metal also leads to an upgraded affinity of bimetallic complexes when compared to the monometallic parent compound.

Due to the excellent luminescence properties of the Ru(II)-Pt(II) complexes, in cellulo studies were conducted with U2OS osteosarcoma cells. Similar to their mononuclear parent compounds, the bimetallic complexes can penetrate the cells to locate within the nuclei and show a weak toxicity in the dark (IC_{50} = 33 to >100 μM), but the cell viability was strongly affected under irradiation (IC_{50} = 0.73 to 2.7 μM) [252].

4. Photoreaction of Ruthenium(II) Complexes with G-quadruplexes

Ru(II) complexes carrying at least two π-deficient ligands, such as TAP or HAT (1,4,5,8,9,12-hexaazatriphenylene), are known to initiate a photoinduced electron transfer (PET) from a guanine base to the excited complex [267–271]. This PET can lead to the formation of a covalently linked adduct between the complex and the guanine, for example, as observed with [Ru(TAP)$_2$(phen)]$^{2+}$ (Figure 31) [272]. This photoreaction of ruthenium(II) complexes was also observed in the presence of G-quadruplexes, notably, the first one being with [{Ru(TAP)$_2$}$_2$(**tpac**)]$^{4+}$ (tpac = tetrapyridoacridine) (Figure 31) [273].
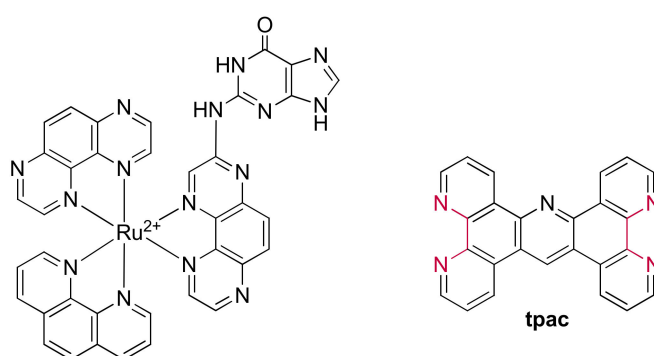
Figure 31. Structure of the photo-adduct of [Ru(TAP)$_2$(phen)]$^{2+}$ with a guanine base. Structure of the tpac bridging ligand used to form the dinuclear photoactive ruthenium(II) complex.

This dinuclear complex, developed within our research group, was shown to be photoreactive and formed covalent adducts with guanine bases of both duplex and G4 DNA. The photoreactivity is mainly due to two factors: a strong interaction with the biomolecule and the independence of each ruthenium center; therefore, allowing each metallic center to keep its excited state properties, which results in the formation of several covalent bonds. After the first photon absorption and the subsequent adduct formation, the newly formed species can absorb a second photon and form a second adduct with another guanine residue, consequently inducing a photocrosslinking between both guanine units. This photocrosslinking is of particular interest since it strongly stabilizes the G4 scaffold and shows significant potential in blocking the telomerase activity. Mass spectrometry also revealed the formation of multiple photo-adducts with G-quadruplexes as well as with duplex DNA, confirming the photocrosslinking phenomenon. However, this dinuclear complex barely shows any selectivity over double-stranded DNA since the binding affinities are of the same order of magnitude (7.6×10^6 M^{-1} and 2.9×10^6 M^{-1} for G-quadruplex and duplex DNA, respectively) [273].

Following this discovery, Thomas et al. developed a dinuclear complex bearing π-deficient ancillary ligands and the structurally similar bridging ligand, **tpphz** (Figure 26) [274]. The TAP analogue of [{Ru(phen)$_2$}$_2$(**tpphz**)]$^{4+}$, namely [{Ru(TAP)$_2$}$_2$(**tpphz**)]$^{4+}$, is capable of promoting photo-oxidation of guanine sites in duplex and G4 DNA. However, the substitution of phen ancillary ligands by the π-deficient TAP ligands results in a lower affinity towards G-quadruplexes than duplexes, namely with a binding constant about an order of magnitude weaker than those set out for duplex binding. In cellulo studies of the photoactive dinuclear tpphz analogue revealed the capacity of this complex to penetrate human C8161 melanoma cells, located primarily in the nuclei. In contrast to [{Ru(phen)$_2$}$_2$(**tpphz**)]$^{4+}$, the TAP derivate also produces bright emission from the cytoplasm after diffusion from the nucleus throughout the cell. Similar to the vast majority of ruthenium(II) complexes, [{Ru(TAP)$_2$}$_2$(**tpphz**)]$^{4+}$ did not show any cytotoxicity

in the dark, whereas it was revealed to be an efficient photosensitizer for PDT as the cell viability dropped to zero after cell irradiation [274].

5. Conclusions

Ruthenium(II) polypyridyl complexes have been widely studied for the last thirty years for their interaction with DNA. However, investigating these complexes to specifically interact with G-quadruplex structures has only started to gain interest in the last fifteen years. These G-quadruplex structures have yet to be fully understood but seem to play an important role as gene expression regulators as well as key targets for potential cancer treatment since they were found in telomeres. In this regard, ruthenium(II) polypyridyl complexes can play a significant role due to their remarkable behavior when interacting with G-quadruplexes. Complexes based on the dppz ligand can act as efficient light-up probes able to selectively localize the position of such G-quadruplexes. Alternatively, other complexes can act as potential anti-cancer drugs either in the dark, by hindering the replication of telomeric sequences leading to the death of tumorous cells, or under light irradiation leading to the formation of reactive oxygen species (ROS) or to the formation of photo-adducts. As shown in this review, the structure and thus the activity of ruthenium(II) complexes can be easily modified, leading to a large array of possible finetuning. However, a deep understanding of the key structural parameters influencing the interaction of these complexes with G-quadruplexes is still lacking. Therefore, the characterization of the interaction geometries of different ruthenium(II) complexes with G-quadruplexes has yet to be determined using advanced techniques such as those exploited for the $[Ru(L)_2(\mathbf{dppz})]^{2+}$ complexes. This should allow the design of new highly selective tools for the recognition, study, and reversible or irreversible marking of G-quadruplexes, which might lead to exciting discoveries in biomedical sciences.

References

1. Watson, J.D.; Crick, F.H.C. Molecular Structure of Nucleic Acids: A Structure for Deoxyribose Nucleic Acid. *Nature* **1953**, *171*, 737–738. [CrossRef] [PubMed]
2. Gehring, K.; Leroy, J.-L.; Guéron, M. A tetrameric DNA structure with protonated cytosine-cytosine base pairs. *Nature* **1993**, *363*, 561–565. [CrossRef]
3. Phan, A.T.; Mergny, J.-L. Human telomeric DNA: G-quadruplexes, i-motif, and Watson-Crick double helix. *Nucleic Acids Res.* **2002**, *30*, 4618–4625. [CrossRef] [PubMed]
4. Ortiz-Lombardía, M.; González, A.; Eritja, R.; Aymamí, J.; Azorin, F.; Coll, M. Crystal structure of a DNA Holliday junction. *Nat. Genet.* **1999**, *6*, 913–917. [CrossRef]
5. Van Rixel, V.H.S.; Busemann, A.; Wissingh, M.F.; Hopkins, S.L.; Siewert, B.; Van de Griend, C.; Siegler, M.A.; Marzo, T.; Papi, F.; Ferraroni, M.; et al. Induction of a Four-Way Junction Structure in the DNA Palindromic Hexanucleotide 5''-d(CGTACG)-3'' by a Mononuclear Platinum Complex. *Angew. Chem. Int. Ed.* **2019**, *58*, 9378–9382. [CrossRef] [PubMed]
6. Gellert, M.; Lipsett, M.N.; Davies, D.R. Helix formation by guanylic acid. *Proc. Natl. Acad. Sci. USA* **1962**, *48*, 2013–2018. [CrossRef] [PubMed]
7. Zimmerman, S.B.; Cohen, G.H.; Davies, D.R. X-ray fiber diffraction and model-building study of polyguanylic acid and polyinosinic acid. *J. Mol. Biol.* **1975**, *92*, 181–192. [CrossRef]

8. Arnott, S.; Chandrasekaran, R.; Marttila, C.M. Structures for polyinosinic acid and polyguanylic acid. *Biochem. J.* **1974**, *141*, 537–543. [CrossRef]
9. Howard, F.B.; Frazier, J.; Miles, H.T. Stable and metastable forms of poly(G). *Biopolymers* **1977**, *16*, 791–809. [CrossRef]
10. Rhodes, D.; Lipps, H.J. G-quadruplexes and their regulatory roles in biology. *Nucleic Acids Res.* **2015**, *43*, 8627–8637. [CrossRef]
11. Kendrick, S.; Hurley, L.H. The Role of G-quadruplex/i-Motif Secondary Structures as Cis-Acting Regulatory Elements. *Pure Appl. Chem.* **2010**, *82*, 1609–1621. [CrossRef]
12. Wright, W.E.; Tesmer, V.M.; Huffman, K.E.; Levene, S.D.; Shay, J.W. Normal human chromosomes have long G-rich telomeric overhangs at one end. *Genes Dev.* **1997**, *11*, 2801–2809. [CrossRef]
13. Sfeir, A.J.; Chai, W.; Shay, J.W.; Wright, W.E. Telomere-End Processing the Terminal Nucleotides of Human Chromosomes. *Mol. Cell* **2005**, *18*, 131–138. [CrossRef]
14. Monchaud, D.; Teulade-Fichou, M.-P. A hitchhiker's guide to G-quadruplex ligands. *Org. Biomol. Chem.* **2007**, *6*, 627–636. [CrossRef]
15. De Cian, A.; Lacroix, L.; Douarre, C.; Temime-Smaali, N.; Trentesaux, C.; Riou, J.-F.; Mergny, J.-L. Targeting telomeres and telomerase. *Biochimie* **2008**, *90*, 131–155. [CrossRef]
16. Zhang, S.; Wu, Y.; Zhang, W. G-quadruplex Structures and Their Interaction Diversity with Ligands. *ChemMedChem* **2014**, *9*, 899–911. [CrossRef]
17. Chambers, V.S.; Marsico, G.; Boutell, J.M.; Di Antonio, M.; Smith, G.P.; Balasubramanian, S. High-throughput sequencing of DNA G-quadruplex structures in the human genome. *Nat. Biotechnol.* **2015**, *33*, 877–881. [CrossRef]
18. Huppert, J.L.; Balasubramanian, S. Prevalence of Quadruplexes in the Human Genome. *Nucleic Acids Res.* **2005**, *33*, 2908–2916. [CrossRef]
19. Todd, A.K.; Johnston, M.; Neidle, S. Highly prevalent putative quadruplex sequence motifs in human DNA. *Nucleic Acids Res.* **2005**, *33*, 2901–2907. [CrossRef]
20. Ou, T.-M.; Lu, Y.-J.; Tan, J.-H.; Huang, Z.-S.; Wong, K.-Y.; Gu, L.-Q. G-quadruplexes: Targets in Anticancer Drug Design. *ChemMedChem* **2008**, *3*, 690–713. [CrossRef]
21. Davis, J.T. G-Quartets 40 Years Later: From 5′-GMP to Molecular Biology and Supramolecular Chemistry. *Angew. Chem. Int. Ed.* **2004**, *43*, 668–698. [CrossRef] [PubMed]
22. Burge, S.; Parkinson, G.N.; Hazel, P.; Todd, A.K.; Neidle, S. Quadruplex DNA: Sequence, topology and structure. *Nucleic Acids Res.* **2006**, *34*, 5402–5415. [CrossRef] [PubMed]
23. Patel, D.J.; Phan, A.T.; Kuryavyi, V. Human telomere, oncogenic promoter and 5′-UTR G-quadruplexes: Diverse higher order DNA and RNA targets for cancer therapeutics. *Nucleic Acids Res.* **2007**, *35*, 7429–7455. [CrossRef] [PubMed]
24. Parkinson, G.N.; Lee, M.P.H.; Neidle, S. Crystal structure of parallel quadruplexes from human telomeric DNA. *Nature* **2002**, *417*, 876–880. [CrossRef] [PubMed]
25. Phan, A.T.; Patel, D.J. Two-Repeat Human Telomeric d(TAGGGTTAGGGT) Sequence Forms Interconverting Parallel and Antiparallel G-quadruplexes in Solution: Distinct Topologies, Thermodynamic Properties, and Folding/Unfolding Kinetics. *J. Am. Chem. Soc.* **2003**, *125*, 15021–15027. [CrossRef]
26. Phan, A.T.; Modi, Y.S.; Patel, D.J. Two-repeat Tetrahymena Telomeric d(TGGGGTTGGGGT) Sequence Interconverts Between Asymmetric Dimeric G-quadruplexes in Solution. *J. Mol. Biol.* **2004**, *338*, 93–102. [CrossRef]
27. Kettani, A.; Bouaziz, S.; Gorin, A.; Zhao, H.; Jones, R.A.; Patel, D.J. Solution structure of a Na cation stabilized DNA quadruplex containing G·G·G·G and G·C·G·C tetrads formed by G-G-G-C repeats observed in adeno-associated viral DNA. *J. Mol. Biol.* **1998**, *282*, 619–636. [CrossRef] [PubMed]
28. Hazel, P.; Parkinson, G.N.; Neidle, S. Topology Variation and Loop Structural Homology in Crystal and Simulated Structures of a Bimolecular DNA Quadruplex. *J. Am. Chem. Soc.* **2006**, *128*, 5480–5487. [CrossRef]
29. Gill, M.L.; Strobel, S.A.; Loria, J.P. 205Tl NMR Methods for the Characterization of Monovalent Cation Binding to Nucleic Acids. *J. Am. Chem. Soc.* **2005**, *127*, 16723–16732. [CrossRef]
30. Haider, S.; Parkinson, G.N.; Neidle, S. Crystal Structure of the Potassium Form of an Oxytricha nova G-quadruplex. *J. Mol. Biol.* **2002**, *320*, 189–200. [CrossRef]
31. Schultze, P.; Hud, N.V.; Smith, F.W.; Feigon, J. The effect of sodium, potassium and ammonium ions on the conformation of the dimeric quadruplex formed by the Oxytricha nova telomere repeat oligonucleotide d(G4T4G4). *Nucleic Acids Res.* **1999**, *27*, 3018–3028. [CrossRef]
32. Schultze, P.; Smith, F.W.; Feigon, J. Refined solution structure of the dimeric quadruplex formed from the Oxytricha telomeric oligonucleotide d(GGGGTTTTGGGG). *Structure* **1994**, *2*, 221–233. [CrossRef]
33. Smith, F.W.; Feigon, J. Quadruplex structure of Oxytricha telomeric DNA oligonucleotides. *Nature* **1992**, *356*, 164–168. [CrossRef]
34. Phan, A.T.; Kuryavyi, V.; Burge, S.; Neidle, S.; Patel, D.J. Structure of an Unprecedented G-quadruplex Scaffold in the Human c-kit Promoter. *J. Am. Chem. Soc.* **2007**, *129*, 4386–4392. [CrossRef]
35. Olsen, C.M.; Gmeiner, W.H.; Marky, L.A. Unfolding of G-quadruplexes: Energetic, and Ion and Water Contributions of G-Quartet Stacking. *J. Phys. Chem. B* **2006**, *110*, 6962–6969. [CrossRef]
36. Marathias, V.M.; Bolton, P.H. Determinants of DNA Quadruplex Structural Type: Sequence and Potassium Binding. *Biochemistry* **1999**, *38*, 4355–4364. [CrossRef]

37. Risitano, A.; Fox, K.R. Inosine substitutions demonstrate that intramolecular DNA quadruplexes adopt different conformations in the presence of sodium and potassium. *Bioorg. Med. Chem. Lett.* **2005**, *15*, 2047–2050. [CrossRef]

38. Rujan, I.N.; Meleney, J.C.; Bolton, P.H. Vertebrate Telomere Repeat DNAs Favor External Loop Propeller Quadruplex Structures in the Presence of High Concentrations of Potassium. *Nucleic Acids Res.* **2005**, *33*, 2022–2031. [CrossRef]

39. Ying, L.; Green, J.J.; Li, H.; Klenerman, D.; Balasubramanian, S. Studies on the structure and dynamics of the human telomeric G quadruplex by single-molecule fluorescence resonance energy transfer. *Proc. Natl. Acad. Sci. USA* **2003**, *100*, 14629–14634. [CrossRef]

40. Lee, J.Y.; Okumus, B.; Kim, D.S.; Ha, T. Extreme conformational diversity in human telomeric DNA. *Proc. Natl. Acad. Sci. USA* **2005**, *102*, 18938–18943. [CrossRef]

41. Zhang, N.; Phan, A.T.; Patel, D.J. (3 + 1) Assembly of Three Human Telomeric Repeats into an Asymmetric Dimeric G-quadruplex. *J. Am. Chem. Soc.* **2005**, *127*, 17277–17285. [CrossRef] [PubMed]

42. Wang, Y.; Patel, D.J. Solution structure of the human telomeric repeat d[AG$_3$(T$_2$AG$_3$)$_3$] G-tetraplex. *Structure* **1993**, *1*, 263–282. [CrossRef]

43. Balagurumoorthy, P.; Brahmachari, S. Structure and stability of human telomeric sequence. *J. Biol. Chem.* **1994**, *269*, 21858–21869. [CrossRef]

44. Li, J.; Correia, J.J.; Wang, L.; Trent, J.O.; Chaires, J.B. Not so Crystal Clear: The Structure of the Human Telomere G-quadruplex in Solution Differs from That Present in a Crystal. *Nucleic Acids Res.* **2005**, *33*, 4649–4659. [CrossRef] [PubMed]

45. Chang, C.-C.; Chu, J.-F.; Kao, F.-J.; Chiu, Y.-C.; Lou, P.-J.; Chen, H.-C.; Chang, T.-C. Verification of Antiparallel G-quadruplex Structure in Human Telomeres by Using Two-Photon Excitation Fluorescence Lifetime Imaging Microscopy of the 3,6-Bis(1-methyl-4-vinylpyridinium)carbazole Diiodide Molecule. *Anal. Chem.* **2006**, *78*, 2810–2815. [CrossRef] [PubMed]

46. Hazel, P.; Huppert, J.; Balasubramanian, S.; Neidle, S. Loop-Length-Dependent Folding of G-quadruplexes. *J. Am. Chem. Soc.* **2004**, *126*, 16405–16415. [CrossRef] [PubMed]

47. Blackburn, E.H. Structure and function of telomeres. *Nature* **1991**, *350*, 569–573. [CrossRef]

48. Kim, N.W.; Piatyszek, M.A.; Prowse, K.R.; Harley, C.B.; West, M.D.; Ho, P.D.L.; Coviello, G.M.; Wright, W.E.; Weinrich, S.L.; Shay, J.W. Specific association of human telomerase activity with immortal cells and cancer. *Science* **1994**, *266*, 2011–2015. [CrossRef]

49. Moyzis, R.K.; Buckingham, J.M.; Cram, L.S.; Dani, M.; Deaven, L.L.; Jones, M.D.; Meyne, J.; Ratliff, R.L.; Wu, J.R. A highly conserved repetitive DNA sequence, (TTAGGG)n, present at the telomeres of human chromosomes. *Proc. Natl. Acad. Sci. USA* **1988**, *85*, 6622–6626. [CrossRef]

50. Blackburn, E.H. Switching and Signaling at the Telomere. *Cell* **2001**, *106*, 661–673. [CrossRef]

51. Stewart, S.A.; Weinberg, R.A. Telomeres: Cancer to Human Aging. *Annu. Rev. Cell Dev. Biol.* **2006**, *22*, 531–557. [CrossRef]

52. D'Adda Di Fagagna, F.; Teo, S.H.; Jackson, S.P. Functional Links between Telomeres and Proteins of the DNA-Damage Response. *Genes Dev.* **2004**, *18*, 1781–1799. [CrossRef]

53. Zaug, A.J.; Podell, E.R.; Cech, T.R. Human POT1 disrupts telomeric G-quadruplexes allowing telomerase extension in vitro. *Proc. Natl. Acad. Sci. USA* **2005**, *102*, 10864–10869. [CrossRef]

54. Denchi, E.L.; De Lange, T. Protection of telomeres through independent control of ATM and ATR by TRF2 and POT1. *Nature* **2007**, *448*, 1068–1071. [CrossRef]

55. Miyoshi, T.; Kanoh, J.; Saito, M.; Ishikawa, F. Fission Yeast Pot1-Tpp1 Protects Telomeres and Regulates Telomere Length. *Science* **2008**, *320*, 1341–1344. [CrossRef]

56. Gomez, D.; O'Donohue, M.-F.; Wenner, T.; Douarre, C.; Macadré, J.; Koebel, P.; Giraud-Panis, M.-J.; Kaplan, H.; Kolkes, A.; Shin-Ya, K.; et al. The G-quadruplex Ligand Telomestatin Inhibits POT1 Binding to Telomeric Sequences In vitro and Induces GFP-POT1 Dissociation from Telomeres in Human Cells. *Cancer Res.* **2006**, *66*, 6908–6912. [CrossRef]

57. Gomez, D.; Wenner, T.; Brassart, B.; Douarre, C.; O'Donohue, M.-F.; El Khoury, V.; Shin-Ya, K.; Morjani, H.; Trentesaux, C.; Riou, J.-F. Telomestatin-induced Telomere Uncapping Is Modulated by POT1 through G-overhang Extension in HT1080 Human Tumor Cells. *J. Biol. Chem.* **2006**, *281*, 38721–38729. [CrossRef]

58. Gunaratnam, M.; Greciano, O.; Martins, C.; Reszka, A.P.; Schultes, C.M.; Morjani, H.; Riou, J.-F.; Neidle, S. Mechanism of acridine-based telomerase inhibition and telomere shortening. *Biochem. Pharmacol.* **2007**, *74*, 679–689. [CrossRef]

59. D'Adda Di Fagagna, F.; Reaper, P.M.; Clay-Farrace, L.; Fiegler, H.; Carr, P.; Von Zglinicki, T.; Saretzki, G.; Carter, N.P.; Jackson, S.P. A DNA Damage Checkpoint Response in Telomere-Initiated Senescence. *Nature* **2003**, *426*, 194–198. [CrossRef]

60. Tauchi, T.; Shin-Ya, K.; Sashida, G.; Sumi, M.; Nakajima, A.; Shimamoto, T.; Ohyashiki, J.H.; Ohyashiki, K. Activity of a novel G-quadruplex-interactive telomerase inhibitor, telomestatin (SOT-095), against human leukemia cells: Involvement of ATM-dependent DNA damage response pathways. *Oncogene* **2003**, *22*, 5338–5347. [CrossRef]

61. Salvati, E.; Leonetti, C.; Rizzo, A.; Scarsella, M.; Mottolese, M.; Galati, R.; Sperduti, I.; Stevens, M.F.; D'Incalci, M.; Blasco, M.A.; et al. Telomere damage induced by the G-quadruplex ligand RHPS4 has an antitumor effect. *J. Clin. Investig.* **2007**, *117*, 3236–3247. [CrossRef]

62. Qi, H.; Lin, C.-P.; Fu, X.; Wood, L.M.; Liu, A.A.; Tsai, Y.-C.; Chen, Y.; Barbieri, C.M.; Pilch, D.; Liu, L. G-quadruplexes Induce Apoptosis in Tumor Cells. *Cancer Res.* **2006**, *66*, 11808–11816. [CrossRef]

63. Kelland, L. Targeting the Limitless Replicative Potential of Cancer: The Telomerase/Telomere Pathway: Figure 1. *Clin. Cancer Res.* **2007**, *13*, 4960–4963. [CrossRef] [PubMed]

64. Oganesian, L.; Bryan, T.M. Physiological relevance of telomeric G-quadruplex formation: A potential drug target. *BioEssays* **2007**, *29*, 155–165. [CrossRef] [PubMed]

65. Siddiqui-Jain, A.; Grand, C.L.; Bearss, D.; Hurley, L.H. Direct evidence for a G-quadruplex in a promoter region and its targeting with a small molecule to repress c-MYC transcription. *Proc. Natl. Acad. Sci. USA* **2002**, *99*, 11593–11598. [CrossRef] [PubMed]

66. Balasubramanian, S.; Hurley, L.H.; Neidle, S. Targeting G-quadruplexes in Gene Promoters: A Novel Anticancer Strategy? *Nat. Rev. Drug Discov.* **2011**, *10*, 261–275. [CrossRef] [PubMed]

67. Murat, P.; Balasubramanian, S. Existence and consequences of G-quadruplex structures in DNA. *Curr. Opin. Genet. Dev.* **2014**, *25*, 22–29. [CrossRef]

68. Sun, D.; Thompson, B.; Cathers, B.E.; Salazar, M.; Kerwin, S.M.; Trent, J.O.; Jenkins, T.C.; Neidle, S.; Hurley, L.H. Inhibition of Human Telomerase by a G-quadruplex-Interactive Compound. *J. Med. Chem.* **1997**, *40*, 2113–2116. [CrossRef]

69. Fedoroff, O.Y.; Salazar, M.; Han, H.; Chemeris, V.V.; Kerwin, S.M.; Hurley, L.H. NMR-Based Model of a Telomerase-Inhibiting Compound Bound to G-quadruplex DNA. *Biochemistry* **1998**, *37*, 12367–12374. [CrossRef]

70. Haider, S.; Parkinson, G.N.; Neidle, S. Structure of a G-quadruplex–Ligand Complex. *J. Mol. Biol.* **2003**, *326*, 117–125. [CrossRef]

71. Gavathiotis, E.; Heald, R.A.; Stevens, M.F.; Searle, M.S. Drug Recognition and Stabilisation of the Parallel-stranded DNA Quadruplex d(TTAGGGT)₄ Containing the Human Telomeric Repeat. *J. Mol. Biol.* **2003**, *334*, 25–36. [CrossRef]

72. Parkinson, G.N.; Ghosh, R.; Neidle, S. Structural Basis for Binding of Porphyrin to Human Telomeres. *Biochemistry* **2007**, *46*, 2390–2397. [CrossRef]

73. Campbell, N.H.; Parkinson, G.N.; Reszka, A.P.; Neidle, S. Structural Basis of DNA Quadruplex Recognition by an Acridine Drug. *J. Am. Chem. Soc.* **2008**, *130*, 6722–6724. [CrossRef]

74. Parkinson, G.N.; Cuenca, F.; Neidle, S. Topology Conservation and Loop Flexibility in Quadruplex–Drug Recognition: Crystal Structures of Inter- and Intramolecular Telomeric DNA Quadruplex–Drug Complexes. *J. Mol. Biol.* **2008**, *381*, 1145–1156. [CrossRef]

75. Kim, M.-Y.; Vankayalapati, H.; Shin-Ya, K.; Wierzba, K.; Hurley, L.H. Telomestatin, a Potent Telomerase Inhibitor That Interacts Quite Specifically with the Human Telomeric Intramolecular G-quadruplex. *J. Am. Chem. Soc.* **2002**, *124*, 2098–2099. [CrossRef]

76. Rodriguez, R.; Müller, S.; Yeoman, J.A.; Trentesaux, C.; Riou, J.-F.; Balasubramanian, S. A Novel Small Molecule That Alters Shelterin Integrity and Triggers a DNA-Damage Response at Telomeres. *J. Am. Chem. Soc.* **2008**, *130*, 15758–15759. [CrossRef]

77. Moorhouse, A.D.; Santos, A.M.; Gunaratnam, M.; Moore, M.; Neidle, S.; Moses, J.E. Stabilization of G-quadruplex DNA by Highly Selective Ligands via Click Chemistry. *J. Am. Chem. Soc.* **2006**, *128*, 15972–15973. [CrossRef]

78. Drewe, W.C.; Nanjunda, R.; Gunaratnam, M.; Beltran, M.; Parkinson, G.N.; Reszka, A.P.; Wilson, W.D.; Neidle, S. Rational Design of Substituted Diarylureas: A Scaffold for Binding to G-quadruplex Motifs. *J. Med. Chem.* **2008**, *51*, 7751–7767. [CrossRef]

79. Delaney, S.; Barton, J.K. Charge Transport in DNA Duplex/Quadruplex Conjugates. *Biochemistry* **2003**, *42*, 14159–14165. [CrossRef]

80. Chen, Q.; Kuntz, I.D.; Shafer, R.H. Spectroscopic recognition of guanine dimeric hairpin quadruplexes by a carbocyanine dye. *Proc. Natl. Acad. Sci. USA* **1996**, *93*, 2635–2639. [CrossRef]

81. Harrison, R.J.; Gowan, S.M.; Kelland, L.R.; Neidle, S. Human telomerase inhibition by substituted acridine derivatives. *Bioorganic Med. Chem. Lett.* **1999**, *9*, 2463–2468. [CrossRef]

82. Read, M.A.; Wood, A.A.; Harrison, J.R.; Gowan, S.M.; Kelland, L.R.; Dosanjh, H.S.; Neidle, S. Molecular Modeling Studies on G-quadruplex Complexes of Telomerase Inhibitors: Structure−Activity Relationships. *J. Med. Chem.* **1999**, *42*, 4538–4546. [CrossRef] [PubMed]

83. Campbell, N.; Patel, M.; Tofa, A.B.; Ghosh, R.; Parkinson, G.N.; Neidle, S. Selectivity in Ligand Recognition of G-quadruplex Loops. *Biochemistry* **2009**, *48*, 1675–1680. [CrossRef]

84. Incles, C.M.; Schultes, C.M.; Kempski, H.; Koehler, H.; Kelland, L.R.; Neidle, S. A G-quadruplex telomere targeting agent produces p16-associated senescence and chromosomal fusions in human prostate cancer cells. *Mol. Cancer Ther.* **2004**, *3*, 1201–1207. [PubMed]

85. Moore, M.J.B.; Schultes, C.M.; Cuesta, J.; Cuenca, F.; Gunaratnam, M.; Tanious, F.A.; Wilson, A.W.D.; Neidle, S. Trisubstituted Acridines as G-quadruplex Telomere Targeting Agents. Effects of Extensions of the 3,6- and 9-Side Chains on Quadruplex Binding, Telomerase Activity, and Cell Proliferation. *J. Med. Chem.* **2005**, *49*, 582–599. [CrossRef]

86. Mergny, J.-L.; Maurizot, J.-C. Fluorescence Resonance Energy Transfer as a Probe for G-Quartet Formation by a Telomeric Repeat. *ChemBioChem* **2001**, *2*, 124–132. [CrossRef]

87. De Cian, A.; Guittat, L.; Kaiser, M.; Sacca, B.; Amrane, S.; Bourdoncle, A.; Alberti, P.; Teulade-Fichou, M.-P.; Lacroix, L.; Mergny, J.-L. Fluorescence-based melting assays for studying quadruplex ligands. *Methods* **2007**, *42*, 183–195. [CrossRef]

88. Burger, A.M.; Dai, F.; Schultes, C.M.; Reszka, A.P.; Moore, M.J.; Double, J.A.; Neidle, S. The G-quadruplex-Interactive Molecule BRACO-19 Inhibits Tumor Growth, Consistent with Telomere Targeting and Interference with Telomerase Function. *Cancer Res.* **2005**, *65*, 1489–1496. [CrossRef]

89. Gowan, S.M.; Harrison, J.R.; Patterson, L.; Valenti, M.; Read, M.A.; Neidle, S.; Kelland, L.R. A G-quadruplex-Interactive Potent Small-Molecule Inhibitor of Telomerase Exhibiting in Vitro and in Vivo Antitumor Activity. *Mol. Pharmacol.* **2002**, *61*, 1154–1162. [CrossRef]

90. Incles, C.M.; Schultes, C.M.; Kelland, L.R.; Neidle, S. Acquired Cellular Resistance to Flavopiridol in a Human Colon Carcinoma Cell Line Involves Up-Regulation of the Telomerase Catalytic Subunit and Telomere Elongation. Sensitivity of Resistant Cells to Combination Treatment with a Telomerase Inhibitor. *Mol. Pharmacol.* **2003**, *64*, 1101–1108. [CrossRef]

91. Tuntiwechapikul, W.; Lee, J.T.; Salazar, M. Design and Synthesis of the G-quadruplex-Specific Cleaving Reagent Perylene-EDTA·Iron(II). *J. Am. Chem. Soc.* **2001**, *123*, 5606–5607. [CrossRef]

92. Duan, W.; Rangan, A.; Vankayalapati, H.; Kim, M.Y.; Zeng, Q.; Sun, D.; Han, H.; Fedoroff, O.Y.; Nishioka, D.; Rha, S.Y.; et al. Design and synthesis of fluoroquinophenoxazines that interact with human telomeric G-quadruplexes and their biological effects. *Mol. Cancer Ther.* **2001**, *1*, 103–120.

93. Mehta, A.K.; Shayo, Y.; Vankayalapati, H.; Hurley, L.H.; Schaefer, J. Structure of a Quinobenzoxazine−G-quadruplex Complex by REDOR NMR. *Biochemistry* **2004**, *43*, 11953–11958. [CrossRef]

94. Lichtman, M.A. A historical perspective on the development of the cytarabine (7 days) and daunorubicin (3 days) treatment regimen for acute myelogenous leukemia: 2013 the 40th anniversary of 7 + 3. *Blood Cells Mol. Dis.* **2013**, *50*, 119–130. [CrossRef]

95. Yang, F.; Teves, S.S.; Kemp, C.J.; Henikoff, S. Doxorubicin, DNA Torsion, and Chromatin Dynamics. *Biochim. Biophys. Acta-Rev. Cancer* **2014**, *1845*, 84–89. [CrossRef]

96. Clark, G.R.; Pytel, P.D.; Squire, C.J.; Neidle, S. Structure of the First Parallel DNA Quadruplex-Drug Complex. *J. Am. Chem. Soc.* **2003**, *125*, 4066–4067. [CrossRef]

97. Barrett, M.P.; Gemmell, C.G.; Suckling, C.J. Minor groove binders as anti-infective agents. *Pharmacol. Ther.* **2013**, *139*, 12–23. [CrossRef]

98. Kopka, M.L.; Yoon, C.; Goodsell, D.; Pjura, P.; Dickerson, R.E. The molecular origin of DNA-drug specificity in netropsin and distamycin. *Proc. Natl. Acad. Sci. USA* **1985**, *82*, 1376–1380. [CrossRef]

99. Pagano, B.; Fotticchia, I.; De Tito, S.; Mattia, C.A.; Mayol, L.; Novellino, E.; Randazzo, A.; Giancola, C. Selective Binding of Distamycin A Derivative to G-quadruplex Structure [d(TGGGGT)]4. *J. Nucleic Acids* **2010**, *2010*, 247137. [CrossRef]

100. Randazzo, A.; Galeone, A.; Mayol, L. 1H-NMR Study of the Interaction of Distamycin A and Netropsin with the Parallel Stranded Tetraplex [d(TGGGT)]4. *Chem. Commun.* **2001**, *11*, 1030–1031. [CrossRef]

101. Cocco, M.J.; Hanakahi, L.A.; Huber, M.D.; Maizels, N. Specific Interactions of Distamycin with G-quadruplex DNA. *Nucleic Acids Res.* **2003**, *31*, 2944–2951. [CrossRef] [PubMed]

102. Martino, L.; Virno, A.; Pagano, B.; Virgilio, A.; Di Micco, S.; Galeone, A.; Giancola, C.; Bifulco, G.; Mayol, L.; Randazzo, A. Structural and Thermodynamic Studies of the Interaction of Distamycin A with the Parallel Quadruplex Structure [d(TGGGGT)]4. *J. Am. Chem. Soc.* **2007**, *129*, 16048–16056. [CrossRef] [PubMed]

103. Mergny, J.-L.; Lacroix, L.; Teulade-Fichou, M.-P.; Hounsou, C.; Guittat, L.; Hoarau, M.; Arimondo, P.B.; Vigneron, J.-P.; Lehn, J.-M.; Riou, J.-F.; et al. Telomerase inhibitors based on quadruplex ligands selected by a fluorescence assay. *Proc. Natl. Acad. Sci. USA* **2001**, *98*, 3062–3067. [CrossRef] [PubMed]

104. Hounsou, C.; Guittat, L.; Monchaud, D.; Jourdan, M.; Saettel, N.; Mergny, J.-L.; Teulade-Fichou, M.-P. G-quadruplex Recognition by Quinacridines: A SAR, NMR, and Biological Study. *ChemMedChem* **2007**, *2*, 655–666. [CrossRef]

105. Bertrand, H.; Bombard, S.; Monchaud, D.; Teulade-Fichou, M.-P. A platinum–quinacridine hybrid as a G-quadruplex ligand. *JBIC J. Biol. Inorg. Chem.* **2007**, *12*, 1003–1014. [CrossRef]

106. Teulade-Fichou, M.-P.; Carrasco, C.; Guittat, L.; Bailly, C.; Alberti, P.; Mergny, J.-L.; David, A.; Lehn, J.-M.; Wilson, W.D. Selective Recognition of G-quadruplex Telomeric DNA by a Bis(quinacridine) Macrocycle. *J. Am. Chem. Soc.* **2003**, *125*, 4732–4740. [CrossRef]

107. Allain, C.; Monchaud, D.; Teulade-Fichou, M.-P. FRET Templated by G-quadruplex DNA: A Specific Ternary Interaction Using an Original Pair of Donor/Acceptor Partners. *J. Am. Chem. Soc.* **2006**, *128*, 11890–11893. [CrossRef]

108. Gabelica, V.; Baker, E.S.; Teulade-Fichou, M.-P.; De Pauw, E.; Bowers, M.T. Stabilization and Structure of Telomeric and c-myc Region Intramolecular G-quadruplexes: The Role of Central Cations and Small Planar Ligands. *J. Am. Chem. Soc.* **2007**, *129*, 895–904. [CrossRef]

109. Haudecoeur, R.; Stefan, L.; Denat, F.; Monchaud, D. A Model of Smart G-quadruplex Ligand. *J. Am. Chem. Soc.* **2012**, *135*, 550–553. [CrossRef]

110. Xu, W.; Tan, J.-H.; Chen, S.-B.; Hou, J.-Q.; Li, D.; Huang, Z.-S.; Gu, L.-Q. Studies on the binding of 5-N-methylated quindoline derivative to human telomeric G-quadruplex. *Biochem. Biophys. Res. Commun.* **2011**, *406*, 454–458. [CrossRef]

111. Tan, J.-H.; Ou, T.-M.; Hou, J.-Q.; Lu, Y.-J.; Huang, S.-L.; Luo, H.-B.; Wu, J.-Y.; Huang, Z.-S.; Wong, K.-Y.; Gu, L.-Q. Isaindigotone Derivatives: A New Class of Highly Selective Ligands for Telomeric G-quadruplex DNA. *J. Med. Chem.* **2009**, *52*, 2825–2835. [CrossRef]

112. Han, F.X.; Wheelhouse, R.T.; Hurley, L.H. Interactions of TMPyP4 and TMPyP2 with Quadruplex DNA. Structural Basis for the Differential Effects on Telomerase Inhibition. *J. Am. Chem. Soc.* **1999**, *121*, 3561–3570. [CrossRef]

113. Izbicka, E.; Wheelhouse, R.; Raymond, E.; Davidson, K.K.; Lawrence, R.A.; Sun, D.; Windle, B.E.; Hurley, L.H.; Von Hoff, D.D. Effects of cationic porphyrins as G-quadruplex interactive agents in human tumor cells. *Cancer Res.* **1999**, *59*, 639–644.

114. Shi, D.-F.; Wheelhouse, R.T.; Sun, D.; Hurley, L.H. Quadruplex-Interactive Agents as Telomerase Inhibitors: Synthesis of Porphyrins and Structure−Activity Relationship for the Inhibition of Telomerase. *J. Med. Chem.* **2001**, *44*, 4509–4523. [CrossRef]

115. Kim, M.-Y.; Gleason-Guzman, M.; Izbicka, E.; Nishioka, D.; Hurley, L.H. The different biological effects of telomestatin and TMPyP4 can be attributed to their selectivity for interaction with intramolecular or intermolecular G-quadruplex structures. *Cancer Res.* **2003**, *63*, 3247–3256.

116. Pirotton, S.; Muller, C.; Pantoustier, N.; Botteman, F.; Collinet, S.; Grandfils, C.; Dandrifosse, G.; Degée, P.; Dubois, P.; Raes, M. Enhancement of Transfection Efficiency Through Rapid and Noncovalent Post-PEGylation of Poly(Dimethylaminoethyl Methacrylate)/DNA Complexes. *Pharm. Res.* **2004**, *21*, 1471–1479. [CrossRef]

117. Sun, D.; Guo, K.; Rusche, J.J.; Hurley, L.H. Facilitation of a structural transition in the polypurine/polypyrimidine tract within the proximal promoter region of the human VEGF gene by the presence of potassium and G-quadruplex-interactive agents. *Nucleic Acids Res.* **2005**, *33*, 6070–6080. [CrossRef]

118. Dexheimer, T.S.; Sun, D.; Hurley, L.H. Deconvoluting the Structural and Drug-Recognition Complexity of the G-quadruplex-Forming Region Upstream of the bcl-2 P1 Promoter. *J. Am. Chem. Soc.* **2006**, *128*, 5404–5415. [CrossRef]

119. Guo, K.; Pourpak, A.; Beetz-Rogers, K.; Gokhale, V.; Sun, D.; Hurley, L.H. Formation of Pseudosymmetrical G-quadruplex and i-Motif Structures in the Proximal Promoter Region of the RET Oncogene. *J. Am. Chem. Soc.* **2007**, *129*, 10220–10228. [CrossRef]

120. Freyer, M.W.; Buscaglia, R.; Kaplan, K.; Cashman, D.; Hurley, L.H.; Lewis, E.A. Biophysical Studies of the c-MYC NHE III1 Promoter: Model Quadruplex Interactions with a Cationic Porphyrin. *Biophys. J.* **2007**, *92*, 2007–2015. [CrossRef]

121. Phan, A.T.; Kuryavyi, V.; Gaw, H.Y.; Patel, D.J. Small-molecule interaction with a five-guanine-tract G-quadruplex structure from the human MYC promoter. *Nat. Chem. Biol.* **2005**, *1*, 167–173. [CrossRef] [PubMed]

122. Ren, J.; Chaires, J.B. Sequence and Structural Selectivity of Nucleic Acid Binding Ligands. *Biochemistry* **1999**, *38*, 16067–16075. [CrossRef] [PubMed]

123. De Cian, A.; Guittat, L.; Shin-Ya, K.; Riou, J.-F.; Mergny, J.-L. Affinity and selectivity of G4 ligands measured by FRET. *Nucleic Acids Symp. Ser.* **2005**, *49*, 235–236. [CrossRef]

124. De Armond, R.; Wood, S.; Sun, D.; Hurley, L.H.; Ebbinghaus, S.W. Evidence for the Presence of a Guanine Quadruplex Forming Region within a Polypurine Tract of the Hypoxia Inducible Factor 1α Promoter. *Biochemistry* **2005**, *44*, 16341–16350. [CrossRef]

125. Monchaud, D.; Allain, C.; Teulade-Fichou, M.-P. Development of a fluorescent intercalator displacement assay (G4-FID) for establishing quadruplex-DNA affinity and selectivity of putative ligands. *Bioorg. Med. Chem. Lett.* **2006**, *16*, 4842–4845. [CrossRef]

126. Haq, I.; Trent, J.O.; Chowdhry, B.Z.; Jenkins, T.C. Intercalative G-Tetraplex Stabilization of Telomeric DNA by a Cationic Porphyrin1. *J. Am. Chem. Soc.* **1999**, *121*, 1768–1779. [CrossRef]

127. Wei, C.; Jia, G.; Yuan, J.; Feng, Z.; Li, C. A Spectroscopic Study on the Interactions of Porphyrin with G-quadruplex DNAs. *Biochemistry* **2006**, *45*, 6681–6691. [CrossRef]

128. Gonçalves, D.P.N.; Rodriguez, R.; Balasubramanian, S.; Sanders, J.K.M. Tetramethylpyridiniumporphyrazines—a new class of G-quadruplex inducing and stabilising ligands. *Chem. Commun.* **2006**, 4685–4687. [CrossRef]

129. Dixon, I.M.; Lopez, F.; Tejera, A.M.; Estève, J.-P.; Blasco, M.A.; Pratviel, G.; Meunier, B. A G-quadruplex Ligand with 10000-Fold Selectivity over Duplex DNA. *J. Am. Chem. Soc.* **2007**, *129*, 1502–1503. [CrossRef] [PubMed]

130. Seenisamy, J.; Bashyam, S.; Gokhale, V.; Vankayalapati, H.; Sun, D.; Siddiqui-Jain, A.; Streiner, N.; Shin-Ya, K.; White, E.; Wilson, A.W.D.; et al. Design and Synthesis of an Expanded Porphyrin That Has Selectivity for the c-MYC G-quadruplex Structure. *J. Am. Chem. Soc.* **2005**, *127*, 2944–2959. [CrossRef]

131. Rezler, E.M.; Seenisamy, J.; Bashyam, S.; Kim, M.-Y.; White, E.; Wilson, W.D.; Hurley, L.H. Telomestatin and Diseleno Sapphyrin Bind Selectively to Two Different Forms of the Human Telomeric G-quadruplex Structure. *J. Am. Chem. Soc.* **2005**, *127*, 9439–9447. [CrossRef]

132. Koeppel, F.; Riou, J.F.; Laoui, A.; Mailliet, P.; Arimondo, P.B.; Labit, D.; Petitgenet, O.; Hélène, C.; Mergny, J.L. Ethidium Derivatives Bind to G-Quartets, Inhibit Telomerase and Act as Fluorescent Probes for Quadruplexes. *Nucleic Acids Res.* **2001**, *29*, 1087–1096. [CrossRef]

133. Riou, J.-F.; Guittat, L.; Mailliet, P.; Laoui, A.; Renou, E.; Petitgenet, O.; Megnin-Chanet, F.; Helene, C.; Mergny, J.-L. Cell senescence and telomere shortening induced by a new series of specific G-quadruplex DNA ligands. *Proc. Natl. Acad. Sci. USA* **2002**, *99*, 2672–2677. [CrossRef]

134. Gomez, D.; Aouali, N.; Londoño-Vallejo, A.; Lacroix, L.; Mégnin-Chanet, F.; Lemarteleur, T.; Douarre, C.; Shin-Ya, K.; Mailliet, P.; Trentesaux, C.; et al. Resistance to the Short Term Antiproliferative Activity of the G-quadruplex Ligand 12459 Is Associated with Telomerase Overexpression and Telomere Capping Alteration. *J. Biol. Chem.* **2003**, *278*, 50554–50562. [CrossRef]

135. Gomez, D.; Lemarteleur, T.; Lacroix, L.; Mailliet, P.; Mergny, J.L.; Riou, J.F. Telomerase Downregulation Induced by the G-quadruplex Ligand 12459 in A549 Cells Is Mediated by HTERT RNA Alternative Splicing. *Nucleic Acids Res.* **2004**, *32*, 371–379. [CrossRef]

136. Douarre, C.; Gomez, D.; Morjani, H.; Zahm, J.M.; O'Donohue, M.-F.; Eddabra, L.; Mailliet, P.; Riou, J.F.; Trentesaux, C. Overexpression of Bcl-2 Is Associated with Apoptotic Resistance to the G-quadruplex Ligand 12459 but Is Not Sufficient to Confer Resistance to Long-Term Senescence. *Nucleic Acids Res.* **2005**, *33*, 2192–2203. [CrossRef]

137. Lemarteleur, T.; Gomez, D.; Paterski, R.; Mandine, E.; Mailliet, P.; Riou, J.-F. Stabilization of the c-myc gene promoter quadruplex by specific ligands' inhibitors of telomerase. *Biochem. Biophys. Res. Commun.* **2004**, *323*, 802–808. [CrossRef]

138. Pennarun, G.; Granotier, C.; Gauthier, L.R.; Gomez, D.; Hoffschir, F.; Mandine, E.; Riou, J.-F.; Mergny, J.-L.; Mailliet, P.; Boussin, F.D. Apoptosis related to telomere instability and cell cycle alterations in human glioma cells treated by new highly selective G-quadruplex ligands. *Oncogene* **2005**, *24*, 2917–2928. [CrossRef]

139. Rodriguez, R.; Miller, K.M.; Forment, J.; Bradshaw, C.; Nikan, M.; Britton, S.; Oelschlaegel, T.; Xhemalce, B.; Balasubramanian, S.; Jackson, S.P. Small-molecule–induced DNA damage identifies alternative DNA structures in human genes. *Nat. Chem. Biol.* **2012**, *8*, 301–310. [CrossRef]

140. Biffi, G.; Di Antonio, M.; Tannahill, D.; Balasubramanian, S. Visualization and selective chemical targeting of RNA G-quadruplex structures in the cytoplasm of human cells. *Nat. Chem.* **2013**, *6*, 75–80. [CrossRef]

141. Lubitz, I.; Borovok, N.; Kotlyar, A. Interaction of Monomolecular G4-DNA Nanowires with TMPyP: Evidence for Intercalation. *Biochemistry* **2007**, *46*, 12925–12929. [CrossRef] [PubMed]

142. Lombardo, C.M.; Welsh, S.J.; Strauss, S.J.; Dale, A.G.; Todd, A.K.; Nanjunda, R.; Wilson, W.D.; Neidle, S. A novel series of G-quadruplex ligands with selectivity for HIF-expressing osteosarcoma and renal cancer cell lines. *Bioorg. Med. Chem. Lett.* **2012**, *22*, 5984–5988. [CrossRef]

143. Anantha, N.V.; Azam, M.; Sheardy, R.D. Porphyrin Binding to Quadruplexed T4G4. *Biochemistry* **1998**, *37*, 2709–2714. [CrossRef]

144. Li, Q.; Xiang, J.; Li, X.; Chen, L.; Xu, X.; Tang, Y.; Zhou, Q.; Li, L.; Zhang, H.; Sun, H.; et al. Stabilizing parallel G-quadruplex DNA by a new class of ligands: Two non-planar alkaloids through interaction in lateral grooves. *Biochimie* **2009**, *91*, 811–819. [CrossRef] [PubMed]

145. Rodriguez, R.; Pantoş, G.D.; Gonçalves, D.P.N.; Sanders, J.K.M.; Balasubramanian, S. Ligand-Driven G-quadruplex Conformational Switching By Using an Unusual Mode of Interaction. *Angew. Chem.* **2007**, *119*, 5501–5503. [CrossRef]

146. Lu, X.-H.; Shi, S.; Yao, J.-L.; Gao, X.; Huang, H.-L.; Yao, T.-M. Two structurally analogous ruthenium complexes as naked-eye and reversible molecular "light switch" for G-quadruplex DNA. *J. Inorg. Biochem.* **2014**, *140*, 64–71. [CrossRef] [PubMed]

147. Yu, H.-J.; Yu, L.; Hao, Z.-F.; Zhao, Y. Interactions of ruthenium complexes containing indoloquinoline moiety with human telomeric G-quadruplex DNA. *Spectrochim. Acta Part A Mol. Biomol. Spectrosc.* **2014**, *124*, 187–193. [CrossRef] [PubMed]

148. Reed, J.E.; Arnal, A.A.; Neidle, S.; Vilar, R. Stabilization of G-quadruplex DNA and Inhibition of Telomerase Activity by Square-Planar Nickel(II) Complexes. *J. Am. Chem. Soc.* **2006**, *128*, 5992–5993. [CrossRef]

149. Keating, L.R.; Szalai, V.A. Parallel-Stranded Guanine Quadruplex Interactions with a Copper Cationic Porphyrin. *Biochemistry* **2004**, *43*, 15891–15900. [CrossRef]

150. Evans, S.E.; Mendez, M.A.; Turner, K.B.; Keating, L.R.; Grimes, R.T.; Melchoir, S.; Szalai, V.A. End-stacking of copper cationic porphyrins on parallel-stranded guanine quadruplexes. *JBIC J. Biol. Inorg. Chem.* **2007**, *12*, 1235–1249. [CrossRef]

151. Romera, C.; Bombarde, O.; Bonnet, R.; Gomez, D.; Dumy, P.; Calsou, P.; Gwan, J.-F.; Lin, J.-H.; Defrancq, E.; Pratviel, G. Improvement of porphyrins for G-quadruplex DNA targeting. *Biochimie* **2011**, *93*, 1310–1317. [CrossRef]

152. Vialas, C.; Pratviel, G.; Meunier, B. Oxidative Damage Generated by an Oxo-Metalloporphyrin onto the Human Telomeric Sequence. *Biochemistry* **2000**, *39*, 9514–9522. [CrossRef]

153. Maraval, A.; Franco, S.; Vialas, C.; Pratviel, G.; Blasco, M.A.; Meunier, B. Porphyrin–aminoquinoline conjugates as telomerase inhibitors. *Org. Biomol. Chem.* **2003**, *1*, 921–927. [CrossRef]

154. Dixon, I.; Lopez, F.; Estève, J.-P.; Tejera, A.M.; Blasco, M.A.; Pratviel, G.; Meunier, B. Porphyrin Derivatives for Telomere Binding and Telomerase Inhibition. *ChemBioChem* **2004**, *6*, 123–132. [CrossRef]

155. Ren, L.; Zhang, A.; Huang, J.; Wang, P.; Weng, X.; Zhang, L.; Liang, F.; Tan, Z.; Zhou, X. Quaternary Ammonium Zinc Phthalocyanine: Inhibiting Telomerase by Stabilizing G quadruplexes and Inducing G-quadruplex Structure Transition and Formation. *ChemBioChem* **2007**, *8*, 775–780. [CrossRef]

156. Mikuma, T.; Ohyama, T.; Terui, N.; Yamamoto, Y.; Hori, H. Coordination Complex between Haemin and Parallel-Quadruplexed d(TTAGGG). *Chem. Commun.* **2003**, *3*, 1708–1709. [CrossRef]

157. Ohyama, T.; Kato, Y.; Mita, H.; Yamamoto, Y. Exogenous Ligand Binding Property of a Heme–DNA Coordination Complex. *Chem. Lett.* **2006**, *35*, 126–127. [CrossRef]

158. Arola-Arnal, A.; Benet-Buchholz, J.; Neidle, S.; Vilar, R. Effects of Metal Coordination Geometry on Stabilization of Human Telomeric Quadruplex DNA by Square-Planar and Square-Pyramidal Metal Complexes. *Inorg. Chem.* **2008**, *47*, 11910–11919. [CrossRef]

159. Campbell, N.H.; Karim, N.H.A.; Parkinson, G.N.; Gunaratnam, M.; Petrucci, V.; Todd, A.K.; Vilar, R.; Neidle, S. Molecular Basis of Structure–Activity Relationships between Salphen Metal Complexes and Human Telomeric DNA Quadruplexes. *J. Med. Chem.* **2011**, *55*, 209–222. [CrossRef]

160. Terenzi, A.; Bonsignore, R.; Spinello, A.; Gentile, C.; Martorana, A.; Ducani, C.; Högberg, B.; Almerico, A.M.; Lauria, A.; Barone, G. Selective G-quadruplex stabilizers: Schiff-base metal complexes with anticancer activity. *RSC Adv.* **2014**, *4*, 33245–33256. [CrossRef]

161. Davis, K.J.; Richardson, C.; Beck, J.L.; Knowles, B.M.; Guédin, A.; Mergny, J.-L.; Willis, A.C.; Ralph, S.F. Synthesis and characterisation of nickel Schiff base complexes containing the meso-1,2-diphenylethylenediamine moiety: Selective interactions with a tetramolecular DNA quadruplex. *Dalton Trans.* **2015**, *44*, 3136–3150. [CrossRef] [PubMed]

162. Terenzi, A.; Lötsch, D.; Van Schoonhoven, S.; Roller, A.; Kowol, C.R.; Berger, W.; Keppler, B.K.; Barone, G. Another step toward DNA selective targeting: Ni(II) and Cu(II) complexes of a Schiff base ligand able to bind gene promoter G-quadruplexes. *Dalton Trans.* **2016**, *45*, 7758–7767. [CrossRef] [PubMed]

163. Ali, A.; Kamra, M.; Roy, S.; Muniyappa, K.; Bhattacharya, S. Novel Oligopyrrole Carboxamide based Nickel(II) and Palladium(II) Salens, Their Targeting of Human G-quadruplex DNA, and Selective Cancer Cell Toxicity. *Chem. Asian J.* **2016**, *11*, 2542–2554. [CrossRef]

164. Lecarme, L.; Prado, E.; De Rache, A.; Nicolau-Travers, M.-L.; Gellon, G.; Dejeu, J.; Lavergne, T.; Jamet, H.; Gomez, D.; Mergny, J.-L.; et al. Efficient Inhibition of Telomerase by Nickel-Salophen Complexes. *ChemMedChem* **2016**, *11*, 1133–1136. [CrossRef] [PubMed]

165. Ali, A.; Kamra, M.; Roy, S.; Muniyappa, K.; Bhattacharya, S. Enhanced G-quadruplex DNA Stabilization and Telomerase Inhibition by Novel Fluorescein Derived Salen and Salphen Based Ni(II) and Pd(II) Complexes. *Bioconjugate Chem.* **2017**, *28*, 341–352. [CrossRef] [PubMed]

166. Davis, K.J.; Assadawi, N.M.O.; Pham, S.Q.T.; Birrento, M.L.; Richardson, C.; Beck, J.L.; Willis, A.C.; Ralph, S.F. Effect of structure variations on the quadruplex DNA binding ability of nickel Schiff base complexes. *Dalton Trans.* **2018**, *47*, 13573–13591. [CrossRef] [PubMed]

167. Farine, G.; Migliore, C.; Terenzi, A.; Lo Celso, F.; Santoro, A.; Bruno, G.; Bonsignore, R.; Barone, G. On the G-quadruplex Binding of a New Class of Nickel(II), Copper(II), and Zinc(II) Salphen-Like Complexes. *Eur. J. Inorg. Chem.* **2021**, *2021*, 1332–1336. [CrossRef]

168. Ruehl, C.L.; Lim, A.H.M.; Kench, T.; Mann, D.J.; Vilar, R. An Octahedral Cobalt(III) Complex with Axial NH 3 Ligands that Templates and Selectively Stabilises G–quadruplex DNA. *Chem. Eur. J.* **2019**, *25*, 9691–9700. [CrossRef]

169. Wu, P.; Ma, D.-L.; Leung, C.-H.; Yan, S.-C.; Zhu, N.; Abagyan, R.; Che, C.-M. Stabilization of G-quadruplex DNA with Platinum(II) Schiff Base Complexes: Luminescent Probe and Down-Regulation of c-myc Oncogene Expression. *Chem. Eur. J.* **2009**, *15*, 13008–13021. [CrossRef]

170. Rakers, V.; Cadinu, P.; Edel, J.B.; Vilar, R. Development of microfluidic platforms for the synthesis of metal complexes and evaluation of their DNA affinity using online FRET melting assays. *Chem. Sci.* **2018**, *9*, 3459–3469. [CrossRef]

171. Abd Karim, N.H.; Mendoza, O.; Shivalingam, A.; Thompson, A.J.; Ghosh, S.; Kuimova, M.K.; Vilar, R. Salphen metal complexes as tunable G-quadruplex binders and optical probes. *RSC Adv.* **2013**, *4*, 3355–3363. [CrossRef]

172. Bertrand, H.; Monchaud, D.; De Cian, A.; Guillot, R.; Mergny, J.-L.; Teulade-Fichou, M.-P. The importance of metal geometry in the recognition of G-quadruplex-DNA by metal-terpyridine complexes. *Org. Biomol. Chem.* **2007**, *5*, 2555–2559. [CrossRef]

173. Bertrand, H.; Bombard, S.; Monchaud, D.; Talbot, E.; Guédin, A.; Mergny, J.-L.; Grünert, R.; Bednarski, P.J.; Teulade-Fichou, M.-P. Exclusive platination of loop adenines in the human telomeric G-quadruplex. *Org. Biomol. Chem.* **2009**, *7*, 2864–2871. [CrossRef]

174. Largy, E.; Hamon, F.; Rosu, F.; Gabelica, V.; De Pauw, E.; Guédin, A.; Mergny, J.-L.; Teulade-Fichou, M.-P. Tridentate N-Donor Palladium(II) Complexes as Efficient Coordinating Quadruplex DNA Binders. *Chem. Eur. J.* **2011**, *17*, 13274–13283. [CrossRef]

175. Trajkovski, M.; Morel, E.; Hamon, F.; Bombard, S.; Teulade-Fichou, M.-P.; Plavec, J. Interactions of Pt-ttpy with G-quadruplexes Originating from Promoter Region of the c-myc Gene Deciphered by NMR and Gel Electrophoresis Analysis. *Chem. Eur. J.* **2015**, *21*, 7798–7807. [CrossRef]

176. Wang, P.; Leung, C.-H.; Ma, D.-L.; Yan, S.-C.; Che, C.-M. Structure-Based Design of Platinum(II) Complexes as c-myc Oncogene Down-Regulators and Luminescent Probes for G-quadruplex DNA. *Chem. Eur. J.* **2010**, *16*, 6900–6911. [CrossRef]

177. Musetti, C.; Krapcho, A.P.; Palumbo, M.; Sissi, C. Effect of G-quadruplex Polymorphism on the Recognition of Telomeric DNA by a Metal Complex. *PLoS ONE* **2013**, *8*, e58529. [CrossRef]

178. Reed, J.E.; Neidle, S.; Vilar, R. Stabilisation of human telomeric quadruplex DNA and inhibition of telomerase by a platinum–phenanthroline complex. *Chem. Commun.* **2007**, 4366–4368. [CrossRef]

179. Ebrahimi, M.; Khayamian, T.; Hadadzadeh, H.; Jannesari, Z.; Khaksar, G. Spectroscopic, biological, and molecular modeling studies on the interactions of [Fe(III)-meloxicam] with G-quadruplex DNA and investigation of its release from bovine serum albumin (BSA) nanoparticles. *J. Biomol. Struct. Dyn.* **2015**, *33*, 2316–2329. [CrossRef]

180. Castor, K.K.; Metera, K.L.; Tefashe, U.M.; Serpell, C.J.; Mauzeroll, J.; Sleiman, H.F. Cyclometalated Iridium(III) Imidazole Phenanthroline Complexes as Luminescent and Electroluminescent G-quadruplex DNA Binders. *Inorg. Chem.* **2015**, *54*, 6958–6967. [CrossRef]

181. Lu, L.; Wang, M.; Mao, Z.; Kang, T.-S.; Chen, X.-P.; Lu, J.-J.; Leung, C.-H.; Ma, D.-L. A Novel Dinuclear Iridirum(III) Complex as a G-quadruplex Selective Probe for the Luminescent Switch-On Detection of Transcription Factor HIF-1α. *Sci. Rep.* **2016**, *6*, 22458. [CrossRef] [PubMed]

182. Wang, M.; Mao, Z.; Kang, T.-S.; Wong, C.-Y.; Mergny, J.-L.; Leung, C.-H.; Ma, D.-L. Conjugating a groove-binding motif to an Ir(iii) complex for the enhancement of G-quadruplex probe behavior. *Chem. Sci.* **2016**, *7*, 2516–2523. [CrossRef] [PubMed]

183. Lin, S.; Lu, L.; Kang, T.-S.; Mergny, J.-L.; Leung, C.-H.; Ma, D.-L. Interaction of an Iridium(III) Complex with G-quadruplex DNA and Its Application in Luminescent Switch-On Detection of Siglec-5. *Anal. Chem.* **2016**, *88*, 10290–10295. [CrossRef] [PubMed]

184. Paris, J.P.; Brandt, W.W. Charge transfer luminescence of a ruthenium(II) chelate. *J. Am. Chem. Soc.* **1959**, *81*, 5001–5002. [CrossRef]

185. Balzani, V.; Juris, A.; Venturi, M.; Campagna, S.; Serroni, S. Luminescent and Redox-Active Polynuclear Transition Metal Complexes. *Chem. Rev.* **1996**, *96*, 759–834. [CrossRef] [PubMed]

186. Campagna, S.; Puntoriero, F.; Nastasi, F.; Bergamini, G.; Balzani, V. Photochemistry and Photophysics of Coordination Compounds: Ruthenium. In *Photochemistry and Photophysics of Coordination Compounds I*; Balzani, V., Campagna, S., Eds.; Springer: Berlin/Heidelberg, Germany, 2007; Volume 280, pp. 117–214.

187. Juris, A.; Balzani, V.; Barigelletti, F.; Campagna, S.; Belser, P.; Von Zelewsky, A. Ru(II) polypyridine complexes: Photophysics, photochemistry, eletrochemistry, and chemiluminescence. *Coord. Chem. Rev.* **1988**, *84*, 85–277. [CrossRef]

188. Di Pietro, M.L.; La Ganga, G.; Nastasi, L.; Puntoriero, F. Ru(II)-Dppz Derivatives and Their Interactions with DNA: Thirty Years and Counting. *Appl. Sci.* **2021**, *11*, 3038. [CrossRef]

189. Olson, E.J.C.; Hu, D.; Hörmann, A.; Jonkman, A.M.; Arkin, M.R.; Stemp, E.D.A.; Barton, A.J.K.; Barbara, P.F. First Observation of the Key Intermediate in the "Light-Switch" Mechanism of [Ru(phen)$_2$dppz]$^{2+}$. *J. Am. Chem. Soc.* **1997**, *119*, 11458–11467. [CrossRef]

190. Olofsson, J.; Önfelt, B.; Lincoln, P. Three-State Light Switch of [Ru(phen)$_2$dppz]$^{2+}$: Distinct Excited-State Species with Two, One, or No Hydrogen Bonds from Solvent. *J. Phys. Chem. A* **2004**, *108*, 4391–4398. [CrossRef]
191. Szalai, V.A.; Thorp, H.H. Electron Transfer in Tetrads: Adjacent Guanines Are Not Hole Traps in G Quartets. *J. Am. Chem. Soc.* **2000**, *122*, 4524–4525. [CrossRef]
192. Rubio-Magnieto, J.; Kajouj, S.; Di Meo, F.; Fossépré, M.; Trouillas, P.; Norman, P.; Linares, M.; Moucheron, C.; Surin, M. Binding Modes and Selectivity of Ruthenium Complexes to Human Telomeric DNA G-quadruplexes. *Chem. Eur. J.* **2018**, *24*, 15577–15588. [CrossRef]
193. Shi, S.; Geng, X.; Zhao, J.; Yao, T.; Wang, C.; Yang, D.; Zheng, L.; Ji, L. Interaction of [Ru(bpy)$_2$(dppz)]$^{2+}$ with human telomeric DNA: Preferential binding to G-quadruplexes over i-motif. *Biochimie* **2010**, *92*, 370–377. [CrossRef]
194. Shi, S.; Zhao, J.; Geng, X.; Yao, T.; Huang, H.; Liu, T.; Zheng, L.; Li, Z.; Yang, D.; Ji, L. Molecular "light switch" for G-quadruplexes and i-motif of human telomeric DNA: [Ru(phen)$_2$(dppz)]$^{2+}$. *Dalton Trans.* **2010**, *39*, 2490–2493. [CrossRef]
195. Shi, S.; Xu, J.-H.; Gao, X.; Huang, H.-L.; Yao, T.-M. Binding Behaviors for Different Types of DNA G-quadruplexes: Enantiomers of [Ru(Bpy)$_2$(L)]$^{2+}$ (L=dppz, Dppz-Idzo). *Chem. Eur. J.* **2015**, *21*, 11435–11445. [CrossRef]
196. Park, J.H.; Lee, H.S.; Jang, M.D.; Han, S.W.; Kim, S.K.; Lee, Y.A. Enantioselective Light Switch Effect of Δ- and Λ-[Ru(Phenanthroline)$_2$Dipyrido[3,2-*a*:2′,3′-*c*]Phenazine]$^{2+}$ Bound to G-quadruplex DNA. *J. Biomol. Struct. Dyn.* **2018**, *36*, 1948–1957. [CrossRef]
197. Devereux, S.J.; Poynton, F.E.; Baptista, F.; Gunnlaugsson, T.; Cardin, C.J.; Sazanovich, I.V.; Towrie, M.; Kelly, J.M.; Quinn, S.J. Caught in the Loop: Binding of the [Ru(phen)$_2$(dppz)]$^{2+}$ Light-Switch Compound to Quadruplex DNA in Solution Informed by Time-Resolved Infrared Spectroscopy. *Chem. Eur. J.* **2020**, *26*, 17103–17109. [CrossRef]
198. Yang, C.; Zhou, Q.; Jiao, Z.; Zhao, H.; Huang, C.-H.; Zhu, B.-Z.; Su, H. Ultrafast excited state dynamics and light-switching of [Ru(phen)$_2$(dppz)]$^{2+}$ in G-quadruplex DNA. *Commun. Chem.* **2021**, *4*, 68. [CrossRef]
199. McQuaid, K.; Hall, J.P.; Baumgaertner, L.; Cardin, D.J.; Cardin, C.J. Three thymine/adenine binding modes of the ruthenium complex Λ-[Ru(TAP)$_2$(dppz)]$^{2+}$ to the G-quadruplex forming sequence d(TAGGGTT) shown by X-ray crystallography. *Chem. Commun.* **2019**, *55*, 9116–9119. [CrossRef]
200. McQuaid, K.; Abell, H.; Gurung, S.P.; Allan, D.R.; Winter, G.; Sørensen, T.L.-M.; Cardin, D.J.; Brazier, J.A.; Cardin, C.J.; Hall, J.P. Structural Studies Reveal Enantiospecific Recognition of a DNA G-quadruplex by a Ruthenium Polypyridyl Complex. *Angew. Chem. Int. Ed.* **2019**, *58*, 9881–9885. [CrossRef] [PubMed]
201. Shi, S.; Lv, C.; Gao, X.; Zhao, J.; Yao, J.; Sun, W.; Huang, H.; Yao, T.; Ji, L. [Ru(bpy)$_2$(bppp)]$^{2+}$ binds two different forms of the human telomeric G-quadruplex structure. *Inorg. Chem. Commun.* **2012**, *24*, 212–215. [CrossRef]
202. Shi, S.; Huang, H.-L.; Gao, X.; Yao, J.-L.; Lv, C.-Y.; Zhao, J.; Sun, W.-L.; Yao, T.-M.; Ji, L.-N. A comparative study of the interaction of two structurally analogous ruthenium complexes with human telomeric G-quadruplex DNA. *J. Inorg. Biochem.* **2013**, *121*, 19–27. [CrossRef] [PubMed]
203. Wachter, E.; Moyá, D.; Glazer, E.C. Combining a Ru(II) "Building Block" and Rapid Screening Approach to Identify DNA Structure-Selective "Light Switch" Compounds. *ACS Comb. Sci.* **2016**, *19*, 85–95. [CrossRef]
204. Wang, X.; Pei, L.; Fan, X.; Shi, S. [Ru(L)$_2$(3-tppp)]$^{2+}$ (L = bpy, phen) stabilizes two different forms of the human telomeric G-quadruplex DNA. *Inorg. Chem. Commun.* **2016**, *72*, 7–12. [CrossRef]
205. Wachter, E.; Moyá, D.; Parkin, S.; Glazer, E.C. Ruthenium Complex "Light Switches" That Are Selective for Different G-quadruplex Structures. *Chem. Eur. J.* **2016**, *22*, 550–559. [CrossRef] [PubMed]
206. Sun, J.; An, Y.; Zhang, L.; Chen, H.-Y.; Wang, Y.-J.; Mao, Z.-W.; Ji, L.-N. Studies on synthesis, characterization, and G-quadruplex binding of Ru(II) complexes containing two dppz ligands. *J. Inorg. Biochem.* **2010**, *105*, 149–154. [CrossRef] [PubMed]
207. Bouzada, D.; Salvadó, I.; Barka, G.; Rama, G.; Martínez-Costas, J.; Lorca, R.; Somoza, Á.; Melle-Franco, M.; Vázquez, M.E.; López, M.V. Selective G-quadruplex binding by oligoarginine-Ru(dppz) metallopeptides. *Chem. Commun.* **2017**, *54*, 658–661. [CrossRef] [PubMed]
208. Wachter, E.; Howerton, B.S.; Hall, E.C.; Parkin, S.; Glazer, E.C. A new type of DNA "light-switch": A dual photochemical sensor and metalating agent for duplex and G-quadruplex DNA. *Chem. Commun.* **2013**, *50*, 311–313. [CrossRef]
209. Liao, G.; Chen, X.; Wu, J.; Qian, C.; Wang, H.; Ji, L.; Chao, H. Novel ruthenium(II) polypyridyl complexes as G-quadruplex stabilisers and telomerase inhibitors. *Dalton Trans.* **2014**, *43*, 7811–7819. [CrossRef]
210. Shi, S.; Zhao, J.; Gao, X.; Lv, C.; Yang, L.; Hao, J.; Huang, H.; Yao, J.; Sun, W.; Yao, T.; et al. Molecular "Light Switch" for G-quadruplex DNA: Cycling the Switch on and Off. *Dalt. Trans.* **2012**, *41*, 5789–5793. [CrossRef]
211. Shi, S.; Gao, X.; Huang, H.; Zhao, J.; Yao, T. Effect of the Ancillary Ligands on the Spectral Properties and G-quadruplexes DNA Binding Behavior: A Combined Experimental and Theoretical Study. *Chem. Eur. J.* **2015**, *21*, 13390–13400. [CrossRef]
212. Yao, J.-L.; Gao, X.; Sun, W.; Fan, X.-Z.; Shi, S.; Yao, T.-M. A Naked-Eye On–Off–On Molecular "Light Switch" Based on a Reversible "Conformational Switch" of G-quadruplex DNA. *Inorg. Chem.* **2012**, *51*, 12591–12593. [CrossRef]
213. Yao, J.-L.; Gao, X.; Sun, W.; Shi, S.; Yao, T.-M. [Ru(bpy)$_2$dppz-idzo]$^{2+}$: A colorimetric molecular "light switch" and powerful stabilizer for G-quadruplex DNA. *Dalton Trans.* **2013**, *42*, 5661–5672. [CrossRef]
214. Hu, X.; Yang, D.; Yao, T.; Gao, R.; Wumaier, M.; Shi, S. Regulation of multi-factors (tail/loop/link/ions) for G-quadruplex enantioselectivity of Δ- and Λ- [Ru(bpy)$_2$(dppz-idzo)]$^{2+}$. *Dalton Trans.* **2018**, *47*, 5422–5430. [CrossRef]

215. Mikek, C.G.; Machha, V.R.; White, J.C.; Martin, L.R.; West, S.J.; Butrin, A.; Shumaker, C.; Gwin, J.C.; Alatrash, N.; MacDonnell, F.M.; et al. The Thermodynamic Effects of Ligand Structure on the Molecular Recognition of Mono- and Birutheniumium polypyridyl Complexes with G-quadruplex DNA. *Eur. J. Inorg. Chem.* **2017**, *2017*, 3953–3960. [CrossRef]

216. Yu, H.-J.; Zhao, Y.; Mo, W.-J.; Hao, Z.-F.; Yu, L. Ru-indoloquinoline complex as a selective and effective human telomeric G-quadruplex binder. *Spectrochim. Acta Part A Mol. Biomol. Spectrosc.* **2014**, *132*, 84–90. [CrossRef]

217. Lefebvre, J.-F.; Saadallah, D.; Traber, P.; Kupfer, S.; Gräfe, S.; Dietzek, B.; Baussanne, I.; De Winter, J.; Gerbaux, P.; Moucheron, C.; et al. Synthesis of three series of ruthenium tris-diimine complexes containing acridine-based π-extended ligands using an efficient "Chemistry on the Complex" approach. *Dalton Trans.* **2016**, *45*, 16298–16308. [CrossRef]

218. Saadallah, D.; Bellakhal, M.; Amor, S.; Lefebvre, J.-F.; Chavarot-Kerlidou, M.; Baussanne, I.; Moucheron, C.; Demeunynck, M.; Monchaud, D. Selective Luminescent Labeling of DNA and RNA Quadruplexes by π-Extended Ruthenium Light-Up Probes. *Chem. Eur. J.* **2017**, *23*, 4967–4972. [CrossRef]

219. Collie, G.W.; Sparapani, S.; Parkinson, G.N.; Neidle, S. Structural Basis of Telomeric RNA Quadruplex–Acridine Ligand Recognition. *J. Am. Chem. Soc.* **2011**, *133*, 2721–2728. [CrossRef]

220. Neidle, S. Quadruplex Nucleic Acids as Novel Therapeutic Targets. *J. Med. Chem.* **2016**, *59*, 5987–6011. [CrossRef]

221. Laguerre, A.; Stefan, L.; Larrouy, M.; Genest, D.; Novotna, J.; Pirrotta, M.; Monchaud, D. A Twice-As-Smart Synthetic G-Quartet: PyroTASQ Is Both a Smart Quadruplex Ligand and a Smart Fluorescent Probe. *J. Am. Chem. Soc.* **2014**, *136*, 12406–12414. [CrossRef]

222. Yang, S.; Amor, S.; Laguerre, A.; Wong, J.M.; Monchaud, D. Real-time and quantitative fluorescent live-cell imaging with quadruplex-specific red-edge probe (G4-REP). *Biochim. Biophys. Acta–Gen. Subj.* **2017**, *1861*, 1312–1320. [CrossRef] [PubMed]

223. Liao, G.-L.; Chen, X.; Ji, L.-N.; Chao, H. Visual specific luminescent probing of hybrid G-quadruplex DNA by a ruthenium polypyridyl complex. *Chem. Commun.* **2012**, *48*, 10781–10783. [CrossRef]

224. Zhang, S.; Wang, L.; Liu, M.; Qiu, Y.; Wang, M.; Liu, X.; Shen, G.; Yu, R. A novel, label-free fluorescent aptasensor for cocaine detection based on a G-quadruplex and ruthenium polypyridyl complex molecular light switch. *Anal. Methods* **2016**, *8*, 3740–3746. [CrossRef]

225. Piraux, G.; Bar, L.; Abraham, M.; Lavergne, T.; Jamet, H.; Dejeu, J.; Marcélis, L.; Defrancq, E.; Elias, B. New Ruthenium-Based Probes for Selective G-quadruplex Targeting. *Chem. Eur. J.* **2017**, *23*, 11872–11880. [CrossRef]

226. Liu, D.; Liu, Y.; Wang, C.; Shi, S.; Sun, D.; Gao, F.; Zhang, Q.; Liu, J. Polypyridyl Complexes of Ruthenium(II): Stabilization of G-quadruplex DNA and Inhibition of Telomerase Activity. *ChemPlusChem* **2012**, *77*, 551–562. [CrossRef]

227. Sun, D.; Liu, Y.; Liu, D.; Zhang, R.; Yang, X.; Liu, J. Stabilization of G-quadruplex DNA, Inhibition of Telomerase Activity and Live Cell Imaging Studies of Chiral Ruthenium(II) Complexes. *Chem.-Eur. J.* **2012**, *18*, 4285–4295. [CrossRef] [PubMed]

228. Yu, Q.; Liu, Y.; Wang, C.; Sun, D.; Yang, X.; Liu, Y.; Liu, J. Chiral Ruthenium(II) Polypyridyl Complexes: Stabilization of G-quadruplex DNA, Inhibition of Telomerase Activity and Cellular Uptake. *PLoS ONE* **2012**, *7*, e50902. [CrossRef]

229. Zhang, Z.; Wu, Q.; Wu, X.-H.; Sun, F.-Y.; Chen, L.-M.; Chen, J.-C.; Yang, S.-L.; Mei, W.-J. Ruthenium(II) complexes as apoptosis inducers by stabilizing c-myc G-quadruplex DNA. *Eur. J. Med. Chem.* **2014**, *80*, 316–324. [CrossRef]

230. Liu, Y.; Liu, Y.; Yang, L.; Cao, C.; Zhou, Y.; Liu, J. Stabilization for loop isomers of c-myc G-quadruplex DNA and anticancer activity by ruthenium complexes. *MedChemComm* **2014**, *5*, 1724–1728. [CrossRef]

231. Sun, D.; Liu, Y.; Yu, Q.; Liu, D.; Zhou, Y.; Liu, J. Selective nuclei accumulation of ruthenium(II) complex enantiomers that target G-quadruplex DNA. *J. Inorg. Biochem.* **2015**, *150*, 90–99. [CrossRef] [PubMed]

232. Zhang, S.; Wu, Q.; Zhang, H.; Wang, Q.; Wang, X.; Mei, W.; Wu, X.; Zheng, W. Microwave-assisted synthesis of ruthenium(II) complexes with alkynes as potential inhibitor by selectively recognizing c-myc G-quadruplex DNA. *J. Inorg. Biochem.* **2017**, *176*, 113–122. [CrossRef]

233. Liu, X.-W.; Liu, N.-Y.; Deng, Y.-Q.; Wang, S.; Liu, T.; Tang, Y.-C.; Chen, Y.-D.; Lu, J.-L. A Luminescence Probe for c-myc G-quadruplex by a Triphenylamine-Appended Ruthenium Complex. Appl. *Organomet. Chem.* **2021**, *35*, e6143. [CrossRef]

234. Yu, Q.; Liu, Y.; Zhang, J.; Yang, F.; Sun, D.; Liu, D.; Zhou, Y.; Liu, J. Ruthenium(II) polypyridyl complexes as G-quadruplex inducing and stabilizing ligands in telomeric DNA. *Metallomics* **2013**, *5*, 222–231. [CrossRef]

235. Zhang, Z.; Mei, W.; Wu, X.; Wang, X.; Wang, B.; Chen, S. Synthesis and Characterization of Chiral Ruthenium(II) Complexes Λ/Δ-[Ru(Bpy)$_2$(H$_2$Iip)](ClO$_4$)$_2$ as Stabilizers of c-Myc G-quadruplex DNA. *J. Coord. Chem.* **2015**, *68*, 1465–1475. [CrossRef]

236. Xu, X.; Wang, S.; Mi, Y.; Zhao, H.; Zheng, Z.; Zhao, X. A hydroxyquinoline-appended ruthenium(II)-polypyridyl complex that induces and stabilizes G-quadruplex DNA. *J. Coord. Chem.* **2019**, *72*, 201–217. [CrossRef]

237. Liu, X.-W.; Liu, N.-Y.; Deng, Y.-Q.; Wang, S.; Liu, T. Topoisomerase I Inhibition, DNA Photocleavage Activity, and G-quadruplex DNA 'Light Switch' Based on Nitro-Substituted Ruthenium Complexes. *Russ. J. Inorg. Chem.* **2020**, *65*, 1186–1195.

238. Liu, X.; Liu, N.; Deng, Y.; Wang, S.; Liu, T.; Tang, Y.; Chen, Y.; Lu, J. An unexpected fluorescent probe for G-quadruplex DNA based on a nitro-substituted ruthenium (II) complex. *Appl. Organomet. Chem.* **2020**, *34*, e5703. [CrossRef]

239. Zhang, J.; Yu, Q.; Li, Q.; Yang, L.; Chen, L.; Zhou, Y.; Liu, J. A ruthenium(II) complex capable of inducing and stabilizing bcl-2 G-quadruplex formation as a potential cancer inhibitor. *J. Inorg. Biochem.* **2014**, *134*, 1–11. [CrossRef]

240. Li, Q.; Zhang, J.; Yang, L.; Yu, Q.; Chen, Q.; Qin, X.; Le, F.; Zhang, Q.; Liu, J. Stabilization of G-quadruplex DNA and inhibition of telomerase activity studies of ruthenium(II) complexes. *J. Inorg. Biochem.* **2014**, *130*, 122–129. [CrossRef]

241. Liu, X.-W.; Liu, N.-Y.; Deng, Y.-Q.; Wang, S.; Liu, T.; Tang, Y.-C.; Chen, Y.-D.; Lu, J.-L. Nitro-Substituted Ruthenium(II) Complex: A New Strategy for a G-quadruplex DNA Fluorescent Probe. *Inorg. Chem.* **2019**, *58*, 16326–16329. [CrossRef]

242. Weynand, J.; Diman, A.; Abraham, M.; Marcélis, L.; Jamet, H.; Decottignies, A.; Dejeu, J.; Defrancq, E.; Elias, B. Towards the Development of Photo-Reactive Ruthenium(II) Complexes Targeting Telomeric G-quadruplex DNA. *Chem. Eur. J.* **2018**, *24*, 19216–19227. [CrossRef] [PubMed]

243. Sheet, S.K.; Rabha, M.; Sen, B.; Patra, S.K.; Aguan, K.; Khatua, S. Ruthenium(II) Complex-Based G-quadruplex DNA Selective Luminescent 'Light-up' Probe for RNase H Activity Detection. *ChemBioChem* **2021**, *22*, 2880–2887. [CrossRef] [PubMed]

244. Chen, X.; Wu, J.-H.; Lai, Y.-W.; Zhao, R.; Chao, H.; Ji, L.-N. Targeting telomeric G-quadruplexes with the ruthenium(II) complexes [Ru(bpy)$_2$(ptpn)]$^{2+}$ and [Ru(phen)$_2$(ptpn)]$^{2+}$. *Dalton Trans.* **2013**, *42*, 4386–4397. [CrossRef] [PubMed]

245. Li, Q.; Sun, N.; Zhou, Y.; Liu, D.; Zhang, Q.; Liu, J. Anticancer activity of novel ruthenium complex with 1,10-phenanthrolineselenazole as potent telomeric G-quadruplex inhibitor. *Inorg. Chem. Commun.* **2012**, *20*, 142–146. [CrossRef]

246. Xia, Y.; Chen, Q.; Qin, X.; Sun, D.; Zhang, J.; Liu, J. Studies of Ruthenium(II)-2,2′-Bisimidazole Complexes on Binding to G-quadruplex DNA and Inducing Apoptosis in HeLa Cells. *New J. Chem.* **2013**, *37*, 3706–3715. [CrossRef]

247. Wumaier, M.; Shi, J.-J.; Yao, T.-M.; Hu, X.-C.; Gao, R.-R.; Shi, S. G-quadruplex and duplex DNA binding studies of novel Ruthenium(II) complexes containing ascididemin ligands. *J. Inorg. Biochem.* **2019**, *196*, 110681. [CrossRef]

248. Zhang, Z.; Wu, X.-H.; Sun, F.-Q.; Shan, F.; Chen, J.-C.; Chen, L.-M.; Zhou, Y.-S.; Mei, W.-J. Synthesis, characterization of ruthenium(II) complex of 1,3,8-trihydroxy-6-methyl-anthraquinone (emodin) and its binding behavior with c-myc G-quadruplex. *Inorg. Chim. Acta* **2014**, *418*, 23–29. [CrossRef]

249. He, L.; Chen, X.; Meng, Z.; Wang, J.; Tian, K.; Li, T.; Shao, F. Octahedral ruthenium complexes selectively stabilize G-quadruplexes. *Chem. Commun.* **2016**, *52*, 8095–8098. [CrossRef]

250. Prasad, B.; Jamroskovic, J.; Bhowmik, S.; Kumar, R.; Romell, T.; Sabouri, N.; Chorell, E. Flexible Versus Rigid G-quadruplex DNA Ligands: Synthesis of Two Series of Bis-indole Derivatives and Comparison of Their Interactions with G-quadruplex DNA. *Chem. Eur. J.* **2018**, *24*, 7926–7938. [CrossRef]

251. Ihmels, H.; Karbasiyoun, M.; Löhl, K.; Stremmel, C. Structural flexibility versus rigidity of the aromatic unit of DNA ligands: Binding of aza- and azoniastilbene derivatives to duplex and quadruplex DNA. *Org. Biomol. Chem.* **2019**, *17*, 6404–6413. [CrossRef]

252. Gillard, M.; Weynand, J.; Bonnet, H.; Loiseau, F.; Decottignies, A.; Dejeu, J.; Defrancq, E.; Elias, B. Flexible Ru(II) Schiff Base Complexes: G-quadruplex DNA Binding and Photo-Induced Cancer Cell Death. *Chem. Eur. J.* **2020**, *26*, 13849–13860. [CrossRef]

253. Friedman, A.E.; Chambron, J.C.; Sauvage, J.P.; Turro, N.J.; Barton, J.K. A molecular light switch for DNA: Ru(bpy)$_2$(dppz)$^{2+}$. *J. Am. Chem. Soc.* **1990**, *112*, 4960–4962. [CrossRef]

254. Hartshorn, R.M.; Barton, J.K. Novel dipyridophenazine complexes of ruthenium(II): Exploring luminescent reporters of DNA. *J. Am. Chem. Soc.* **1992**, *114*, 5919–5925. [CrossRef]

255. Rajput, C.; Rutkaite, R.; Swanson, L.; Haq, I.; Thomas, J.A. Dinuclear Monointercalating Ru(II) Complexes That Display High Affinity Binding to Duplex and Quadruplex DNA. *Chem. Eur. J.* **2006**, *12*, 4611–4619. [CrossRef]

256. Wilson, T.; Williamson, M.P.; Thomas, J.A. Differentiating quadruplexes: Binding preferences of a luminescent dinuclear ruthenium(II) complex with four-stranded DNA structures. *Org. Biomol. Chem.* **2010**, *8*, 2617–2621. [CrossRef]

257. Wilson, T.; Costa, P.J.; Félix, V.; Williamson, M.P.; Thomas, J.A. Structural Studies on Dinuclear Ruthenium(II) Complexes That Bind Diastereoselectively to an Antiparallel Folded Human Telomere Sequence. *J. Med. Chem.* **2013**, *56*, 8674–8683. [CrossRef]

258. Gill, M.; Garcia-Lara, J.; Foster, S.J.; Smythe, C.; Battaglia, G.; Thomas, J. A ruthenium(II) polypyridyl complex for direct imaging of DNA structure in living cells. *Nat. Chem.* **2009**, *1*, 662–667. [CrossRef]

259. Gonzalez, V.; Wilson, T.; Kurihara, I.; Imai, A.; Thomas, J.A.; Otsuki, J. A dinuclear ruthenium(II) complex that functions as a label-free colorimetric sensor for DNA. *Chem. Commun.* **2008**, 1868–1870. [CrossRef]

260. Zhao, X.-L.; Zhao, H.-Q.; Xu, X.-X.; Li, Z.-S.; Wang, K.-Z. Inducement and stabilization of G-quadruplex DNA by a thiophene-containing dinuclear ruthenium(II) complex. *J. Coord. Chem.* **2017**, *70*, 2094–2112. [CrossRef]

261. Zhao, H.; Xu, X.; Wang, S.; Mi, Y.; Zheng, Z.; Zhao, X. A dinuclear ruthenium(II) complex as an inducer and potential luminescent switch-on probe for G-quadruplex DNA. *Transit. Met. Chem.* **2018**, *43*, 539–548. [CrossRef]

262. Xu, L.; Zhang, D.; Huang, J.; Deng, M.; Zhang, M.; Zhou, X. High fluorescence selectivity and visual detection of G-quadruplex structures by a novel dinuclear ruthenium complex. *Chem. Commun.* **2009**, *46*, 743–745. [CrossRef] [PubMed]

263. Zheng, C.; Liu, Y.; Liu, Y.; Qin, X.; Zhou, Y.; Liu, J. Dinuclear ruthenium complexes display loop isomer selectivity to c-MYC DNA G-quadruplex and exhibit anti-tumour activity. *J. Inorg. Biochem.* **2016**, *156*, 122–132. [CrossRef] [PubMed]

264. Shi, S.; Gao, S.; Cao, T.; Liu, J.; Gao, X.; Hao, J.; Lv, C.; Huang, H.; Xu, J.; Yao, T. Targeting Human Telomeric G-quadruplex DNA and Inhibition of Telomerase Activity With [(dmb)$_2$Ru(obip)Ru(dmb)$_2$]$^{4+}$. *PLoS ONE* **2013**, *8*, e84419. [CrossRef]

265. Xu, L.; Chen, X.; Wu, J.; Wang, J.; Ji, L.; Chao, H. Dinuclear Ruthenium(II) Complexes That Induce and Stabilise G-quadruplex DNA. *Chem. Eur. J.* **2015**, *21*, 4008–4020. [CrossRef] [PubMed]

266. Xu, L.; Liao, G.-L.; Chen, X.; Zhao, C.-Y.; Chao, H.; Ji, L.-N. Trinuclear Ru(II) polypyridyl complexes as human telomeric quadruplex DNA stabilizers. *Inorg. Chem. Commun.* **2010**, *13*, 1050–1053. [CrossRef]

267. Lecomte, J.-P.; Kirsch-De Mesmaeker, A.; Feeney, M.M.; Kelly, J. Ruthenium(II) Complexes with 1,4,5,8,9,12-Hexaazatriphenylene and 1,4,5,8-Tetraazaphenanthrene Ligands: Key Role Played by the Photoelectron Transfer in DNA Cleavage and Adduct Formation. *Inorg. Chem.* **1995**, *34*, 6481–6491. [CrossRef]

268. Blasius, R.; Moucheron, C.; Kirsch-De Mesmaeker, A. Photoadducts of Metallic Compounds with Nucleic Acids—Role Played by the Photoelectron Transfer Process and by the TAP and HAT Ligands in the RuII Complexes. *Eur. J. Inorg. Chem.* **2004**, *2004*, 3971–3979. [CrossRef]

269. Wagenknecht, H.-A.; Stemp, E.D.A.; Barton, J.K. Evidence of Electron Transfer from Peptides to DNA: Oxidation of DNA-Bound Tryptophan Using the Flash-Quench Technique. *J. Am. Chem. Soc.* **1999**, *122*, 1–7. [CrossRef]

270. Moucheron, C. From cisplatin to photoreactive Ru complexes: Targeting DNA for biomedical applications. *New J. Chem.* **2008**, *33*, 235–245. [CrossRef]

271. Keane, P.M.; O'Sullivan, K.; Poynton, F.E.; Poulsen, B.C.; Sazanovich, I.V.; Towrie, M.; Cardin, C.J.; Sun, X.-Z.; George, M.W.; Gunnlaugsson, T.; et al. Understanding the factors controlling the photo-oxidation of natural DNA by enantiomerically pure intercalating ruthenium polypyridyl complexes through TA/TRIR studies with polydeoxynucleotides and mixed sequence oligodeoxynucleotides. *Chem. Sci.* **2020**, *11*, 8600–8609. [CrossRef]

272. Ghizdavu, L.; Pierard, F.; Rickling, S.; Aury, S.; Surin, M.; Beljonne, D.; Lazzaroni, R.; Murat, P.; Defrancq, E.; Moucheron, C.; et al. Oxidizing Ru(II) Complexes as Irreversible and Specific Photo-Cross-Linking Agents of Oligonucleotide Duplexes. *Inorg. Chem.* **2009**, *48*, 10988–10994. [CrossRef]

273. Rickling, S.; Ghisdavu, L.; Pierard, F.; Gerbaux, P.; Surin, M.; Murat, P.; Defrancq, E.; Moucheron, C.; Kirsch-De Mesmaeker, A. A Rigid Dinuclear Ruthenium(II) Complex as an Efficient Photoactive Agent for Bridging Two Guanine Bases of a Duplex or Quadruplex Oligonucleotide. *Chem. Eur. J.* **2010**, *16*, 3951–3961. [CrossRef]

274. Archer, S.A.; Raza, A.; Dröge, F.; Robertson, C.; Auty, A.J.; Chekulaev, D.; Weinstein, J.A.; Keane, T.; Meijer, A.J.H.M.; Haycock, J.W.; et al. A dinuclear ruthenium(II) phototherapeutic that targets duplex and quadruplex DNA. *Chem. Sci.* **2019**, *10*, 3502–3513. [CrossRef]